Analysis and Optimization of Medium Voltage-Line Voltage Regulators

Pankaj Raghav Partha Sarathy

Master of Science Thesis

TU Delft Delft University of Technology

EWEM

NTNU Norwegian University of Science and Technology

Challenge the future

Analysis and Optimization of Medium Voltage-Line Voltage Regulators

by

Pankaj Raghav Partha Sarathy

in partial fulfillment of the requirements for the degrees of
MSc in Electrical Engineering at Delft University of Technology
&
MSc-Technology in Wind Energy at Norwegian University of Science and Technology,
under the European Wind Energy Masters programme (EWEM).
To be defended publicly on Friday August 31, 2018 at 02:00 PM.

Student number:	4597524	
Thesis committee:	Dr. ir. Pavol Bauer,	TU Delft, supervisor
	Dr. Kjell Sand,	NTNU Trondheim, supervisor
	Dr. ir. L.M. Ramirez Elizondo,	TU Delft
Company supervisors:	Frank Cornelius,	ABB, Germany
	Tobias Asshauer,	ABB, Germany

TU Delft ABB NTNU Norwegian University of Science and Technology

Abstract

In recent years, distribution networks have been facing voltage quality issues due to the influx of renewable energy. Rural areas which are ideal for renewable energy development due to large vacant areas are faced with grid voltage variations due to long distribution lines. Because of the stringent conditions laid by the Distribution System Operators (DSOs) on voltage variations, voltage regulation is becoming increasingly important in the distribution grid. A complete grid reinforcement by replacing the conductors can be very expensive for the DSOs. Active solutions such as shunt and series compensation provides an economical solution to address the voltage regulation issues in the distribution grids.

The initial part of this work focuses on quantitatively studying the impact of series and shunt compensation on increasing the grid capacity of a Medium Voltage(MV) line compared to a grid reinforcement with conductor upgradation. The analysis was done on a 20 kV, 10 MVA radial line with 5 loads distributed equally along the line, and a generator at the end of the line. An algorithm was developed in MATLAB/ Simulink to determine the allowable grid capacity to stay within the thermal and voltage limits for different voltage regulation strategies. The study indicates that the series voltage regulation with Line Voltage Regulators(LVR) is an effective solution in increasing the grid capacity by actively regulating the voltage in the grid. The MV-LVR product offered by ABB consists of dry-type transformers and mechanical contactors for changing the tap position. However, dry-type transformers are bigger in size and more expensive than oil-type transformers. To reduce the cost and the size of the MV-LVR, the study is focused on the feasibility of a MV-LVR with oil-type transformers and On-Load Tap-Changers (OLTCs). The second part of the project work focuses on developing an economical LVR configuration with an oil-type transformer and a mechanical OLTC. ECOTAP VPD III 100 from Maschinenfabrik Reinhausen (MR) was selected as the mechanical OLTC to perform the tap changing operation in the LVR. ECOTAP OLTC enables low maintenance of transformers due to the use of vacuum switches for quenching the arc during tap-changes. 7 LVR configurations with single and two active parts are investigated. All the configurations are finally compared for their cost and range of operation. The final part of the work focuses on a feasibility study of a power electronics based OLTC for LVR applications as mechanical OLTCs require regular maintenance. Anti-parallel thyristors are used as the solid-state switches for the LVR application due to its low cost and losses. Commutation instants are defined for the complete power factor range for the thyristor based OLTC to have no/controlled short circuit during tap-changes.

The two active parts LVR configuration constructed with a center tapped feeder transformer and a booster transformer with the ECOTAP VPD III 100 OLTC is economical for a 20 kV, 10 MVA feeder line. A LVR rated at 20 kV, 10 MVA with ±6% voltage regulation using the selected configuration was simulated in MATLAB/ Simulink. A 400 V, 5 kVA low voltage setup was built with the ECOTAP VPD III 100 OLTC, and the LVR configuration was verified with experimental results. The feeder transformer model with two taps was simulated in MATLAB/Simulink for switching up and switching down operation with a thyristor based OLTC for capacitive, inductive and resistive power factors. The complete LVR system with thyristor based OLTC placed in a MV distribution line was simulated to verify the control algorithm used for the commutation. The thyristor based OLTC successfully performs tap-changes for a LVR system with a low voltage stress on the thyristor, and low short circuit currents between the taps for certain power factor angles during the commutation process.

Acknowledgements

I would like to express my sincere gratitude to my professors Pavol Bauer from TU Delft and Kjell Sand from NTNU Trondheim for giving me the opportunity to work under their supervision. I am deeply grateful to Tobias Asshauer and Frank Cornelius from ABB Brilon for allowing me to be a part of this project at the company and keeping the doors open whenever I ran into trouble during my research. I would like to sincerely thank Gautham Ram from TU Delft for his valuable inputs and motivation which gave me a lot of confidence in moments of doubt. I would like to thank professor Pavol Bauer again for his valuable advice which made me stay on track in moments of uncertainty.

I would like to take this opportunity to show my appreciation towards European Wind Energy Masters (EWEM) consortium for the generous scholarship to pursue my Erasmus Mundus programme. I would also like to thank my friends Andres and Isidora from electrical power systems track and other friends from the EWEM programme for always being together throughout these two years of the Master programme.

Finally, I must express my very deepest gratitude to my parents and to my brother for providing me with unfailing support and encouragement throughout my study. This accomplishment would not have been possible without them. I would like to also thank Niranchana Venkatesh for being the ever supportive companion and helping me see this thesis through to the finish.

Pankaj Raghav Partha Sarathy
Delft, August 2018

The impediment to action advances action.
What stands in the way becomes the way.

- Marcus Aurelius

Contents

List of Figures

List of Tables

Nomenclature

$a_{booster}$ Turns ratio of booster transformer

a_{feeder} Turns ratio of feeder transformer

α Firing angle of the thyristor

δ Extinction angle

δ_q Thyristor turn-off angle

γ Overlap angle during commutation

ω Angular frequency (rad/s)

ϕ Power factor angle

CCC Current carrying capacity

DSO Distribution system operator

e_r Per unit resistance drop

e_x Per unit reactance drop

I_m Peak value of the current

I_{T1} Current in thyristor pair T1

I_{T2} Current in thyristor pair T2

L_{tap} Per-tap leakage inductance

N_{Bpri} No. of turns on the booster transformer the primary windings

N_{Bsec} No. of turns on the booster transformer secondary winding

N_{pri} No. of tunrs on the the feeder transformer primary windings

$N_{sec}(OLTC)$ Effective number of turns for feeder transformer secondary with OLTC

N_{taps} No. of taps

PF Power Factor

S_k Short circuit power

$S_{booster}$ Power rating of booster transformer

S_{feeder} Power rating of feeder transformer

SCR Short circuit ratio

t_q Thyristor turn-off time

$tan(\psi)$ Network impedance angle

V_L Load voltage

V_m Peak value of the voltage

V_S Source voltage

V_{1T} Feeder transformer secondary OLTC voltage

V_1 Feeder transformer primary voltage

V_{2T} Booster transformer primary OLTC voltage

V_2 Series compensation voltage

V_{comp} Compensation Voltage

V_{GEN} Generator voltage

V_{Snew} New voltage set-point

V_{step} Step voltage

V_{T1} Voltage across thyristor pair T1

V_{T2} Voltage across thyristor pair T2

V_{tap} Per-tap voltage of the transformer

Reg. range Regulation range of LVR (pu)

RMS Root Mean Square

SCADA Supervisory Control and Data Acquisition technology

1

Introduction

There has been a huge push by governments all around the world to move towards renewable energy to reduce greenhouse gas emissions. Fig. 1.1 shows the installed capacity of global renewable energy from 2006 - 2015 and the percentage increase for each technology. The installed capacity of the wind and solar energy based technology are growing at a very rapid rate with a percentage change of 487.7% and 3404.9% respectively from 2006-15. With the recent Paris agreement, the share of renewable energy is expected to increase at a faster rate. Apart from the large wind and solar parks to produce huge amounts of renewable power, integrating renewable energy sources (RES) in to the distribution system has started to become increasingly popular [9].

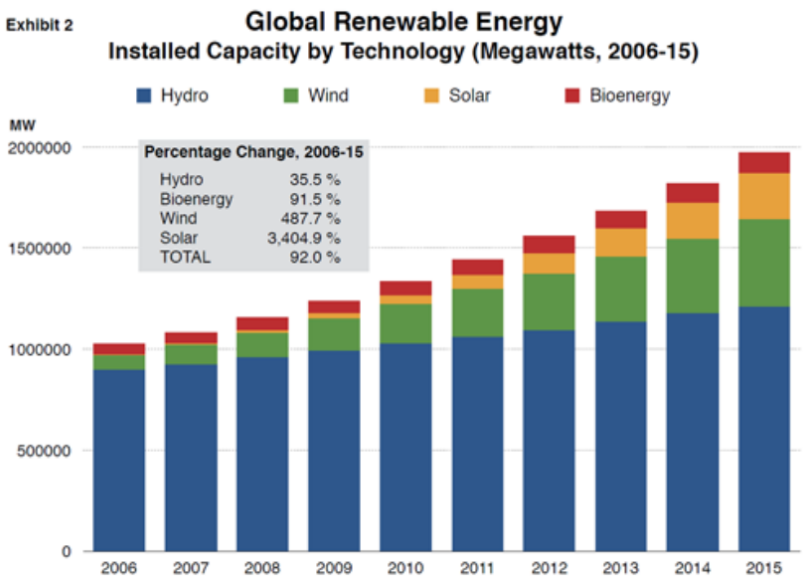

Figure 1.1: Global renewable energy share and percentage change of installed capacity of different technologies(source: International renewable energy agency, Renewable Capacity Statistics,2016) [7]

Increasing the amount of DG penetration into the Medium Voltage (MV) and Low Voltage (LV) grid causes voltage regulation issues in the distribution network[76]. Injection of active power by the DGs to the distribution network can directly impact the feeder voltage due to high R/X ratio [77]. The voltage variation is more pronounced in rural networks due to long feeders compared to urban networks with shorter lines[19].

Rural areas are ideal for renewable energy development due to their sparse population and large vacant areas [3]. With the growing rural renewable energy development, evacuating the power from rural areas requires long overhead lines. The connection cost for a renewable energy project can be reduced by connecting the generators to a lower voltage level network at the point of common coupling (PCC). The higher the voltage

level, the higher the connection cost for the developer [40]. But, active power injection by the DGs to a low voltage level network can have a more direct impact on voltage variation than when they are connected to a high voltage level network. To bridge the gap, the developers and DSOs should deploy economically active solutions to maintain the voltage, especially in long rural networks with renewable energy.

The traditional active voltage regulation methods used by the DSOs are as follows [41]:

- Distribution transformer with On-Load Tap-Changers (OLTC)
- Shunt capacitors and reactors
- Series Voltage Regulators (SVRs) or Line Voltage Regulators (LVRs)

This thesis focuses specifically on the Line Voltage Regulators (LVRs). LVRs or SVRs are located along the feeder to provide voltage regulation. They are constructed using a transformer with tap changing mechanism to regulate the voltage. LVRs have the ability to individually regulate the voltage in a particular feeder without affecting other feeders connected to a common bus [37].
The MV-LVR product offered by ABB consists of dry-type transformers and mechanical contactors for changing the tap position [8]. However, dry-type transformers are bigger in size and more expensive than oil-type transformers. The main objective of this thesis is to evaluate the feasibility of a MV-LVR with oil-type transformers and OLTCs. Feasibility with both mechanical and power electronic based OLTCs are considered in this thesis. A system level study of different voltage regulation strategies is added to the objectives to have a more holistic understanding of LVRs.

Research objectives:

The research objectives of the study are as follows:

1. Technical benefit analysis of different voltage regulation strategies for medium voltage (MV) radial grids using load flow studies to assess its impact on grid capacity.
2. Analyze different MV-LVR configurations with oil-type transformers and mechanical OLTCs, and develop an economical MV-LVR for series voltage regulation in a distribution grid.
3. Feasibility study of a power electronics based OLTC solution for MV-LVRs.

Thesis outline:

The thesis has been divided into three major parts to focus on different aspects of the LVR. The first part deals with a system level study of LVRs and their impact on improving the grid capacity in a MV distribution grid. This analysis is performed to understand how active solutions can avoid conductor upgradation and operate the distribution grid without violating the voltage and power limits. The second part focuses on selecting an oil-type mechanical OLTC and analyzing different configurations to develop an economical and low maintenance design for LVRs. Simulations and a low power experimental validations are performed to verify the selected configuration. The final part investigates the feasibility of a power electronics based on-load tap-changer solution to enable faster tap-changes and avoid maintenance compared to LVRs with mechanical OLTCs. A bi-directional solid-state switch is selected and an appropriate control algorithm is formulated. Simulations are performed to validate the control algorithm of the power electronics based OLTC. Finally, a brief comparison is presented between power electronics based OLTCs and mechanical OLTCs for LVR applications.

2

Voltage Variation and Regulation in a Medium Voltage Grid

2.1. Introduction

In a traditional power system, generators are located at a significant distance from the consumers and the power flow is typically unidirectional. The system is designed so that the consumers connected at the end of a line do not experience voltage violation even during high load conditions. With increase in Distributed Generators (DGs), distribution networks are challenged by the reverse power flow. Traditionally designed distribution networks are not designed to handle the DG penetration. The increase in distributed generation is challenging the DSOs to maintain the voltage within the statuatory limits. This chapter elaborates on voltage variation problems faced in the distribution grids and the methods used to tackle the issue.

2.2. Voltage quality standards

There are various voltage quality standards laid out by the TSOs and DSOs around the world to maintain the voltage within a reasonable range to avoid maloperation of various components connected to the grid. Table 2.1 presents a comparison of standards for long duration voltage variation limits from different parts of the world [5], [4], [1], [2].

Table 2.1: Long duration supply voltage variation statutory limits in different countries

Standard	Statistical evaluation	Compliance w.r.t U_N
EN 50160 (Europe)	95 % of the time in 1 week	± 10 %
ANSI C84.1 (USA)	100 % of the time	-2,5% to + 5%
NVE (Norway)	100 % of the time	± 10 %
NRS-048-2 (South Africa)	95 % of the time in 1 week 100 % of the time in 1 week	± 5 % ± 10 %
GB/T 12325-2003 (China)	100 % of the time	± 10 %
CEA (India)	Not specified	-10% to + 6%

The Distribution System Operators (DSOs) have laid down the above stringent regulations for long duration supply voltage variation to avoid any detrimental effect on the customers connected to the grid. There have been various studies which show the negative effects of voltage variation on industries and residential customers [62], [49], [61].

2.3. Medium voltage grid

Power produced by traditional large power plants are transferred to the consumers via the electrical grid. A typical AC electrical grid can be generally subdivided into four main networks based on the voltage levels:

- Transmission network (225kV - 765kV)

- Sub-transmission network (25kV - 275 kV)
- Medium voltage network (1kV - 25 kV)
- Low voltage network (up to 1kV)

The most commonly used medium voltage levels in Europe are between 10kV and 20kV due to its optimal power transfer capability and the cost of components. The most commonly used grid layouts for medium voltage are (i) Radial structure (ii) Open loop structure [58]. A brief description of layout is given below:

2.3.1. Radial structure

Fig.2.1 shows the radial network layout. Radial grids operate on a single supply line for the connected consumers, and in this structure there is only one possible electrical supply path to any consumer connected to the grid. Advantages of this structure are simple layout, lower installation cost and easier operation. Disadvantage of this structure is the low reliability to the connected consumers. Radial grid topology is used for rural overhead distribution lines.

2.3.2. Open loop structure

The right hand side of the fig.2.1 shows the open loop network layout. The main idea behind an open loop network layout is the possibility of supplying the power via two electrical networks. Only one electrical path is activated at any point of time to the consumers by having an open point in the line. In case of any fault in one of the networks, back up power is provided from the other electrical path by closing the open point. This increases the reliability of supply to the consumers connected to the grid. In normal operation, it still works like two independent radial grid network as the tie breaker is open. Advantages of this structure are simple layout, higher reliability. Disadvantages are the higher cost and more complex operation than simple radial grid network. Open loop topology is generally used for urban underground cable distribution lines.

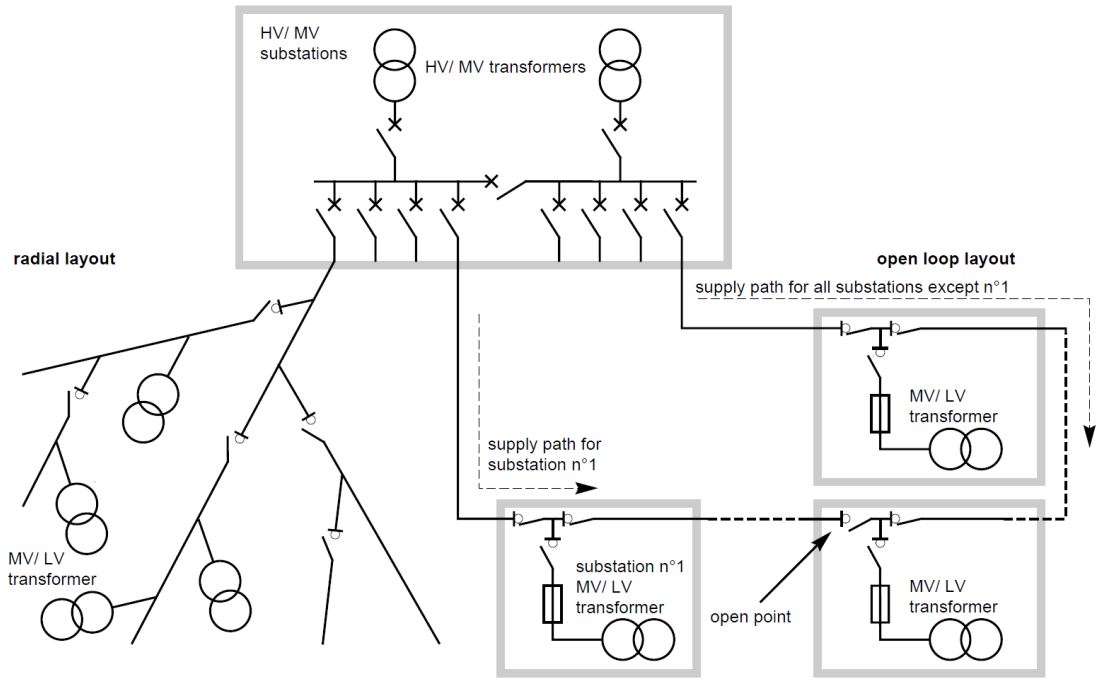

Figure 2.1: Radial and open loop layout employed in medium voltage distribution grid [58]

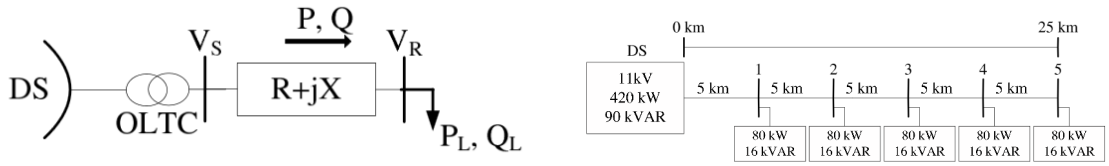

(a) (b)

Figure 2.2: (a) A typical two bus distribution system (b) A conventional radial distribution system [40]

2.4. Voltage drop in a conventional distribution grid

A traditional grid is designed for a unidirectional power flow from a conventional source located far away from the consumption point and it is transmitted via different voltage level networks.

A distribution network can be modeled as a passive network with resistance and inductance. A lumped resistance (R) and inductance (X) model is considered as shown in fig. 2.2a. V_S represents the bus voltage, V_R represents the load voltage. P and P_L represents the active power through the line and consumed by the load respectively. Q represents the reactive power through the line and Q_L represents the reactive power consumed by the load. The voltage drop equation can be derived based on the phasor relationship between the source and the load.

$$\begin{aligned} \overline{V_S} &= \overline{V_R} + \overline{I} * (R + jX) \\ \overline{V_S} * \overline{I^*} &= P + jQ \end{aligned} \tag{2.1}$$

By rearranging the second part of eq. 2.1, the following equation can be derived for the current (I) flowing in the system.

$$\overline{I} = \frac{P - jQ}{\overline{V_S}}$$

Substituting the above equation in the first part of eq.2.1, the following equation can be derived for the sending end voltage.

$$\begin{aligned} \overline{V_S} &= \overline{V_R} + \left(\frac{P - jQ}{\overline{V_S}}\right) * (R + jX) \\ \overline{V_S} &= \overline{V_R} + \left(\frac{RP + XQ}{\overline{V_S}}\right) + j\left(\frac{XP - RQ}{\overline{V_S}}\right) \end{aligned} \tag{2.2}$$

Therefore, the voltage drop between the source and the load can be written as:

$$\Delta V = \left(\frac{RP + XQ}{\overline{V_S}}\right) + j\left(\frac{XP - RQ}{\overline{V_S}}\right) \tag{2.3}$$

The angle between the source and the load is not large, and in most cases it is very small [40]. The imaginary part of the eq. 2.3 can be safely neglected to arrive at an approximate solution for the voltage drop in the system. Taking the source voltage as the slack bus reference voltage , the $\overline{V_S}$ can be represented with just the magnitude $|V_S|$ or V_S. Eq. 2.3 can now be approximately rewritten as:

$$\Delta V \approx \left(\frac{RP + XQ}{V_S}\right)$$

To keep the analysis comparable for different distribution voltage levels, a per unit (p.u.) system is used. In p.u. system calculation, the slack or the source bus voltage is assumed to be 1 for simplicity. The voltage drop equation now becomes:

$$\Delta V \approx RP + XQ \tag{2.4}$$

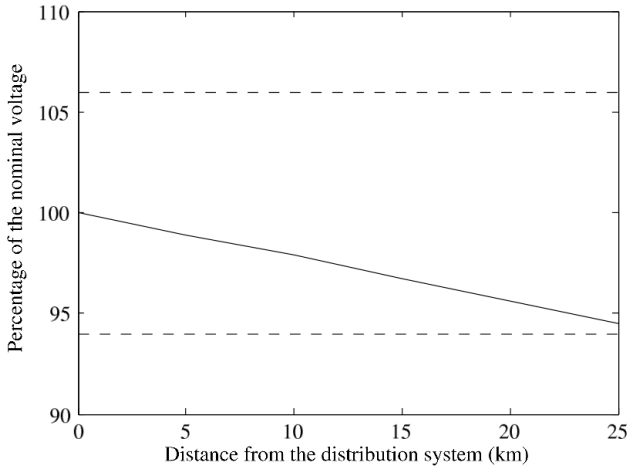

Figure 2.3: Voltage profile in a radial distribution system

Eq. 2.4 gives the voltage drop in a line with active and reactive power flow. It is very important to note that both active and reactive power will affect the voltage along a distribution line, i.e, both RP & XQ terms from eq. 2.4 affect the voltage profile in a line. This is not the case in a transmission line where only reactive power majorly affects the voltage profile. This difference mainly arises due to the low X/R ratios in distribution lines as compared to transmission lines. X/R ratios are also expressed in terms of network impedance angle ψ and it is defined as:

$$tan(\psi) = \frac{X}{R}$$

The higher the network impedance angle, the higher is the X/R ratio. Fig. 2.3 shows the voltage profile for the radial distribution line in fig. 2.2b. A resistance of 0.625 ohm/km and a reactance of 0.3125 ohm/km has been considered in the analysis by the author of [40]. The dotted lines represent a ±6 voltage limit. As it can be seen in the voltage profile from fig. 2.3, loading creates a considerable voltage reduction in the medium voltage distribution line. The same equation can be rearranged to determine the maximum load that can be connected at a particular distance so that the voltage limits are not violated. For systems with high R/X ratio and a low reactive power consumption by the load, the term 'XQ' can be neglected to determine the maximum load that can be connected at any distance. The equation in p.u can be derived as follows:

$$P_{Lmax} \approx \frac{V_S - V_R}{R_L * L} \tag{2.5}$$

The above equation represents the maximum load that can be connected at a distance for a unity power factor two bus system.

2.5. Voltage rise due to Distributed Generators

There is a steady increase to move towards decentralized generation of intermittent renewable energy to reduce the carbon footprint. CHP plants are being employed by industrial users to effectively use the waste heat from the plant and reduce energy consumption by injecting power back to the grid. These recent trends have changed the conventional flow of power in a distribution grid. To assess the impact on the voltage, a two bus system is considered with a reverse power flow as shown in the fig.2.4a.

The voltage at the grid is stronger than that at the generator. The voltage deviation equation for reverse power flow can be written as follows:

$$\overline{V_{GEN}} = \overline{V_S} + \left(\frac{P - jQ}{\overline{V_S}}\right) * (R + jX) \tag{2.6}$$

In the above equation, P represents P_G - P_L, Q represents $\pm Q_C$ $\pm Q_G$ - Q_L. Where P_G is the active power generated, P_L is the active power consumed by the load, Q_C is the reactive power generated by the compensator, Q_G is the generator reactive power and Q_L is the reactive power consumed by the load. Assuming genertor

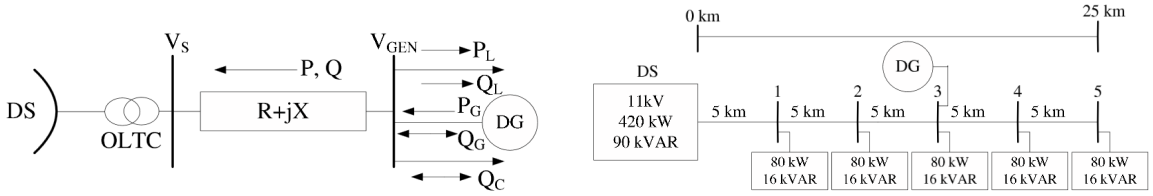

(a) (b)

Figure 2.4: (a) A typical two bus distribution system with DG connected (b) A radial distribution system with DG connected [40]

voltage (V_{GEN}) to be unity (in p.u.), and following the assumptions made in the section 2.4, the equation for voltage rise is written as follows:

$$V_{GEN} - V_S \approx \Delta V \approx RP + XQ \tag{2.7}$$

Consider the generator shown in the fig. 2.4b connected to the existing distribution system. Eq. 2.7 proves that the active power changes in the system will affect the voltage profile. As the generator is connected along the line, if the power generated is higher than the active power consumed by the feeder, then the point of common coupling (PCC) of the generator will increase its voltage to feed the excess power to the primary substation. If the generation from the generator is consumed locally, then the power flow is still from the primary substation as the load power is greater than the generated power. If there is an excessive power generation from the generator, this will result in reverse flow of active power in the line. ΔV is positive for Eq. 2.7, i.e., the voltage at the generator point is higher than that at the primary substation. This ΔV depends on the magnitude of power injection by the generator connected. Fig. 2.5a shows the voltage profile along the line when the connected DG is supplying a power of 240 kW. As the power supplied by the DG is less than the load consumption, there is still an active power flow from the substation. Fig. 2.5a shows the voltage profile along the line when the connected DG is supplying a power of 1 MW. The voltage rise goes beyond the critical limit leading to voltage violation in this case. Another major problem with this scenario is that the local control and protection of the generator might sense this over voltage and give a trip signal or reduce the active power output to the generator [55]. Reduction in output or complete disconnection is seriously detrimental to the green energy integration targets set by many countries.

For a two bus system, the maximum generation that can be connected to avoid voltage violation can be determined by rearranging the eq.2.7. For unity power factor systems, the maximum generation P_{Gmax} can be approximately given as follows:

$$P_{Gmax} \approx \frac{V_G - V_S}{R_L * L} \tag{2.8}$$

The value for $V_G - V_S$ is given by the DNO based on the statutory requirements. This equation gives an approximate relationship for the maximum generation that can be connected at a distance 'L' from the source/ substation.

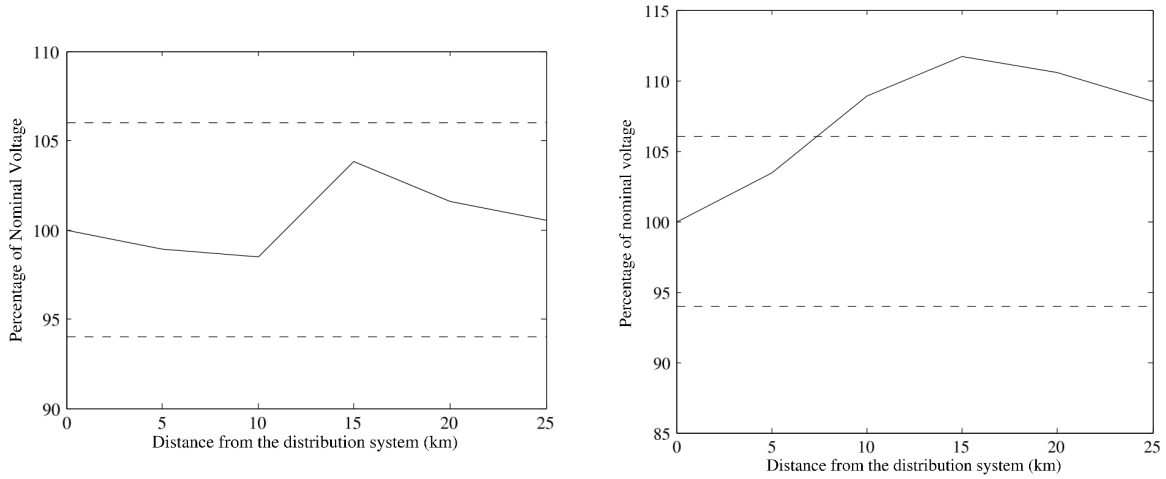

(a) (b)

Figure 2.5: (a) Voltage profile when P_G = 240 kW (b) Voltage profile when P_G = 1 MW [40]

2.6. Impact of line parameters on voltage profile

With increasing bi-directional flow of renewable energy, the distribution system will be playing an active role in the future power systems. Wind turbines are built in rural areas due to availability of high wind resource. Even the installation of rooftop PV panels are common in rural places due to less obstruction of sunlight. It is clear that a reverse power flow in a traditionally designed grid will cause voltage rise and affect the grid's performance. Understanding the grid parameters will predict up to what extent the integration can affect the grid's performance. It is important to understand the cause and the effect of the voltage rise to devise necessary compensation strategy. Fig. 2.6a shows the Thevenin equivalent of a wind farm connected to a voltage source via a network. The wind farm is connected to BUS A and the source is connected to BUS B via the network of impedance $Z_{eq}e^{j\psi}$. $Z_{eq}e^{j\psi}$ is the polar representation of the impedance, R + jX is the complex represenation of the impedance.

The network impedance angle, the short circuit power (S_k) and ratio (SCR) are written as follows:

$$tan(\psi) = \frac{X}{R}$$

$$S_k = \frac{V_S^2}{\sqrt{R^2 + X^2}}$$

$$SCR = \frac{S_k}{P_n}$$

The short circuit power gives an idea of how high or low is the impedance in the line. The voltage along the line will depend on power injection or consumption for high impedance lines. The network impendance angle determines the type of the line. Transmission lines with higher X/R ratio will have a higher angle. Rural grids generally have a lower X/R ratio (low network impedance angle ψ) and in most cases a very low short circuit power ratio. Distribution line with low short circuit powers are considered weak due to the effect of active and reactive power flow on the voltage in and around the point of connection.

Fig. 2.6b depicts the impact on voltage due to the rated active power injection P_n as a function of SCR and network impedance angle ψ. Typically, wind farms connected to rural distribution grids will have a lower short circuit ratio < 25 and a network impedance angle in the range of 25^o and 55^o due to its resistive nature [70]. It can be clearly seen from the graph that the active power injection has a significant effect on the voltage as observed by the 'ΔV' parameter for rural distribution lines compared to a transmission lines. With growing distributed energy technology connected to the distribution grid, the need for a proper voltage regulation strategy is becoming critical to enable smooth operation without violating the voltage limits of the line.

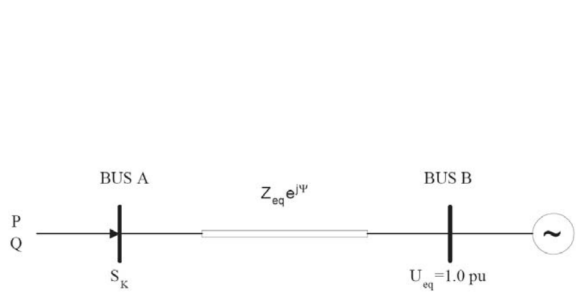

(a)

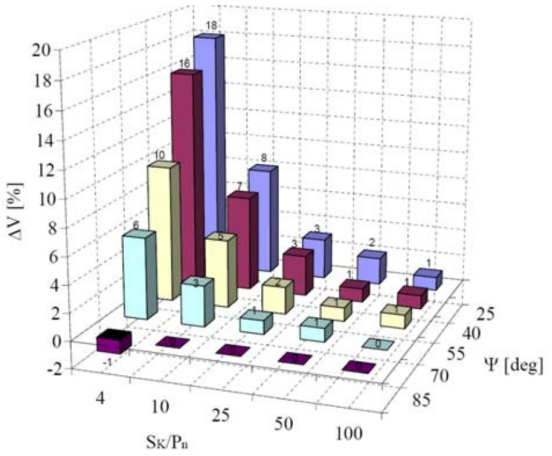

(b)

Figure 2.6: (a) A thevenin equivalent circuit for a wind farm (Bus A) connected to a grid (Bus B) (b) Voltage variation due to injected power P_n [70]

2.7. Voltage regulation strategies

Voltage regulation is of less importance in urban areas due to short distribution lines. The main limiting factor for urban distribution lines are the thermal ratings of the cable and the components connected in the system. However, rural lines are very long and in many cases voltage regulation becomes a bottleneck instead of the thermal capacity of the line. With increased unpredictability during generation in the distribution line, DSOs must implement voltage regulation strategies to keep the voltage under regulation limits. The Regulation methodologies that are used in the distribution grid are outlined in the following sections.

2.8. Series voltage regulation

Series voltage regulation in a distribution system is performed by either one of the methods discussed as follows:

1. By dynamically or manually changing the voltage set-point of the distribution line
2. By injecting a voltage in the line in-phase or out-of-phase at an optimal location in the line
3. By connecting a passive element in series to change the impedance of the line

Due to lack of controllability in the third method, the first two methodologies are the most preferred type of series voltage regulation in a medium voltage distribution system.

Voltage set-points in the line are varied by using the in-built on-load tap-changer (OLTC) of the HV/MV transformer to set a different voltage at the beginning of the line based on the load conditions. In some cases, this voltage regulating function is given to a voltage regulator which is placed at an optimal place chosen along the line, and changes the voltage based on the grid conditions. The voltage function is varied such that eq. 2.9 is always satisfied to ensure satisfactory operation. V_{Snew} indicates the new voltage set-point at the source using OLTC in the substation or the set-point where the LVR is placed.

$$V_{Smin} < V_{Snew} + \Delta V < V_{Smax} \tag{2.9}$$

2.8.1. OLTC in HV/MV substation

The most common type of series voltage regulation used in medium voltage distribution grid is controlling the HV/MV voltage using an OLTC. HV/MV transformers will have a voltage drop based on the short circuit impedance, transformer load losses and the PF of the system [54]. The Voltage drop in a transformer system is given by the following equation[56]:

$$\Delta V_{transformer} = e_r cos(\phi) \pm e_x sin(\phi)$$

e_r & e_x are the per unit resistance and reactance drop respectively, and ϕ is the power factor angle. According to the IEC 60076-5 standard, the minimum impedance of the transformer, z_t, is 12.5% for transformers with a nominal power capacity ranging from 63 - 100 MVA. This will have a direct impact on the voltage drop during loaded conditions. Usually, the last controllable OLTC is present in a HV/MV transformer to offset this voltage drop at any given time and maintain a steady MV voltage. As there are only off-load tap changers present in MV/LV transformers, maintaining an optimal voltage is necessary in the MV grid. If the the load drop compensation (LDC) is enabled, the voltage set points of the bus are changed so that the voltage range is not violated for the loads connected to the distribution line. This is shown in the fig. 2.7 below. OLTC changes the voltage set point based on the load profile present at that moment to maintain the voltage within prescribed limits.

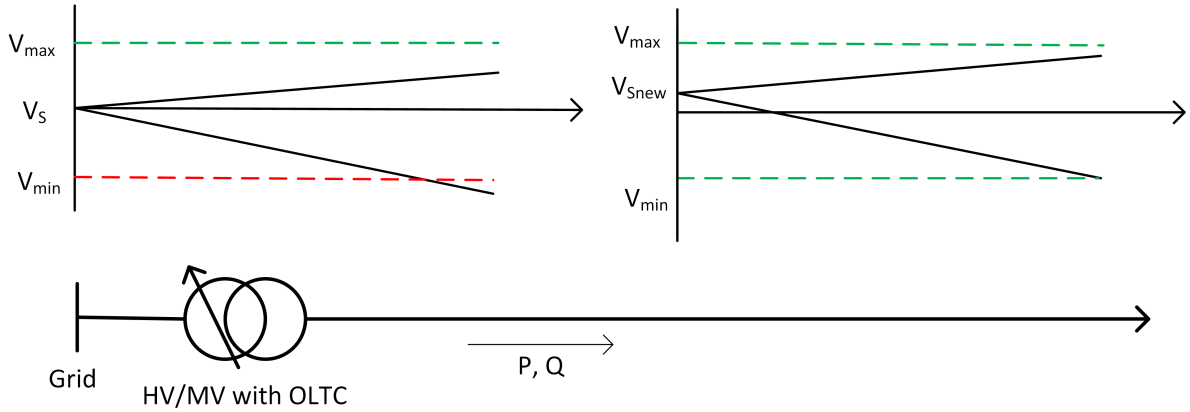

Figure 2.7: Voltage set-point adjustment by HV/MV transformer OLTC in a distribution line

The main challenge for this type of control is that there are multiple feeders connected to the same MV busbar. In practical scenarios, most of the feeders will not have the same load and generation profile. Hence, maintaining the voltage within the range for all the feeders with a single OLTC at the HV/ MV substation becomes more complicated[17]. The authors of [21] & [52] discusses a control algorithm which utilizes substation parameters along with the peripheral unit's information to determine the appropriate voltage set point to avoid any voltage violation. These algorithms also require telecommunication functions and in some cases, they are required to control the generator active and reactive power.

2.8.2. Line voltage regulators

Line Voltage Regulator (LVR) or Series Voltage Regulator (SVR) systems are more commonly used in a distribution system to have individual control over the feeder [37]. These systems effectively decouple the medium voltage line and reset the voltage bandwidth of the line. By controlling the individual feeder, other feeders are not affected. LVRs can be placed in a specific feeder where there are voltage violations due to different load and generation profiles. Fig. 2.8 shows the schematic of a LVR. The LVR is able to move the voltage set-point while the voltage is maintained constant at the HV/MV substation.

2.8.3. Dynamic voltage regulator

A dynamic voltage regulator (DVR) is similar to a LVR with respect to the basic functionality. Fig.2.9 shows the typical layout of a DVR system. It has an intermediate power electronics based AC-DC to DC- AC conversion. The regulated AC from the DC-AC inverter is fed into the injecting transformer based on the line conditions. Due to the presence of power electronics based control, the DVR can typically respond very quickly[69]. DVRs are mainly used in distribution grids to protect critical loads from all kinds of disturbances except for complete system outages. DVRs are used to solve more critical problems such as temporary voltage sag/swells, imbalances and more advanced issues such as flicker and harmonics. Hence, using DVRs for long-duration supply voltage variation might not be economical due to high investment costs involved because of the power electronic based converters.

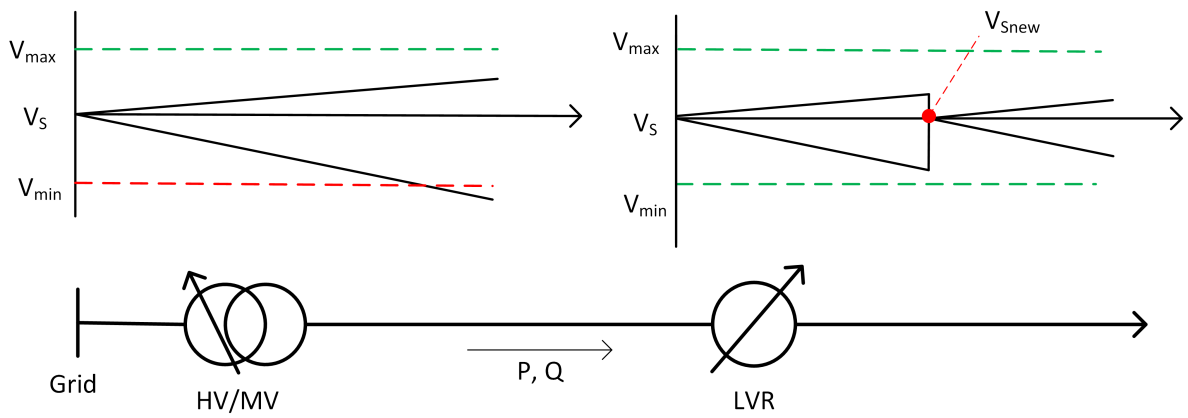

Figure 2.8: Effect of series voltage injection along the line by a LVR in a distribution line

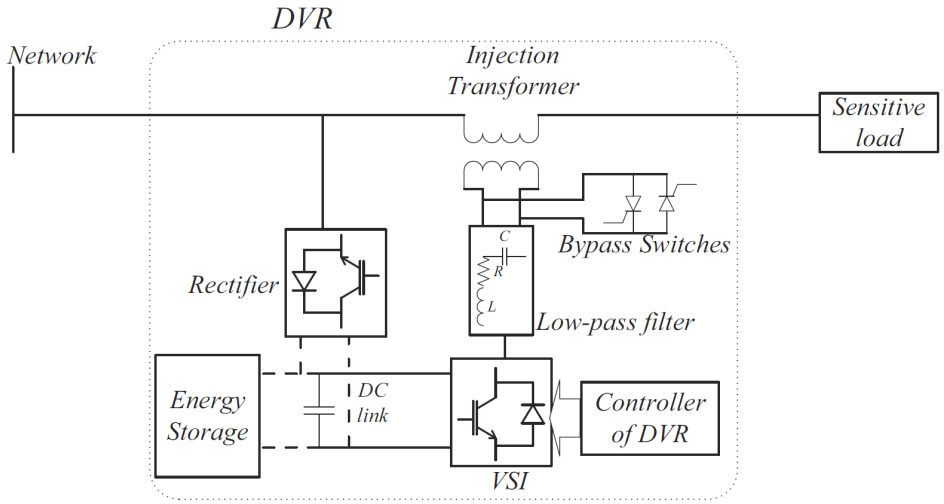

Figure 2.9: General structure of a dynamic voltage restorer [69]

2.9. Shunt voltage regulation

This method uses a reactive element, active or passive, in shunt to import or export reactive power to achieve voltage regulation in the grid. The voltage rise due to the generator is given by the equation below and the reactive power parameter that is controlled to perform voltage regulation is expressed in the equation.

$$V_{GEN} - V_S \approx RP + X\mathbf{Q}$$

With the inclusion of reactive power control, the parameter Q, is a combination of reactive power consumed by the line, load and shunt regulation elements. The effective Q is given as follows:

$$Q = Q_{line} + Q_{load} \pm Q_{shunt}$$

Q_{line} is the reactive power consumed by the line, Q_{load} is the reactive power consumed by the load and Q_{shunt} is the reactive power consumed or generated by the shunt regulation element. By effectively controlling the Q_{shunt}, the XQ factor in the voltage difference equation can be made negative to reduce the impact of the voltage variation.

Recently, DGs are being used extensively to produce reactive power to control the voltage at the point of common coupling (PCC)[67]. Fig. 2.10 shows the field demonstration from a US medium voltage distribution rural line [45]. Photovoltaic (PV) plants connected in the line created voltage rise during lightly loaded condition, and the inverter was operated at a lagging power factor of 0.95 to reduce the impact on the voltage

rise [45]. Reactive power compensation shows clear benefit by reducing the voltage rise by the local control. The sub-transmission and transmission system provides the bulk reactive power to compensate for the 0.95 lagging operation of the PV system. It was noted that during the demonstration the capacitor banks situated in the line did not provide reactive power for the PV system as they are switched based on the voltage level in the system, which is under control when the PV system is injecting the reactive power[45]. This stresses the transmission system and produces more losses. Hence the utility should take measures so that the voltage reduction is implemented in an economical way with minimal losses.

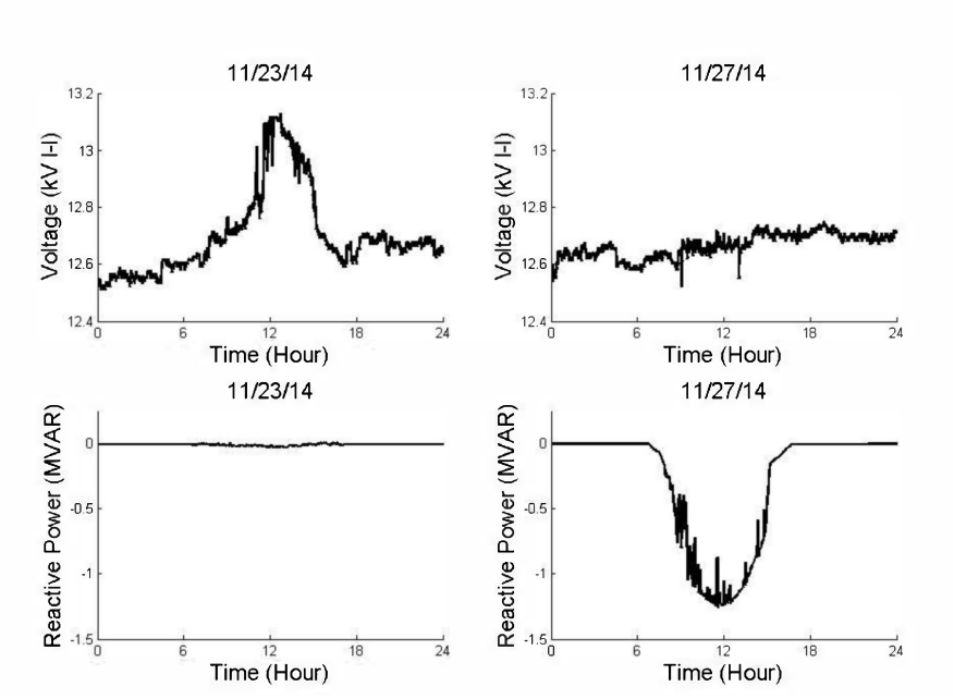

Figure 2.10: Comparison of PV system voltage at PCC without (left) and with (right) reactive power compensation[45]

2.9.1. Traditional shunt compensation technologies

Fixed or mechanically switched shunt capacitors and inductors have been in use for a long time in power systems. Shunt capacitors are connected to increase the voltage at the point of connection and shunt reactors are connected to decrease the voltage at the point of connection [66]. Fixed shunt capacitors and reactors possess the inherent problem of over-compensation or under-compensation when there are fluctuating loads and generations in the grid [22].

Fig.2.11 shows the effect of voltage reduction from the sending end voltage due to capacitor compensation at the load. This case considers the receiving end voltage to be constant, therefore, causing a reduction in the sending end voltage. But in practical scenarios, the sending end voltage is from a substation where the voltage is fixed. The net effect will be a voltage increase in the receiving end of the line.

Synchronous condensers have been employed in electrical network for many years to provide reactive power support. Synchronous condensers are synchronous machines without a prime mover. They are installed in the system to provide the voltage support through reactive power injection and increase the short circuit capacity of the system[38]. Due to the inherent inertia possessed in the synchronous generator, modern synchronous condensers are increasingly used to provide the inertia support to the modern full converter wind turbines [43]. The main limiting factors of synchronous condensers are the cost, space requirements and the maintenance required due to mechanical components compared to the modern day Flexible AC Transmission system (FACTS) devices.

2.9.2. FACTS based shunt compensation technologies

FACTS technology for reactive power compensation are used extensively to suppress voltage fluctuations in the distribution grids [35]. Static VAr Compensators (SVCs) and Synchronous Static Compensators (STAT-

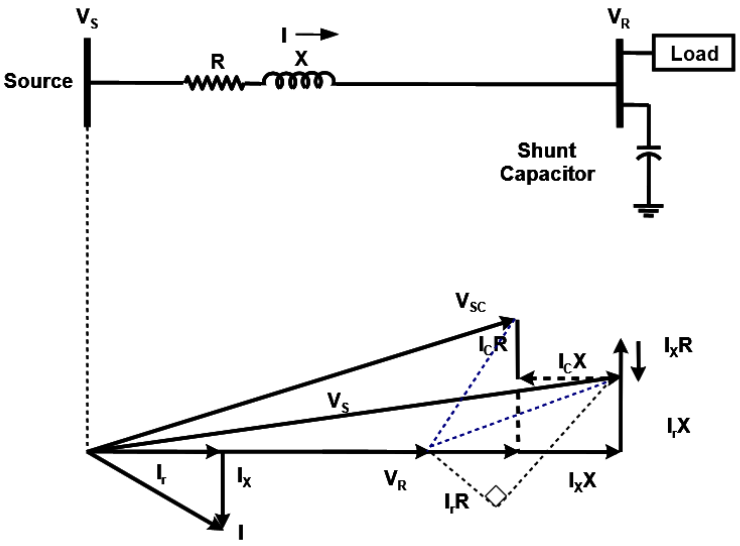

Figure 2.11: Phasor diagram of the reduction in sending end voltage due to shunt compensation [20]

COMs) are the main shunt compensation technologies used with static switches.

The two types of SVCs that can be realized are Fixed Capacitor - Thyristor Controlled Reactor (FC-TCR) and Thyristor Switched Capacitor - Thyristor Controlled Reactor (TSC-TCR)[51].

Fig. 2.12a shows the TSC- TCR combination which has more flexibility and smaller rating of the reactor compared to FC-TCR. SVCs act as a controlled shunt susceptance in the line. The controller varies the effective susceptance of the SVCs to maintain the voltage by providing the necessary reactive power to the system. Due to the presence of static switches and lack of any rotating machines, SVCs have a very small inertia and are capable of reacting quickly for any voltage variations. SVCs can typically react within 2-3 cycles for any voltage variation, thereby, increasing the stability of the system. The high-pass and tuned filters can also supply reactive power at fundamental frequencies and act as a filter for higher order harmonics generated by the system.

A simple layout of a STATCOM, a Voltage Source Converter (VSC) connected to the grid is shown in the fig. 2.12b. VSC acts like a controllable reactor and capacitor by injecting the appropriate reactive current in to the grid. VSCs requires self-commutated switches to perform the operation. The main advantages of a STATCOM compared to a SVC are the faster response to disturbances and compactness due to less bulky reactive elements[74].

The modern day DGs such as wind and PV systems are predominantly using a full power electronic converter to interface with the grid. This has motivated the DSOs from several countries to demand reactive power control from the DGs. Power electronic converters interfacing with the grid creates an opportunity to provide reactive power support at a modest additional cost [67]. The increase in cost is mainly due to the over sizing of the components in the converter to provide reactive power support.

2.10. Conductor upgradation

Upgrading the conductor with a higher cross-section not only enables the cable to carry higher current but it also has a positive effect on the voltage regulation. Resistance in a conductor decreases inversely with the cross-sectional area of the conductor but the reduction in inductance is less because it also depends on the conductor spacing. Higher reduction in R with smaller reduction in inductance reduces the R/X ratio of the conductor with higher cross-sectional area. Assuming the reactive power and the active power to be constant in the system, the long duration voltage variation can be given as follows:

$$\Delta V \propto R$$

With a minimal change in inductance and higher change in resistance, the above equation shows that the voltage rise or drop directly depends on the resistance of the conductor. Upgrading the conductor increases

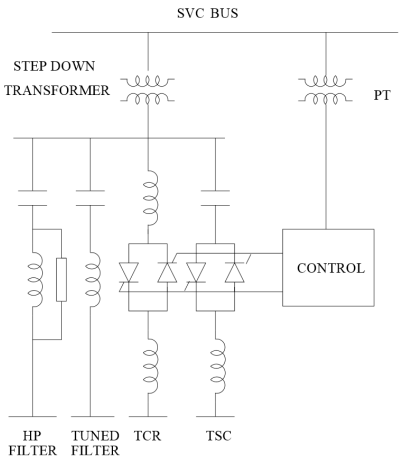

(a)

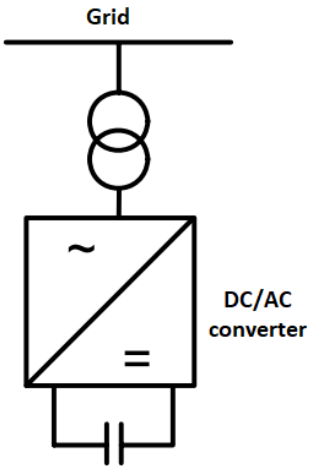

(b)

Figure 2.12: (a) A Typical layout diagram of a SVC (TCR-TSC) [74] (b) A typical layout diagram of a STATCOM (VSC) [42]

the power capacity, thereby allowing the DSO to connect more generators and loads in the system. DSOs generally do not consider upgrading the conductor in order to alleviate the voltage variation issues [40] as it is a tedious and expensive task for the DSOs. A typical 10kV, 100 mm^2 cable can roughly cost up to **30,000 USD per km**[71]. The final cost can vary from country to country but it can still be very expensive for long lines. With the recent developments in voltage regulation technologies, DSOs should first evaluate the possibility of using a voltage regulation technology which is much more easy to install and an economical option in most cases.

2.11. Future challenges in the distribution grids

There have been many recent developments in generators and consumption equipment for distribution grids which was not foreseen in the past. Plug-in hybrid vehicles (PHEVs), plug-in vehicles (PEVs), heat pumps, etc., have introduced high power consumption for a short period of time. The electric vehicles such as cars and buses are on the rise in Europe and in other parts of the world [14], [28]. EV chargers are placed to charge the electric vehicles in residential and public places. These chargers can stress the distribution grid in terms of power congestion and voltage drop in both MV and LV distribution grids [39]. Fig. 2.13 shows the power consumption of an average residential load in USA with power from EV charging profile superimposed in dotted lines [33]. This study only considers a EV charger rated at 1.6 kW, while there are already EV fast chargers from 6.6 kW to 120 kW commercially available. If not properly designed, high power demand for a short period of time will create voltage dips in the system. A vehicle-to-grid (V2G) concept of using EVs battery for peak shaving operations can also contribute to reverse power flow in the future apart from the renewable energy in-feed.

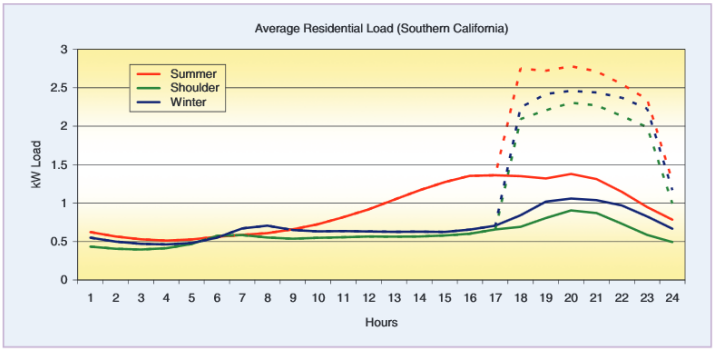

Figure 2.13: Typical load profile of residential load with EV charging profile superimposed as dotted lines [33]

3

Impact of Different Voltage Regulation Strategies on Grid Capacity

Every country has tailored their voltage regulation standards for optimal operation of the network pertaining to their grid conditions. This study focuses on the European grid where the DSOs are expected to maintain the long duration voltage variation within ±10% for the MV grids. According to EN 50160, the voltage in the MV and LV grid should be within ±10%. In order to maintain the LV grid within ±10%, the voltage deviation allowed is divided as shown in the fig. 3.1. In order to maintain the LV grid within the regulation limits, DSOs exercise more stringent limits to MV grids to avoid the cascading effect on voltage drop from MV to LV grid [53]. In this study the allowable voltage deviation in the MV grid is set to ±4%. In long lines with dispersed load and generation, these limits can be easily violated leading to unreliable supply for the customers. A quantitative technical benefit analysis is conducted to determine the most effective active solution for MV distribution lines with DGs.

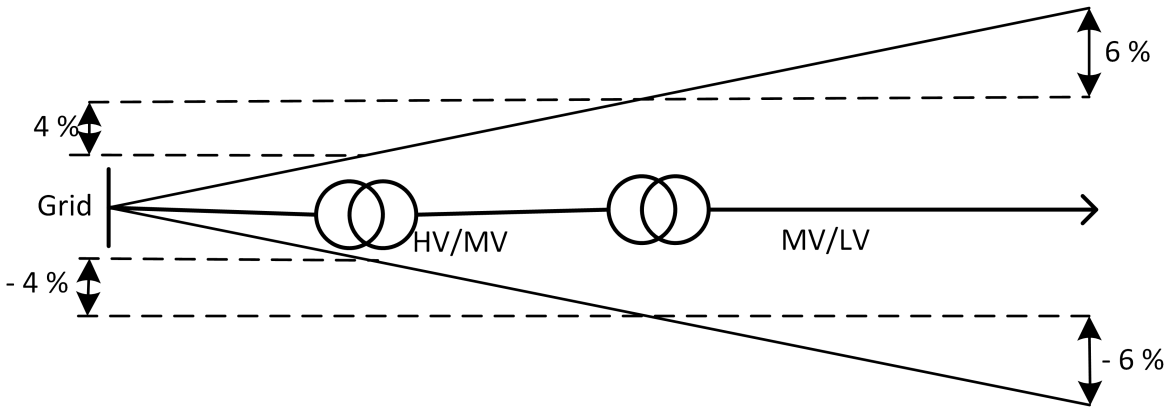

Figure 3.1: Voltage variation limits (%) for the MV and LV grid considered in this study

3.1. Technical benefit analysis

The previous chapter discussed various possible regulation methods used by the utilities to restrict the voltage violation. From an economic standpoint, the impact of voltage regulation methodologies such as series and shunt regulation should first be studied to avoid a complete replacement of the existing conductor [67]. [12] discusses algorithm to assess the hosting capacity of a LV grid with DGs. [31]evaluates the effect of different voltage regulation methods on hosting capacity for LV distribution grid for line lengths less than 3 KM. In LV grids, due to high R/X ratio, the influence of 'X' is much less compared to medium voltage grids. In this study, the focus is given on evaluating the effect on grid capacity by different voltage regulation methods for medium voltage distribution grid.

3.2. System description

Urban networks have underground cables due to short lines and rural networks are constructed with overhead structures due to long lines [23]. As discussed in sec. 2.3, radial grids are predominantly used in long distance feeders leading to voltage regulation problems. A radial system with a equally spaced loads and generators connected to the end of the line is considered for the study. Fig. 3.2 shows the single line diagram of the system considered. S_L is the load which is modeled as a constant power block with a power factor of 0.95. S_{gen} is the generator which injects only active power to the system (cos (ϕ) = 1). The MV side voltage from the HV/MV substation is considered to operate and maintain a constant 20kV (1 pu). As discussed previously, in the sec. 2.8, in the case of multiple feeders with different load and generation profiles, finding one optimal point for the MV becomes more complex and challenging. Table 3.1 shows the overhead line parameters taken from the IEC standards for the bare stranded conductors. The ambient temperature is considered to be 20 °C and the temperature of the aluminium conductor is considered to be at 100 °C. A rated power of 10 MVA is considered for the line. The current carrying capacity is calculated as per the ideal conditions considered in IEC 61597 standard. The inductive reactance value given in the IEC 61597 is due to the magnetic flux within a 0.3m radius of the conductor. Considering the geometric mean distance in a MV overhead line to be small, the inductive reactance value from the IEC is taken directly for calculations. This also provides a basis for comparison while studying the effect of conductor upgradation. The effect of capacitance can be neglected in MV lines with network voltage less than 69 kV and for line lengths less than 80 km[30]. The short medium voltage distribution line model is used in the study. The MV line is modeled as a series impedance with resistance and inductance.

Table 3.1: Type A1 conductor parameters used for the study taken from IEC 61597

Code number	Stranding	Diameter (mm)	CCC (A)	Resistance(Ω/km)	Inductive reactance (Ω/km)
A1_40	7	8.09	293	0.7165	0.2917

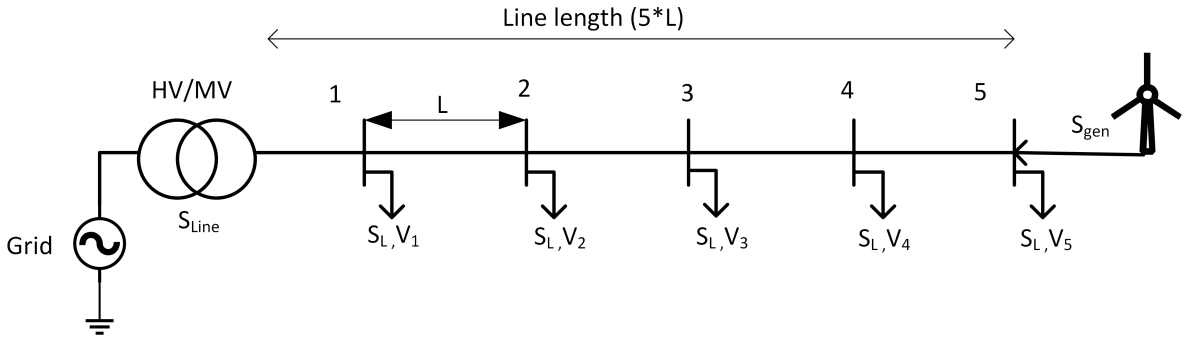

Figure 3.2: Single line diagram of the 20kV, 10 MVA distribution system under study

3.3. Algorithm for evaluation

An algorithm is devised to determine the line power at which primary line limits are violated for different line lengths. The primary technical line limits considered in this study are the admissible line capacity and voltage variation in the line. The primary limiting factor for shorter line lengths is the rated power capacity of the conductor and components present in the line. The primary limiting factor for longer line lengths is the violation of voltage limits. The two scenarios that leads to extreme voltage rise/ drop from the feeder source along the line are:

- Maximum voltage drop - no generation and only load consumption
- Maximum voltage rise - only generation and no load consumption

A brief description of the limits are discussed below:

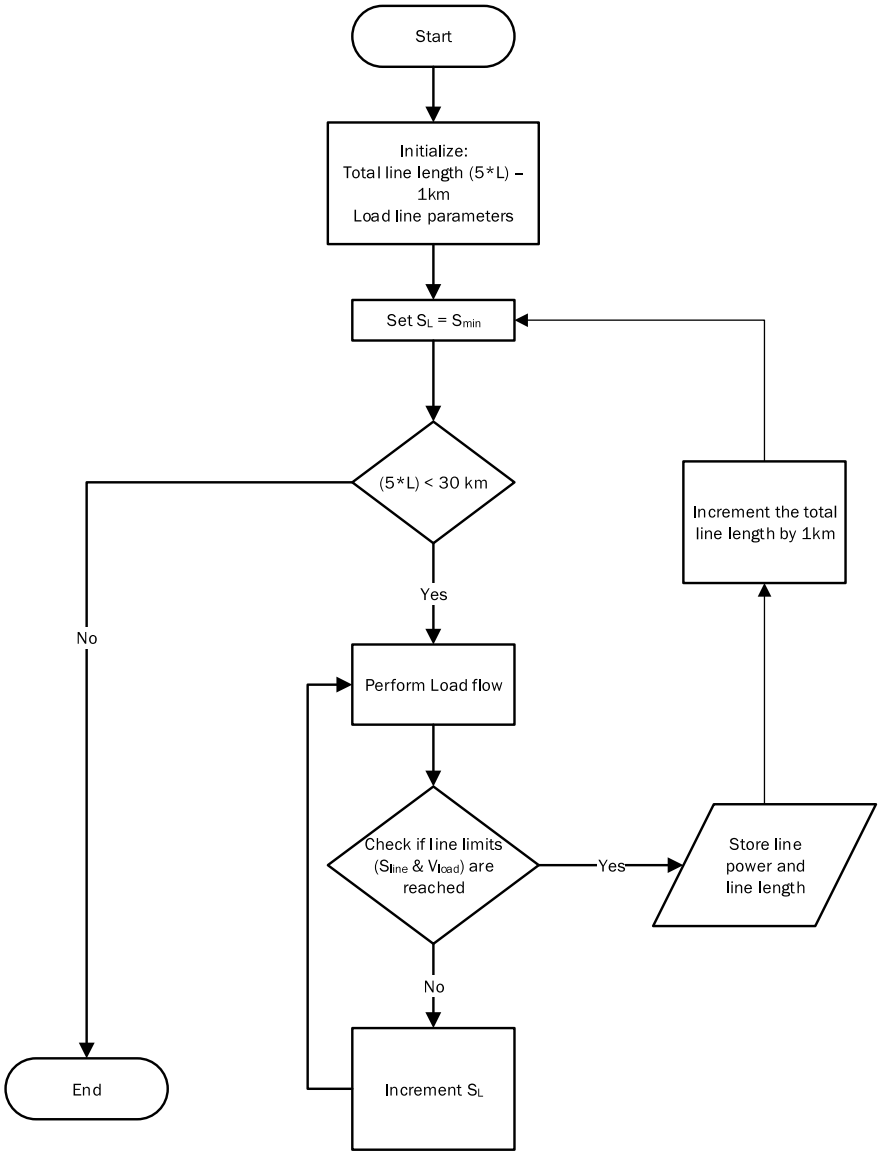

Figure 3.3: Algorithm used to assess the grid capacity with primary line limits

Thermal capacity of the line:

The thermal capacity of a line depends on various parameters such as ambient temperature, wind conditions, condition of the conductor, conductor type and ground clearance [6]. The ampacity of the line varies based on the above mentioned parameters. To keep the study general, nominal power of the line is considered as the thermal constraint. S_{line} should always be less than or equal to 1 pu (10 MVA).

Steady state voltage variation:

According to EN50160[5], a steady state voltage variation of ±10% is allowed in a MV grid. As any variations in an MV grid directly affects the LV grid, only ±4% is allowed in the MV grid. The voltage in the line is allowed to vary only between 0.96 pu to 1.04 pu.

As the system considered is a radial grid topology, the first voltage violation will occur at the end of the line. The two parameters that are checked for violations in each iteration are the line power and the voltage at all load and generation points.

Fig.3.3 shows the algorithm used for the evaluation. The algorithm starts with initializing the line length as 1 km and setting all the load and generation to zero. The line length is now fixed and the power of the load/ generator is increased in steps for the respective scenario. For each increment of the power, load flow is executed and the parameters are extracted from the model, and checked for primary line violations. Once any of the line limits are violated, the corresponding line power and the line lengths are stored. The line power at which any of the limits are violated is the line capacity of the grid. The final graph is plotted against the line capacity and line length to understand the effect of voltage violation in long distribution lines.

The same algorithm is executed with a shunt and series voltage regulation strategy. Line capacity is obtained with respect to the line lengths and the percentage increase in the grid capacity is presented. In each section, a load and a generation scenario is considered and studied in detail.

3.4. No regulation

3.4.1. Load scenario

In this case, it is assumed that there is only load consumption in the grid without any generation. Fig.3.4 shows the line diagram of the system without any voltage compensation. Fig. 3.5 shows the grid capacity as a function of line length with the primary line limits. It can be seen that for the initial 3 km, the primary line limitation is the thermal or power capacity of the line. As the line length gets higher, the voltage deviation of - 4% is reached at the end of the line before the full power capacity is reached. The reduction in line capacity due to voltage limit violation is non-linear with the line length. This leads to large reduction in line capacity for long lines.

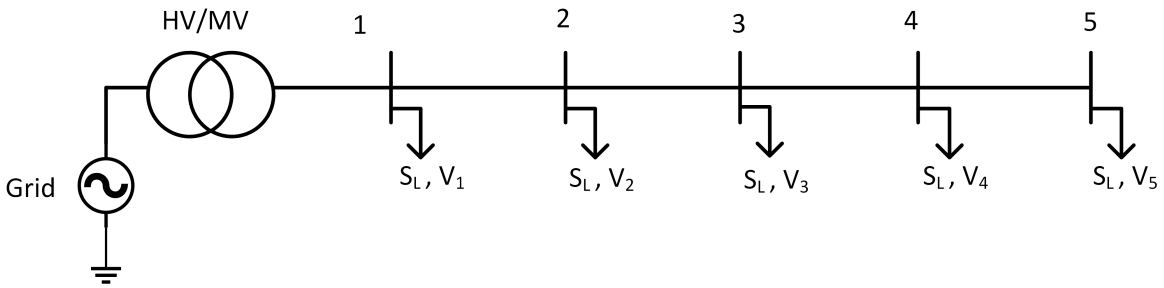

Figure 3.4: Single line diagram of the system with no regulation for load scenario

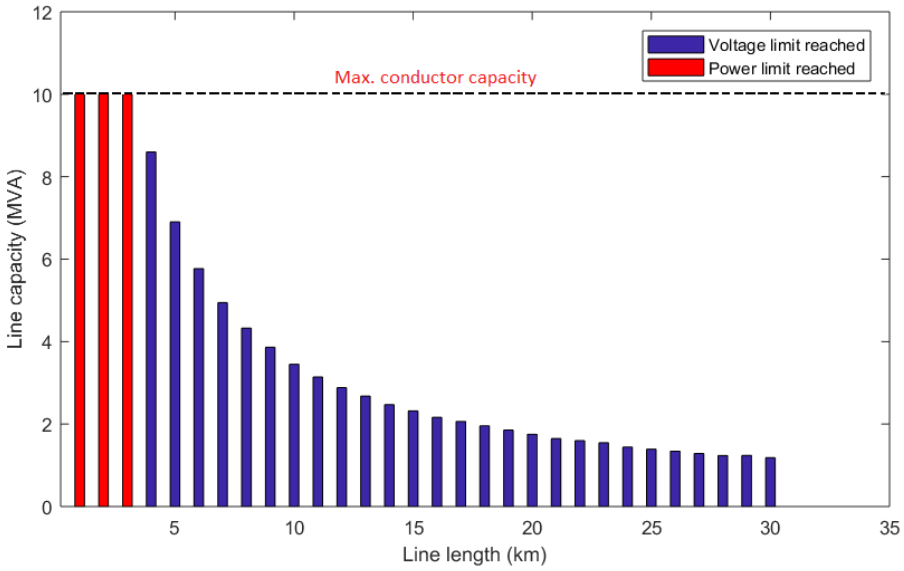

Figure 3.5: Line capacity vs Line length for the load scenario without any regulation

3.4.2. Generation scenario

There is only generation of power due to distributed generators and no load consumption is considered in this case to assess the power capacity reduction with the voltage rise of the system due to reverse active power flow. Fig.3.6 shows the line diagram of the system considered for this scenario. Fig. 3.7 shows the restriction of the line power as function of line length with the primary line limits included in the algorithm. The primary line limitation with thermal limits is reached in the initial 2 km of the line as indicated in the fig. 3.7 with a red legend. The main difference between this scenario and previous load scenario arises due to the amount of power that flows through each section of the line. In the load scenario, as the loads are equally spaced, the total power is reduced by a factor of the load power in each section leading to lesser power in the subsequent section of the line. This effect leads to a less severe voltage drop compared to the voltage rise in the generation scenario, where all of the power generated flows through all the sections of the line. This effect leads to quicker voltage rise violation, thereby, restricting the line capacity that can be supplied through the grid.

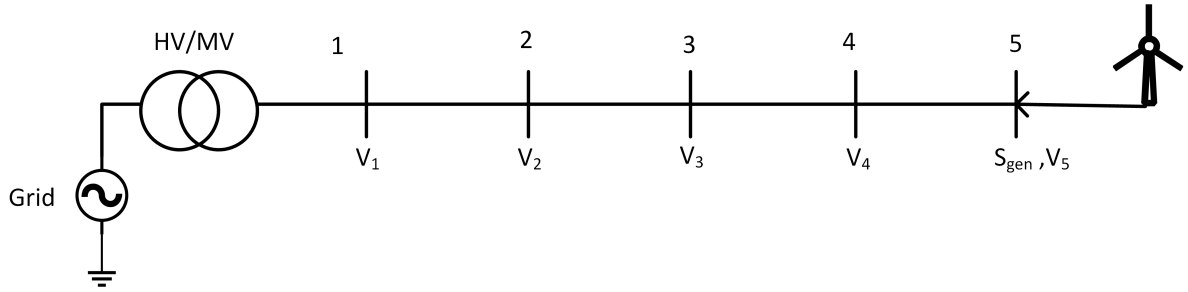

Figure 3.6: Single line diagram of the system with no regulation for generation scenario

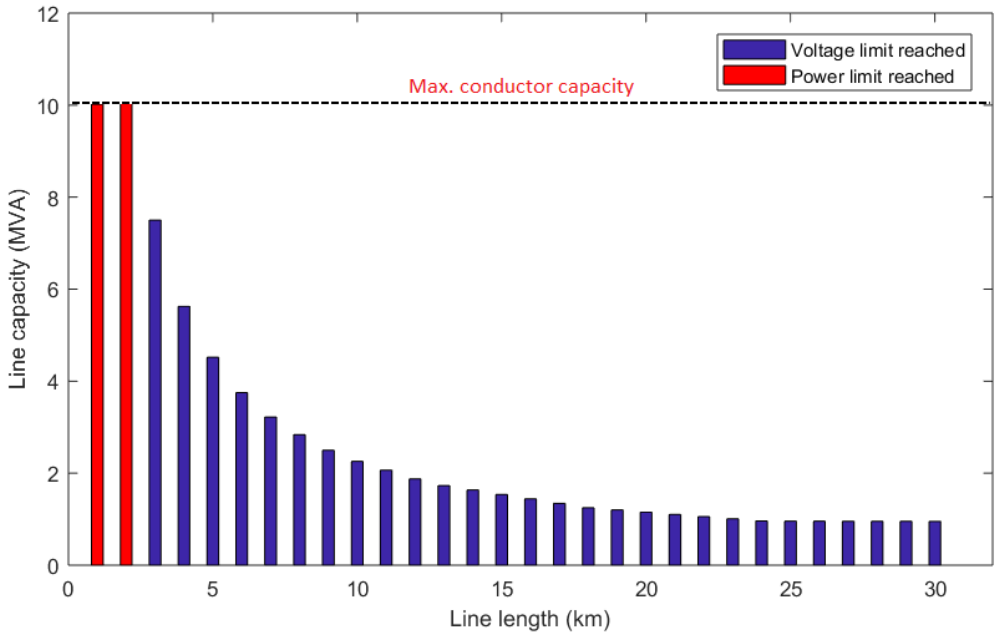

Figure 3.7: Line capacity vs Line length for the generation scenario without any regulation

3.5. Shunt voltage regulation

Reactive power based shunt compensation is studied in detail in this section. Section 2.9 elaborated various shunt compensation technologies that are being actively used by the utilities to control the voltage. As it was seen in the previous section, voltage limit becomes a serious bottleneck that can hinder the DSOs to completely utilize the grid capacity. Fig. 3.8 shows the shunt compensator connected to all the load and generation center. The shunt compensator block is a traditional or FACTS based technology and it is used to provide the reactive power based on the requirements. Transient performance of the shunt compensation device will not affect the results as only the steady state long duration voltage dip/ rise is of particular interest.

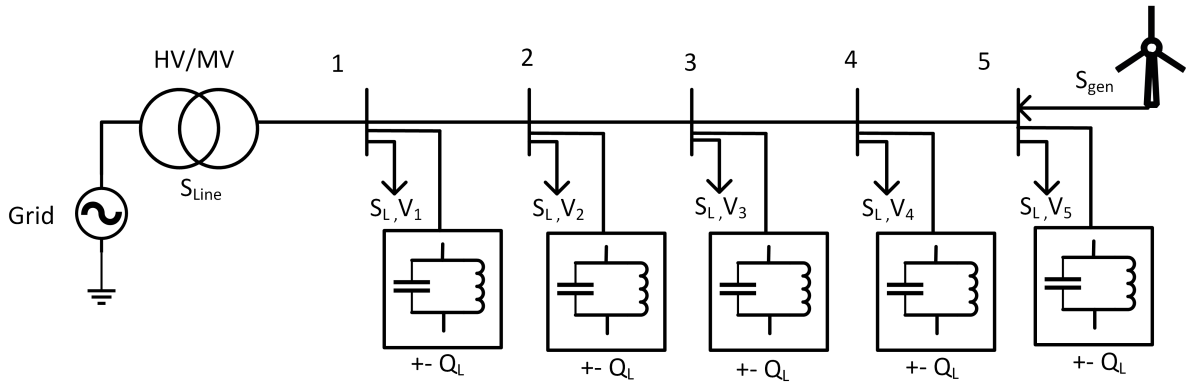

Figure 3.8: Single line diagram of a 20kV, 10 MVA distribution system under study with shunt compensation

3.5.1. Load scenario

Only loads are connected to the grid and no distributed generation is considered in this scenario. The shunt compensation effectively compensates for the lagging power factor load by providing capacitive power. This increases the voltage at the load point. Also the provision of reactive power locally reduces the reactive current from the grid. Thereby the $I^2 * R$ losses are reduced in the system. Shunt compensation provides an effective solution for the voltage regulation and decreasing losses in the grid. It is assumed in this case that the capacitive power is provided by one of the shunt compensation technologies to completely offset the lagging power produced by the inductive load. It can be argued that the further increase in capacitive power can increase the voltage at the load points, thereby increasing the grid capacity. Excess capacitive power injection can lead to the over-sizing of the equipment and increased losses in the grid. Fig.3.9 shows that the additional power that can be utilized in the grid when compared to the no compensation scenario. The additional power added is due to the voltage regulation capabilities of the capacitive compensation by delaying the voltage limit violation. Fig. 3.10 shows the percentage increase in power compared to the base power. It can be clearly seen that the positive effect of adding a shunt compensation for load case becomes less prominent with distance. Shunt compensation in this scenario is able to add 6.7% of base power at 3 km. The effectiveness of shunt regulator on voltage regulation decreases with the increasing distance.

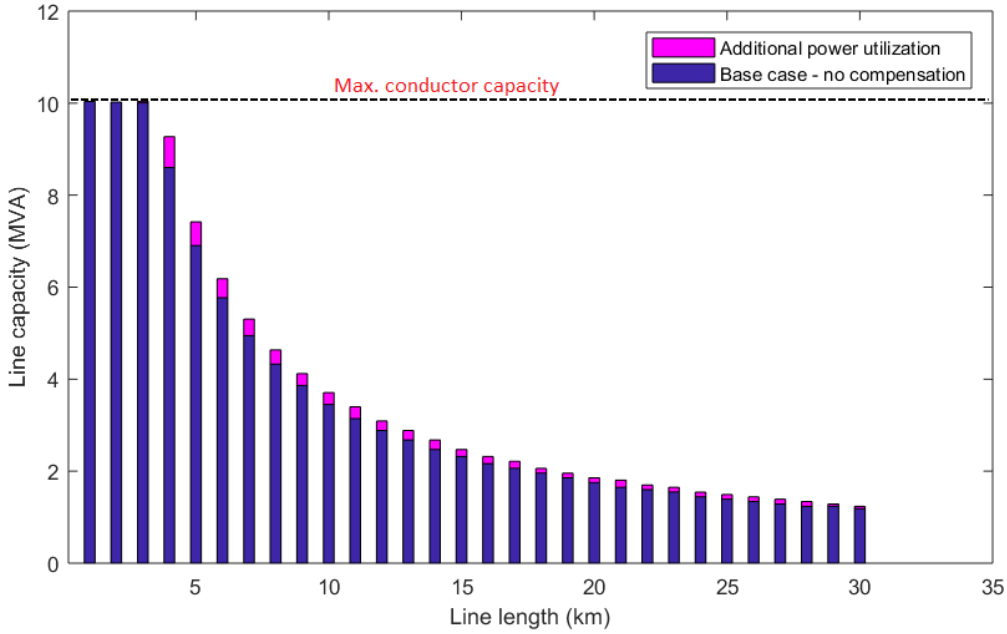

Figure 3.9: Line capacity vs Line length for the load scenario with shunt compensation

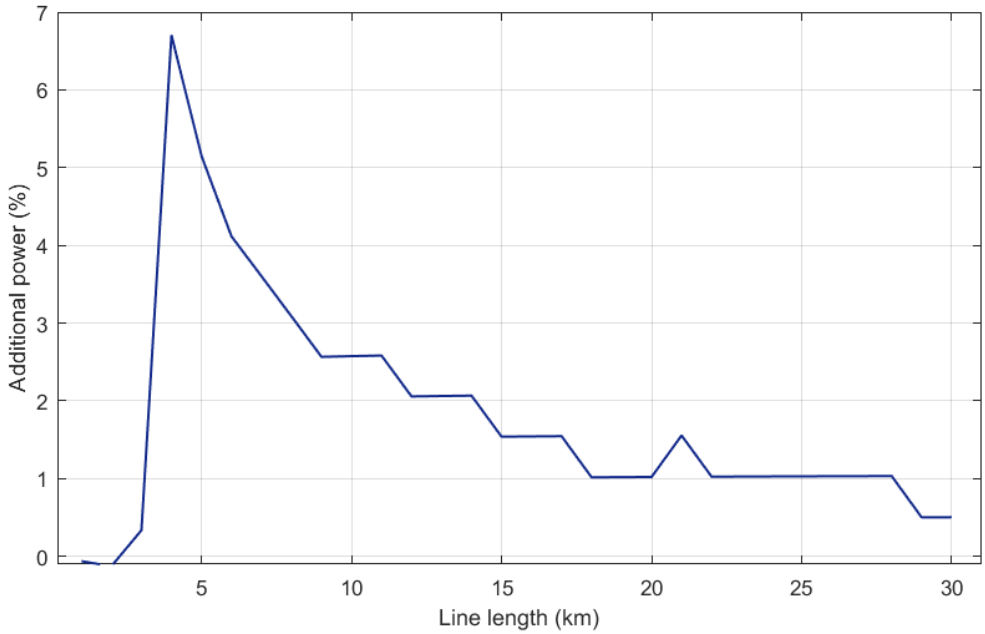

Figure 3.10: Percentage increase in the line capacity as a function of line length for the load scenario with shunt compensation

3.5.2. Generation scenario

As per the BDEW technical guideline for MV DG connected to the German grid, the DGs should be able to operate from 0.95 lagging to 0.95 leading power factor to provide voltage support at minimal additional cost[67] [50]. This requirement varies from country to country. The shunt compensation on bus 5 with the generator is made to operate at 0.95 power factor to reduce the voltage rise at the generator location. Due to voltage rise caused by the generation in MV grids, the associated shunt compensation should operate at a lagging power factor to decrease the impact on voltage rise. However, this reactive power should be supplied by a capacitor bank or by the distribution grid which increases the losses in the system to regulate the voltage.

The shunt compensator is always made to operate at 0.95 lagging power factor to evaluate the best case scenario. Fig. 3.11 shows the additional power capacity due to voltage support by the shunt compensation. As noted in the previous case, the effectiveness of a shunt compensation decreases quickly with distance. Shunt compensation is able to add up to 16.85% of the base power at 3 km distance from the substation. At 30 km it has minimal or no impact on the system performance as shown in fig. 3.12. This is mainly due to the fact that at longer distances, the drop due to 'RP' component is much higher than the XQ component. The XQ component has little impact to reduce the voltage rise. Voltage regulation by shunt compensation technique to increase the grid capacity is effective only for short distribution lines.

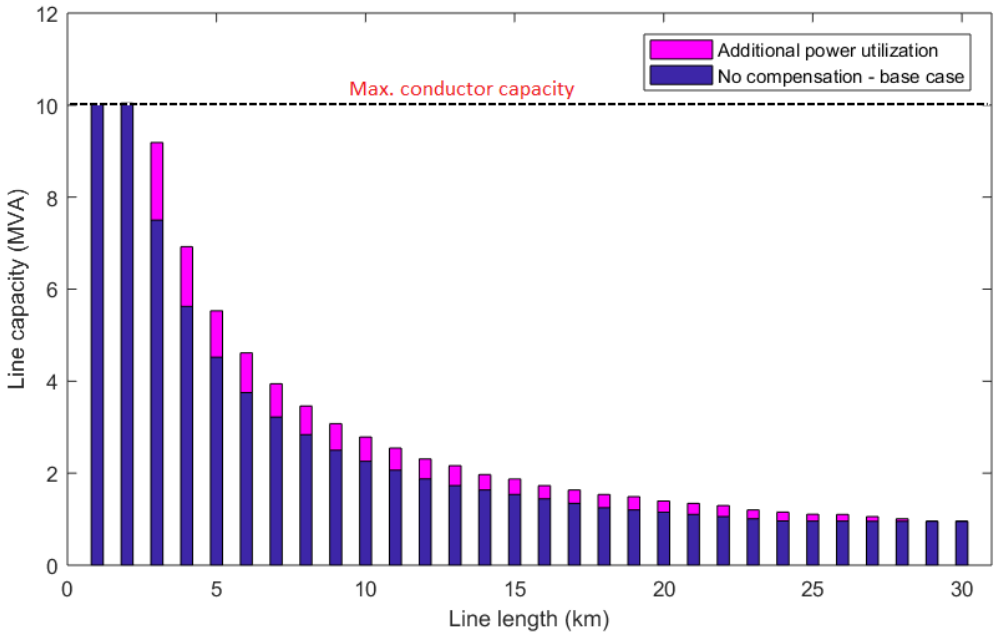

Figure 3.11: Line capacity vs Line length for the generation scenario with individual shunt compensation

3.6. Series voltage regulation

The series voltage regulation considered in this section are regulators which can inject voltage in-phase or out-of-phase at any point in the system to avoid voltage limits violation. Fig.3.13 shows the line diagram of the system with a LVR for series voltage regulation. This can be achieved by either a LVR or a DVR system as described in the section 2.8. Even though voltage regulation is possible by dynamically changing the set-point in the HV/MV substation with the use of OLTCs, HV/MV substations have multiple feeders and regulation cannot be done based on one single feeder. This section studies the effect of individual feeder regulation using a LVR or a DVR system with 10% regulation range. A DVR system is used for short duration voltage variations such as voltage sags/swells, flicker, etc. As the focus here is on long duration voltage variation, the cost effective solution available in the market is a LVR or a SVR. As the regulators are studied at a system level, the results are applicable for both LVR and DVR.

3.6.1. Load scenario

The thumb rule used for the placement of a LVR is usually 1/3 or 2/3 along the length of the line [37]. This placement depends on the load and the generation profile present in the system. LVR can also be placed in the substation at the starting point of the feeder. The main effect of adding a LVR is that it gives the flexibility to the feeder by adding an extra bandwidth for voltage variation equivalent to the regulation range of the compensation system. To make the analysis more generic and applicable to different LVR locations along the line, the simulation for load scenario is carried out by increasing the voltage at the beginning to be at 1.1 pu. This emulates the scenario of placing an LVR with 10% regulation at the beginning of the line. The results obtained by this method are also applicable for the placement of LVR at any point along the line as the loads are modeled as a constant power block which do not depend on the voltage. The voltage limit still

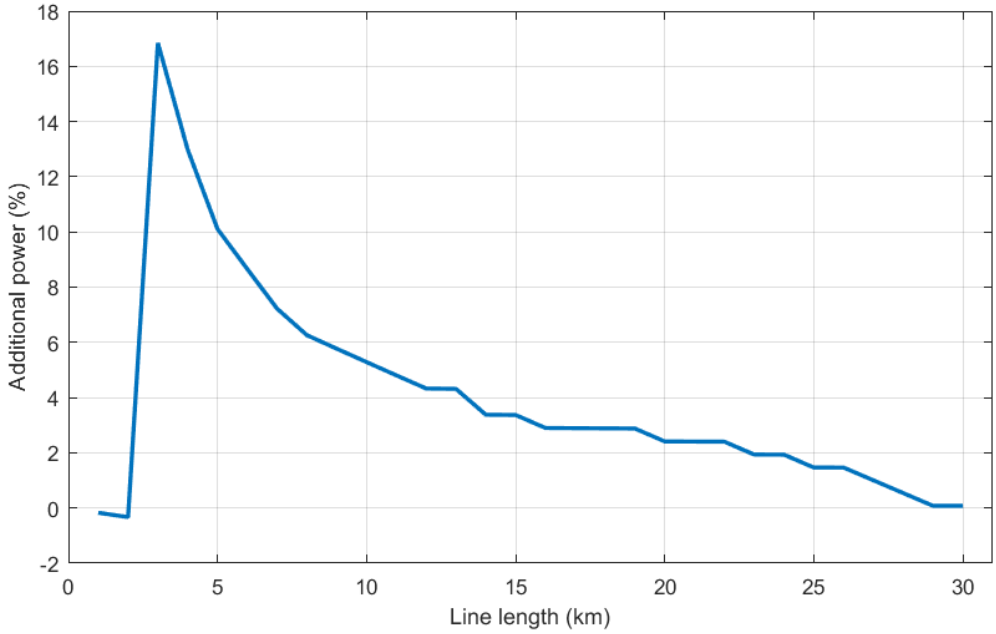

Figure 3.12: Percentage increase in the line capacity as a function of line length for the generation scenario due to shunt voltage compensation

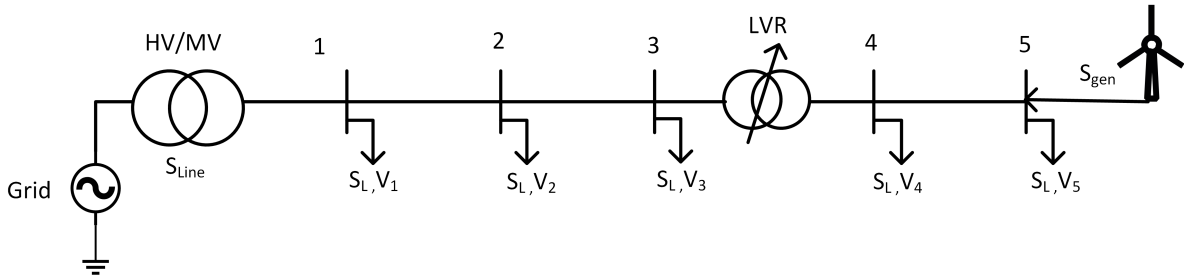

Figure 3.13: Single line diagram of the 20kV, 10 MVA distribution system under study with series voltage compensation

remains the same at 0.96pu for the loads connected to the system. Fig.3.14 shows the additional grid capacity available due to the presence of a LVR in the system. Series voltage regulation enables the grid to utilize full grid capacity until 13 km without any voltage violation. LVR acts in positive regulation mode by boosting the voltage up in the system. In the base case without any compensation, voltage limits were violated after 3 km in the load scenario. Fig. 3.15 shows the additional power in percentage that can be utilized from the existing grid due to the installation of LVR in the system. LVR enables the grid to utilize up to 73.59% of the base grid capacity without any line violations.

3.6.2. Generation scenario

Voltage rise caused by the renewable integration can be effectively alleviated by using a LVR in the system. As discussed in the previous subsection, LVR placement depends on the load and generation profile in the system. LVR should operate in buck operation to reduce the voltage by 10 % to maintain the line voltage within the limits. The voltage at the start of the line is made to 0.9pu and the voltage rise limit is set as 1.04pu in the line. Fig. 3.16 shows the additional line capacity available compared to no compensation scenario due to the presence of LVR in the system. LVR allows the existing cable to be utilized to full capacity until 7 km as shown in fig. 3.16. Fig. 3.17 shows the additional reverse active power in percentage that can be utilized from the existing grid due to the installation of LVR in the system. LVR enables the grid to utilize up to 63.78% of the base grid capacity without any line violations.

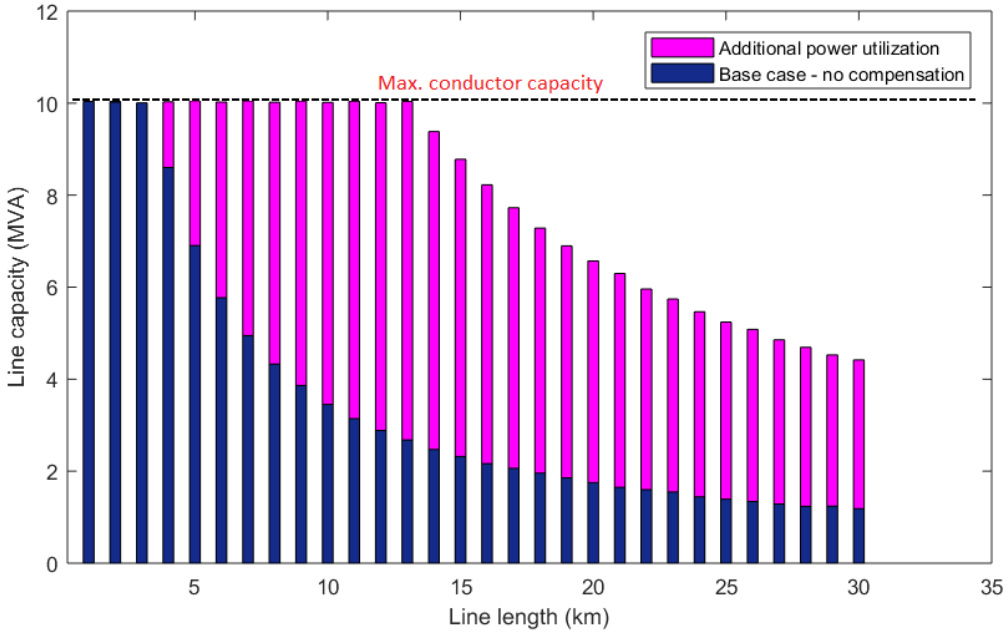

Figure 3.14: Line capacity vs Line length for the load scenario with a ±10% line voltage regulator

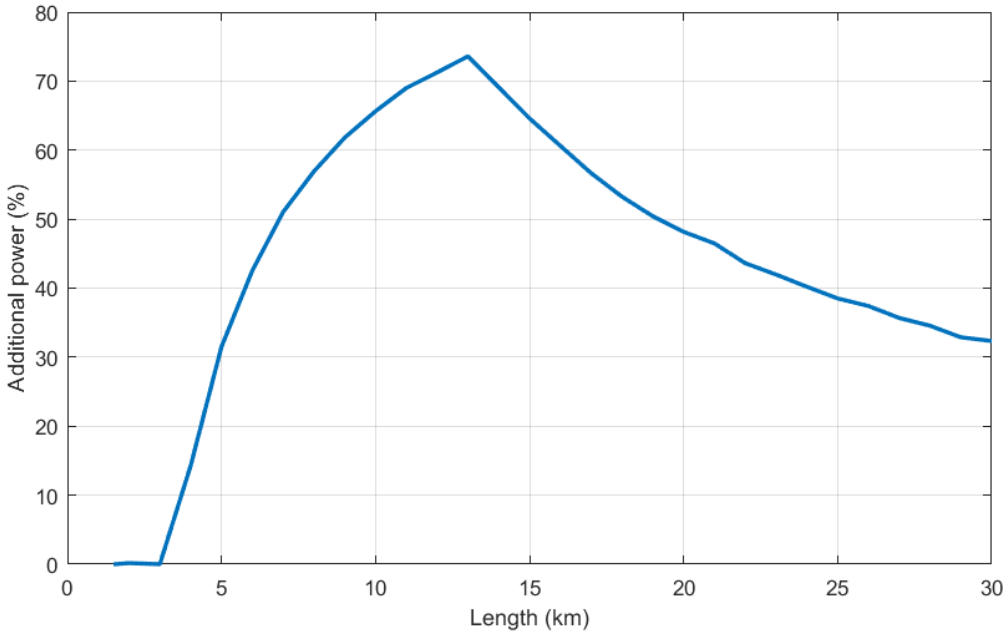

Figure 3.15: Percentage increase in the line capacity as a function of line length due to series compensation with ±10% line voltage regulator

3.7. Conductor upgradation

Increasing the cross-sectional area of the conductor has a positive effect in reducing the voltage rise/ drop due to reduction in R/X ratio in the system. The main aim of this study is to see the effect of the conductor upgradation with respect to the voltage regulation capabilities. Even though the power carrying capability of the conductor is increased due to larger area of the conductor, the power limit considered in the study still remains the same at 10 MVA. Table 3.2 shows the overhead aluminum conductors that are used in the simulation to study the effect on grid capacity.

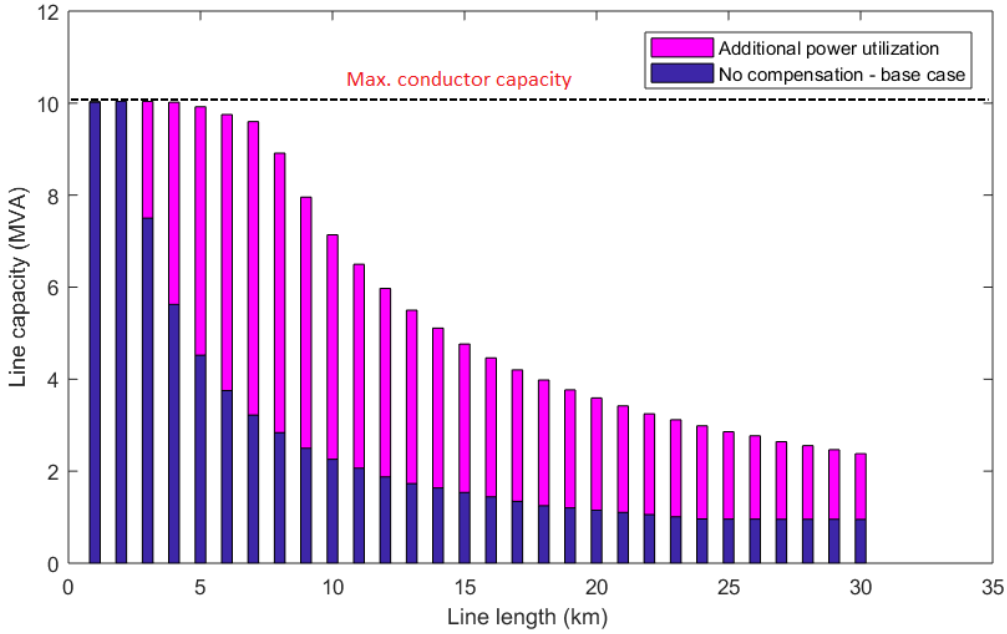

Figure 3.16: Line capacity vs Line length for the generator scenario with a ±10% line voltage regulator

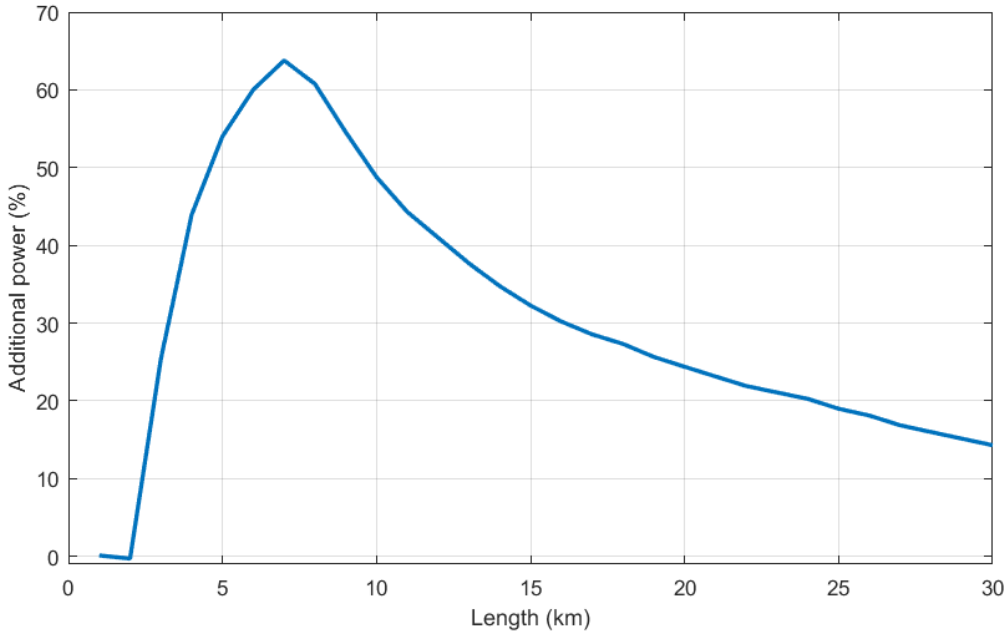

Figure 3.17: Percentage increase in the line capacity as a function of line length due to series compensation with a ±10% line voltage regulator

Table 3.2: Type A1 conductor parameters used for the study taken from IEC 61597

Code number	Stranding	Diameter (mm)	CCC (A)	Resistance(Ω/km)	Inductive reactance (Ω/km)
A1_63	7	10.2	393	0.4550	0.2772
A1_100	19	12.9	529	0.2883	0.2597

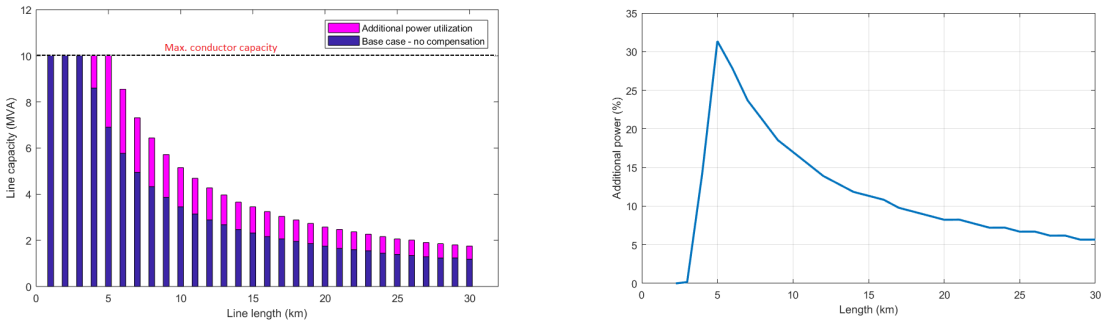

(a) (b)

Figure 3.18: (a) Line capacity (MVA) vs line length (km) for the load scenario with A1_63 conductor (b) Percentage increase in the line capacity as a function of line length for the load scenario with A1_63 conductor

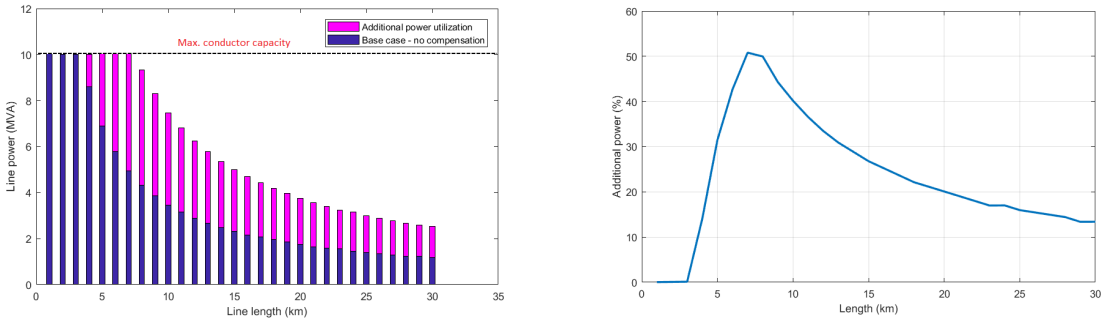

(a) (b)

Figure 3.19: (a) Line capacity (MVA) vs line length (km) for the load scenario with A1_100 conductor (b)Percentage increase in the line capacity as a function of line length for the load scenario with A1_100 conductor

3.7.1. Load scenario

The effect of a conductor upgradation for the load scenario with no generation is studied here. Reducing the R/X ratio will allow lower voltage drop for the same amount of power transfer from the substation to the loads connected in the grid. Fig. 3.18a shows the effect of conductor upgradation with A1_63 conductor and Fig. 3.19a shows the effect of conductor upgradation with A1_100 conductor. With A1_63 conductor upgradation, voltage violation is avoided till 5 km and it allows complete 10 MVA power utilization. After 5 km, even though there is additional grid capacity available compared to the base case scenario, but voltage limits are violated before the complete power utilization in the conductor. This is seen in the inverse relationship between the grid capacity and and length after 5km. This conductor upgradation is enabling the grid to utilize up to 32.1% of the base grid capacity without any line violations as shown in the fig. 3.18b. With the A1_100 conductor, the system is able to utilize full power until 7 km. After 7 km, the system is able to provide additional grid capacity better than the base case and A1_63 conductor case but voltage violation is reached before full power utilization as seen in the fig.3.19a. This conductor upgradation is enabling the grid to utilize up to 50.81% of the base grid capacity without any line violations as shown in the fig. 3.19b. Definitely conductor upgradation does improve the grid capacity due to the effective reduction in R/X ratio but a complete techno-economic analysis should be done before it can be replaced. In case of long rural lines, the effective increase in grid capacity utilization might not be justified due to high investment costs involved.

3.7.2. Generation scenario

Voltage rise caused due to generation without any load consumption is studied here with the upgraded conductor. Reduction in R/X ratio is able to increase the grid capacity for longer distances without any voltage violation. Fig.3.20a shows the additional grid capacity available with the conductor upgradation. With a A1_63 conductor, rated 10 MVA power can be transmitted until 4 km without any voltage violations. This conductor upgradation enables the grid to utilize up to 32.7% of the base grid capacity without any line viola-

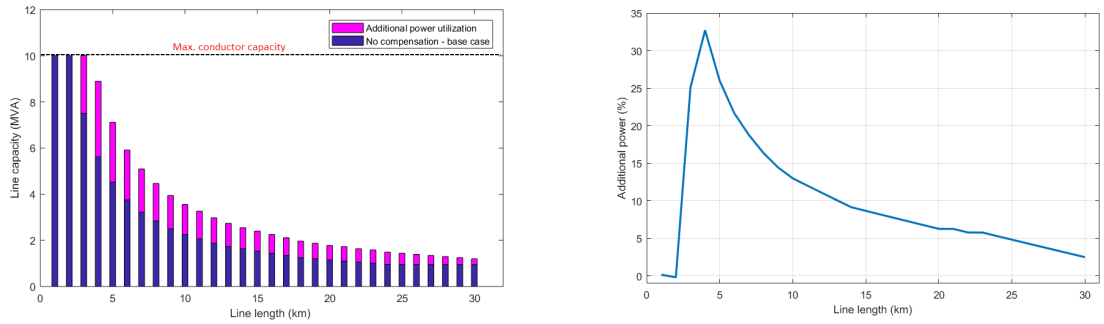

(a) (b)

Figure 3.20: (a) Line capacity (MVA) vs line length (km) for the generation scenario with A1_63 conductor (b) Percentage increase in the line capacity as a function of line length for the generation scenario with A1_63 conductor

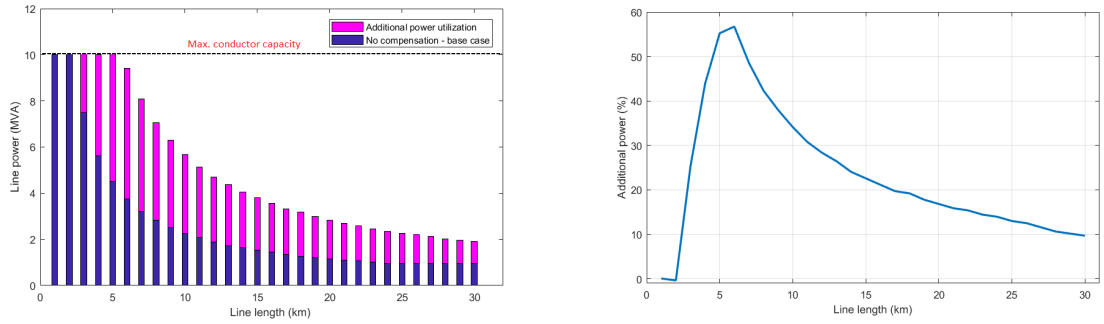

(a) (b)

Figure 3.21: (a) Line capacity (MVA) vs line length (km) for the generation scenario with A1_100 conductor (b) Percentage increase in the line capacity as a function of line length for the generation scenario with A1_100 conductor

tions as shown in the fig. 3.20b. The effect of cable upgradation has minimal effects on the voltage regulation for the generators connected to the long lines due to large impedance. Fig. 3.21a shows the additional grid capacity available with A1_100 conductor. Rated 10 MVA power can be transmitted until 6 km without any voltage violation with the A1_100 conductor. This conductor upgradation enables the grid to utilize up to 56.75% of the base grid capacity without any line violations as shown in the fig. 3.21b.

3.8. Voltage regulation impact on grid capacity

Various voltage regulation strategies were analyzed in this chapter. The impact of voltage regulation on enhancing the grid capacity was quantitatively studied. Table 3.3 & 3.4 shows the results from the simulation. The following conclusions can be derived from the study:

- The series compensation with a LVR has a positive impact on grid capacity and it is also able to utilize the existing conductor for longer lengths without any voltage violations. This is an effective active solution which can provide feeder specific voltage regulation.
- Shunt compensation is not very effective in providing voltage regulation support. In low power factor distribution systems, shunt based power factor correction devices will decrease losses, and it can also provide some voltage regulation in the line. But shunt compensation is not effective in its voltage regulation capabilities compared to series voltage regulation for MV distribution grids.
- Conductor replacement with a larger cross sectional area has a positive effect on the voltage regulation due to reduction in R/X ratio. The cost and time involved in conductor upgradation is very high. It is not an economical solution to solve the voltage regulation issues. In areas where future load consumption and generation is foreseen, this can be the only option to the DSO as the active solutions cannot increase the power capacity of the conductor.

Table 3.3: Grid capacity results for load scenario(* Conductor A1_40 (60 mm^2) was used in the study)

	Load scenario	
	Maxmimum grid capacity added (%)	Line length with rated grid capacity (km)
No regulation*	NA	3
Shunt compensation*	6.71 %	3
Series compensation*	73.59 %	13
Conductor A1_63 (95 mm^2)	32.1%	5
Conductor A1_100 (150mm^2)	50.81 %	7

Table 3.4: Grid capacity results for generation scenario(* Conductor A1_40 (60 mm^2) was used in the study)

	Generation scenario	
	Maxmimum grid capacity added (%)	Line length with rated grid capacity (km)
No regulation*	NA	2
Shunt compensation*	16.85 %	3
Series compensation*	63.78 %	7
Conductor A1_63 (95 mm^2)	32.7%	4
Conductor A1_100 (150mm^2)	56.75 %	6

The effectiveness of series voltage regulation with a LVR makes it an economical active solution to increase the grid capacity of an existing conductor without violating the voltage limits for longer line lengths compared to shunt compensation solutions.

4

Analysis of LVR configurations with mechanical OLTCs

4.1. Introduction

From chapter 3 it was deduced that line voltage regulators are able to solve the long duration voltage variation problems faced in feeder lines. The main components present in a LVR are transformers and OLTCs. Transformers convert the medium voltage to a lower voltage which will be used in series in the network to regulate the line voltage. OLTCs dynamically change the series voltage to meet the voltage requirements. ABB's line voltage regulator is manufactured with dry-type transformers and mechanical contactors [8]. Fig.4.1 shows a typical layout of the LVR system manufactured by ABB. The LVR uses a two active parts "booster/feeder" configuration with RESIBLOC dry-type transformer. The secondary side of the feeder transformer is connected with the primary side of the booster transformer by an intermediate circuit consisting of mechanical contactors to perform the tap changes(Patent No: US9618950B2 [16]). Dry-type transformers are larger than a liquid-filled oil transformers for the same voltage and capacity, as it uses air for insulation and cooling. Due to this reason, more material for core and coil is used in dry-type transformers leading to higher cost and losses. The drawbacks of dry-type transformer are their **larger space requirement** and **higher cost** compared to an oil transformer of same voltage and power capacity. This chapter will be focused on the analysis of different LVR configurations with oil-type transformers and mechanical OLTCs.

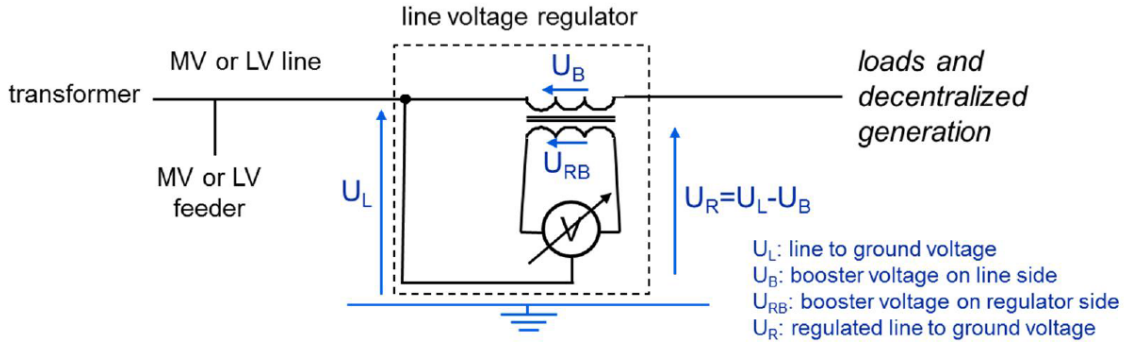

Figure 4.1: Typical layout of a Line Voltage Regulator system [37]

The three main suppliers for SVRs with oil-type transformers are GE, with its VR-1 series; Siemens, with its JFR series; and Cooper Power Systems with its VR- 32 series [15]. This chapter will analyze different LVR configurations with oil-type transformer and mechanical OLTCs.

The final LVR configuration is selected based on the following criteria:

- Technical feasibility for the chosen network
- Cost-effectiveness

- Lower maintenance

4.2. Transformers

Transformers are static devices which can transfer energy from one circuit to another circuit, usually at a very high efficiency. Transformers couple both the electrical circuit and transfer energy through a common magnetic iron core. They are designed for various purposes such as for measurement of currents & voltages, transferring signals or electrical power applications. The focus on the thesis is given for transformers used to transfer electrical power in distribution systems. They are used to transfer the power from one voltage level to another voltage level in a electrical network or a grid.

4.2.1. Transformer basics

A transformer is constructed by two windings coupled with a magnetic core and magnetically connected by a mutual flux between two windings. An ideal transformer can transfer power without any losses. The main assumptions made for analyzing ideal transformer are as follows [72]:

- No eddy and hysteresis losses are present - core losses are zero.
- Conductors have zero resistance - no resistive losses.
- Windings are perfectly coupled with the core - no leakage flux is present.
- Core has a linear B-H curve with no magnetic reluctance.

The above assumptions are used to derive the transformer equation for ideal scenarios. Maxwell's equation which relates the electric field and the magnetic field in a circuit is given as follows:

$$\nabla \times \vec{E} = -\frac{\partial \vec{B}}{\partial t}$$

This equation can be extended for a simple transformer system to derive the governing principle - faraday's law. Faraday's law states that a changing magnetic field in a circuit or a closed loop gives rise to a Electro Motive Force (EMF) in the system. The relationship between e (EMF) and ϕ_m (mutual flux) can be written as follows:

$$e = -\frac{d\phi}{dt}$$

Assuming a sinusoidal variation in the flux, following equation can be derived:

$$\phi = \phi_m cos(\omega t)$$
$$e = \omega \phi_m sin(\omega t)$$

The 'e' represents the per-turn EMF of the winding. If the total EMF is 'E' and total number of turns is 'N', the RMS equation can be given as follows:

$$\frac{E}{N} = \frac{\omega \phi_m}{\sqrt{2}}$$
$$\frac{E}{N} = \frac{\omega B_m * A_{core}}{\sqrt{2}}$$

This is a very important equation which states that the per-turn EMF should be constant for a system with constant frequency and depends only on ϕ_m. ϕ_m is given as a product of B_m and area of the cross-section of the core (A_{core}). B_m depends on the transformer designer and operating conditions of the transformer. The designer ensures that B_m does not exceed B_{max} of the core material which will lead to core saturation.

As the same mutual flux is coupled between both the windings as shown in fig.4.2, the following equation between the transformer can be written:

$$\frac{E_H}{E_X} = \frac{N_H}{N_X} \tag{4.1}$$

As the reluctance of the magnetic path is considered very low (in ideal cases it is zero), ampere turns on both windings should be balanced. Equation relating to currents on primary and secondary side is given as:

$$N_H I_H = N_X I_X \tag{4.2}$$

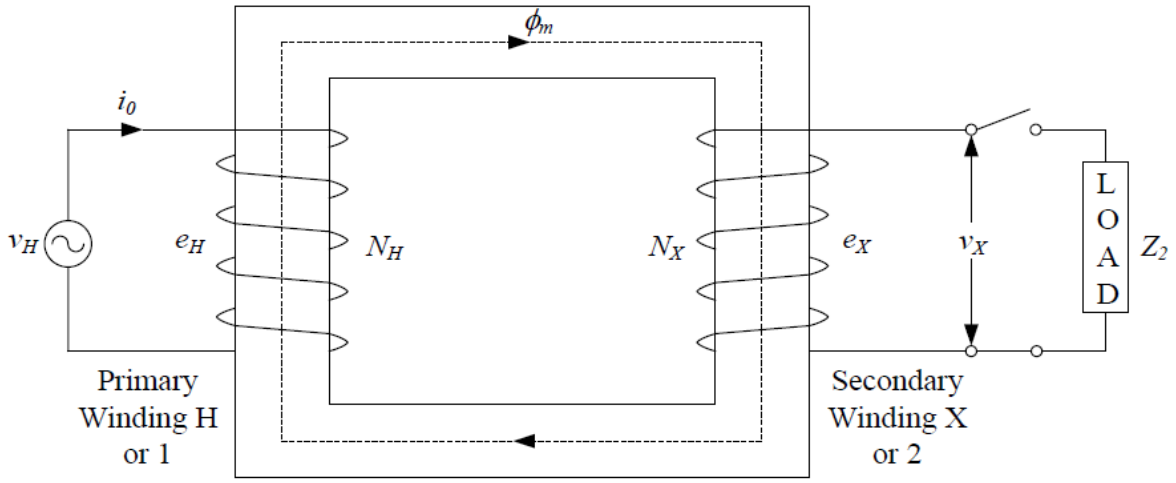

Figure 4.2: An ideal two-winding transformer with primary and secondary windings [72]

It is very important to note that the transformer saturates only when the voltage exceeds the prescribed limits. Even during high currents on the secondary and primary windings, the ampere turns relation will still hold good as the Magneto Motive Force (MMF) from both the windings oppose each other to create a low value of mutual flux. This scenario will not lead to saturation, hence, the eq. 4.2 will always hold good.

4.2.2. Practical transformer and parameters identification

The Following effects are considered in modeling a practical transformer:

- Magnetization current to set up the flux in the magnetic core is not zero due to the presence of finite reluctance.
- Leakage inductances are present as flux produced by the primary winding is not completely linked by the secondary winding of the transformer.
- Conductor and core losses are present in the transformer due to non-ideal nature of components in practical transformers.

Fig.4.3 depicts the equivalent circuit of a practical transformer including all the major non-idealities. R_H, R_X are the equivalent series resistance that includes the conductor losses for the primary and secondary windings respectively. L_H, L_X are the series leakage inductance for the primary and secondary windings respectively. R_M is the core losses and L_M is the magnetization inductance of the transformer. L_M is considered to be linear for all the power system calculation purposes. But in most cases, the shunt branch can be neglected without any error in calculation [36].

Let 'a' be the turn's ratio N_H/N_X, then the equivalent resistance and inductance referred to the primary side can be given as follows:

$$R_{eq,primary} = R_H + a^2 R_X$$
$$L_{eq,primary} = L_H + a^2 L_X$$

Z is determined by conducting a short-circuit test on transformers. The conductor resistance contribution to the impedance of the transformer is taken into the account only for very small distribution transformers. The main impedance (Z) contribution comes from the leakage inductance of the transformer. The leakage inductance can be calculated by using this assumption.

$$Z = R_{eq,primary} + jX_{eq,primary} \approx jX_{eq,primary} \tag{4.3}$$

Impedance is given as a percentage with respect to the base impedance of the transformer as follows:

$$u_{Z\%} = 100 * \frac{I_r Z}{V_r} \tag{4.4}$$

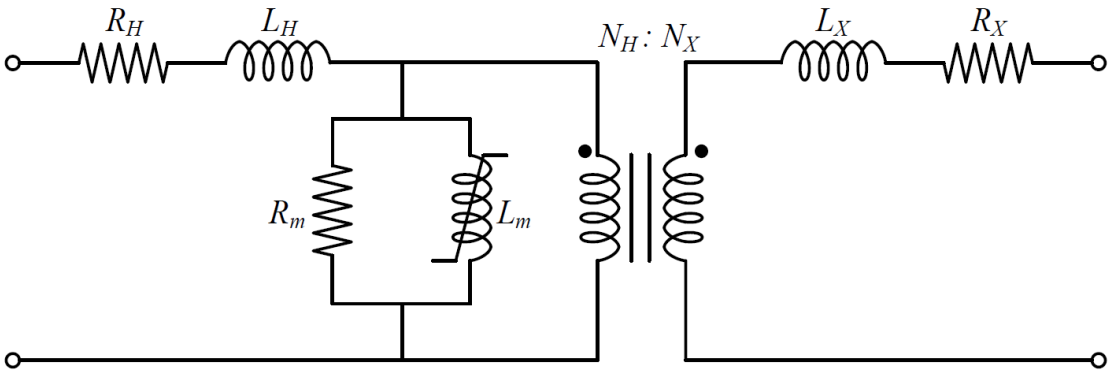

Figure 4.3: Equivalent circuit of a practical transformer with non-idealities [72]

V_r, I_r represents the rated voltage and current of the transformer. Individual leakage inductance can be approximately determined as follows:

$$Z = X_{eq,primary} \tag{4.5}$$

$$L_{eq,primary} = \frac{X_{eq,primary}}{\omega} \tag{4.6}$$

$$\frac{L_{eq,primary}}{2} = L_H = a^2 L_X \tag{4.7}$$

The above assumption has been used widely to model the individual leakage inductance in a transformer [72].

4.2.3. Autotransformer

Autotransformers have the same working principle as a regular two-winding transformer except for electrical isolation between primary and secondary windings. The main advantage of an auto transformer is the reduction in core size and copper usage compared to a two-winding transformer of the same rating [72]. Fig.4.4a depicts a step down autotransformer. As the winding is in the same core, volts per turn is constant leading to proportionality between the voltage and the number of turns. Considering ideal conditions, the voltage equation is given as follows:

$$V_H : V_X = N_H : N_X \tag{4.8}$$

Similar to a two-winding transformer, MMF balance equation can be written to find the relationship between the primary and secondary currents as follows:

$$I_H(N_H - N_X) = N_X(I_X - I_H)$$

$$I_H N_H = I_X N_X \tag{4.9}$$

As seen in fig.4.4a, the primary and secondary currents are out of phase leading to reduced current through the common winding of the transformer. This reduction in current leads to copper savings as the cross sectional area of the conductor required is reduced. As the same windings are used for the both primary and secondary circuits, the effective core window of the transformer is reduced leading to savings in the core. The effective core size of an autotransformer in terms of core or magnetic power as a function of autotransformer power can be given as follows:

$$S_{core} = \frac{V_H - V_X}{V_H} * S_{autotransformer} \tag{4.10}$$

The above equation signifies the fact that when the secondary voltage is close to the primary voltage, most of the power is transferred electrically and only the remaining power is transferred magnetically via the

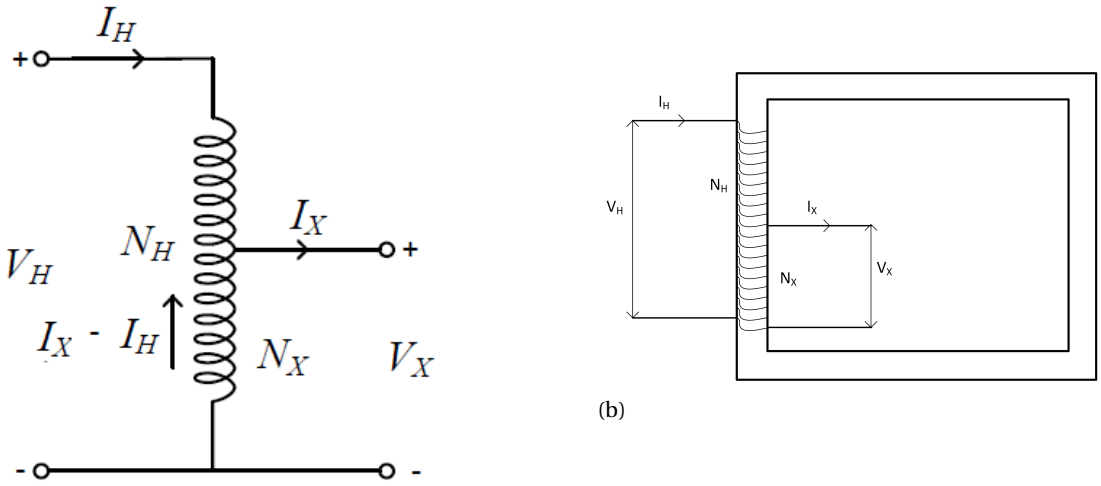

(a)

(b)

Figure 4.4: (a) Schematic diagram of an autotransformer [72] (b) Physical arrangement of an autotransformer

core. Assuming the cross sectional area of the selected conductor is proportional to the current carried in the conductor, the copper savings of an autotransformer with respect to a two-winding transformer can be given as follows:

$$\frac{Cu_{Autotransformer}}{Cu_{2WdgTransformer}} = \frac{I_H(N_H - N_X) + N_X(I_X - I_H)}{I_H N_H + I_X N_X}$$

Using the ampere turns balance eq.4.9 & eq. 4.8 in the above expression,

$$\frac{Cu_{Autotransformer}}{Cu_{2WdgTransformer}} = 1 - \frac{V_{sec}}{V_{pri}} \tag{4.11}$$

From eq. 4.10 & 4.11 it can be clearly seen that the savings is higher only when the secondary voltage is close to the primary voltage. When the secondary voltage approaches the primary voltage, the power transfer is mainly through electrical circuit and only partial power is transferred through the magnetic network. This is applicable when the purpose of using an autotransformer is similar to a regular two winding transformer. For e.g., if it is used to step up or step down voltages in a power network. In those cases it is highly beneficial to have autotransformers when the voltage transformation ratio is close to each other.

The equivalent resistance and leakage impedance in an autotransformer is given by the following equation:

$$R_{eq,primary} = R_H + k^2 R_X$$

$$L_{eq,primary} = L_H + k^2 L_X$$

Where k is defined as:

$$k = (\frac{N_H}{N_X} - 1)$$

For autotransformers, 'k' is referred to as co-ratio. This term is similar to ratio 'a' defined for two winding transformers.

A two winding transformer can be used as an autotransformer to increase or decrease the voltage. This kind of application is widely used in SVRs to perform the voltage regulation in a line/feeder. For this application, the savings on the copper and core derived previously is not applicable. Fig. 4.5b shows a two winding transformer connected as an autotransformer to boost the input voltage V_H. The voltage of the secondary winding with respect to the neutral point is the primary voltage plus the secondary voltage. Effectively, the

schematic diagram of the two winding transformer connected as an autotransformer is shown in fig: 4.5a. This configuration of the autotransformer is widely used as a series voltage regulator to boost the voltage. The relationship between the input/output voltage ratio and the number of turns in the winding for this configuration can be written as follows:

$$\frac{Outputvoltage}{inputvoltage} = \frac{V_H + V_X}{V_H} = \frac{N_H + N_X}{N_H}$$
$$\frac{Outputvoltage}{inputvoltage} = 1 + \frac{N_X}{N_H}$$

To obtain the same output voltage for a two winding transformer, following equations can be applied.

$$\frac{Outputvoltage}{inputvoltage} = \frac{V_H + V_X}{V_H} = \frac{N_X}{N_H}$$

In LVR applications where the output voltage regulation percentage is usually in the range of 6% to 10 %, the amount of winding turns required for a auto transformer is very less compared to a two winding transformer. For a 6% boost in voltage, the secondary winding for autotransformer should be 0.06 pu compared to a two winding transformer which requires 1.06 pu turns to perform the same operation considering the primary winding number of turns is 1pu. Usually a reversing switch is provided to connect the series winding in opposite fashion to reduce or buck the input voltage. This is explained in detail in the sec: 4.3. For buck operation, the output voltage is the input voltage minus the series transformer voltage. The copper savings can be obtained as follows:

$$\frac{Outputvoltage}{inputvoltage} = \frac{V_H - V_X}{V_H} = \frac{N_H - N_X}{N_H}$$
$$\frac{Outputvoltage}{inputvoltage} = 1 - \frac{N_X}{N_H}$$

To obtain the same output voltage in a two winding transformer, the voltage and number of turns relationship is written as follows:

$$\frac{Outputvoltage}{inputvoltage} = \frac{V_H - V_X}{V_H} = \frac{N_X}{N_H}$$

For a 6% reduction in voltage, the number of turns on the secondary side of an autotransformer will be only 0.06pu compared to 0.94 pu in a two winding transformer. For a regulator which provides 6% voltage regulation, assuming there is a load current of 1 pu, the power through the secondary winding which is in series can be given as follows for both boost and buck operation:

$$S_{series} = V_{series} * I_{load}$$
$$S_{series} = 0.06 * 1 = 0.06pu$$

Based on the theory of transformer action, the primary side of the transformer should also have the same power. If 1 pu of power is considered entering the input or source side of the transformer, the power transferred through the magnetic action is only 0.06 pu and rest of the power of 0.94 p.u is transferred electrically to the load. Due to this reason, the S_{core} of the autotransformer will also be rated at 0.06pu. In a two-wind transformer, boost operation requires a transformer with a rated power of 1.06 pu, and buck operation requires a transformer with a rated power of 0.94 pu . It can be clearly seen that when an autotransformer is used to perform voltage regulation operations, the power rating of the autotransformer (in pu) is same as that of the voltage regulation range (in pu) of the regulator. The copper used on the secondary side of the transformer is only a small fraction compared to a two-winding transformer.

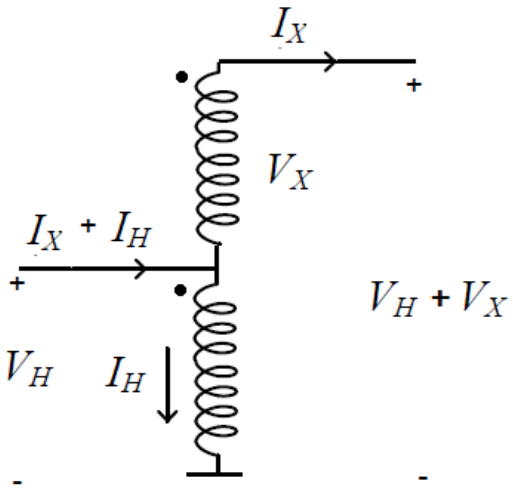

(a)

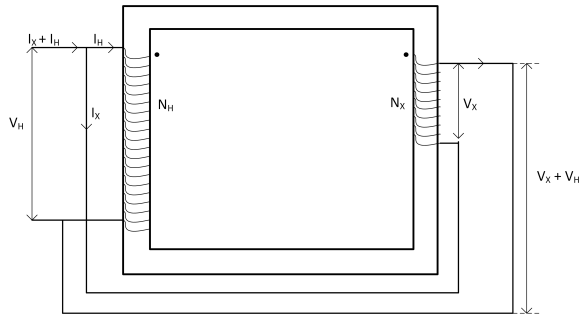

(b)

Figure 4.5: A two-winding transformer connected as a autotransformer to boost the voltage (a) Schematic diagram (b) Physical arrangement

4.3. Modeling of line voltage regulators

LVRs or SVRs uses the principle of two winding transformers connected as an autotransformer in series to the feeder to boost or buck the supply voltage. There are also other variations of LVRs available such as employing a feeder and a booster (series) transformer to perform the same function. LVRs are installed with an on-load tap-changer to vary the output voltage based on the control system input. The control system uses various algorithms such as constant voltage mode or line drop compensation or impedance compensation to compensate for the voltage variation depending on the DNO preference. A typical LVR is shown in the fig. 4.6a. This structure is similar to a two winding transformer connected as a autotransformer, but the reversing switch gives the flexibility of positive and negative compensation. The OLTC connected to the LVR can vary the series voltage according to the controller commands.

For an ideal transformer, equations for positive regulation can be given as follows:

$$V_S = V_1 \qquad I_S = I_1 + I_2$$
$$\frac{V_2}{V_1} = \frac{N_2}{N_1} \qquad I_2 = (\frac{N_1}{N_2})I_1$$
$$V_L = V_1 + V_2 \qquad I_L = I_2$$
$$V_L = V_1 + (\frac{N_2}{N_1})V_1 \qquad I_1 = I_S - I_2$$
$$V_L = V_1(1 + \frac{N_2}{N_1}) \qquad I_2 = (\frac{N_1}{N_2})(I_S - I_2)$$
$$V_L = V_S * a_p \qquad I_L = \frac{I_S}{1 + (\frac{N_2}{N_1})} = \frac{I_S}{a_p}$$

For an ideal transformer, equations for negative regulation can be given as follows:

$$V_S = V_1 \qquad I_S = I_1 + I_2$$
$$\frac{V_2}{V_1} = -\frac{N_2}{N_1} \qquad I_2 = -(\frac{N_1}{N_2})I_1$$
$$V_L = V_1 + V_2 \qquad I_L = I_2$$
$$V_L = V_1 - (\frac{N_2}{N_1})V_1 \qquad I_1 = I_S - I_2$$
$$V_L = V_1(1 - \frac{N_2}{N_1}) \qquad I_2 = -(\frac{N_1}{N_2})(I_S - I_2)$$
$$V_L = V_S * a_n \qquad I_L = \frac{I_S}{1 - (\frac{N_2}{N_1})} = \frac{I_S}{a_n}$$

The regulation coefficient for positive regulation a_p and coefficient for negative regulation a_n can be combined together to form a regulation coefficient a_{Reg}. The equation for positive and negative regulation is written as follows:

$$a_{Reg} = 1 \pm (\frac{N_2}{N_1})$$

$$V_L = V_S * a_{Reg} \qquad I_L = \frac{I_S}{a_{Reg}} \tag{4.12}$$

The above equation is derived for single phase LVR where V_S is the source voltage, V_L is the load or output voltage, I_S is the source current and I_L is the load or output current from the LVR. These individual units can be connected to make three phase regulation in the network [13]. Due to low imbalances in European medium voltage network , three phase three wire networks are predominantly used to reduce the cost of the line. A Wye connected LVR is considered here in detail due to its wide use in MV networks and due to its ease in application compared to a closed delta connection [27]. Fig. 4.6b shows a three phase wye connected LVR. The reversing switch and OLTC is not shown in the figure. The equation of a single phase LVR can extended for the wye connected three phase LVR systems. The matrix equation 4.13 & 4.14 shows the relationship between the source and the load voltage. V_{SR}, V_{SY} & V_{SB} represents three phase source voltages and V_{LR}, V_{LY} & V_{LB} represents three phase load or output voltages of the LVR. I_{SR}, I_{SY} & I_{SB} represents three phase source currents and I_{LR}, I_{LY} & I_{LB} represents three phase load or output currents of the LVR.

$$V_{LR} = a_{RegR} * V_{SR} \qquad I_{LR} = \frac{I_{SR}}{a_{RegR}}$$
$$V_{LY} = a_{RegY} * V_{SY} \qquad I_{LY} = \frac{I_{SY}}{a_{RegY}}$$
$$V_{LB} = a_{RegB} * V_{SB} \qquad I_{LB} = \frac{I_{SB}}{a_{RegB}}$$

$$\begin{bmatrix} V_{LR} \\ V_{LY} \\ V_{LB} \end{bmatrix} = \begin{bmatrix} a_{RegR} & 0 & 0 \\ 0 & a_{RegY} & 0 \\ 0 & 0 & a_{RegB} \end{bmatrix} * \begin{bmatrix} V_{SR} \\ V_{SY} \\ V_{SB} \end{bmatrix} \tag{4.13}$$

$$\begin{bmatrix} I_{LR} \\ I_{LY} \\ I_{LB} \end{bmatrix} = \begin{bmatrix} \frac{1}{a_{RegR}} & 0 & 0 \\ 0 & \frac{1}{a_{RegY}} & 0 \\ 0 & 0 & \frac{1}{a_{RegB}} \end{bmatrix} * \begin{bmatrix} I_{SR} \\ I_{SY} \\ I_{SB} \end{bmatrix} \tag{4.14}$$

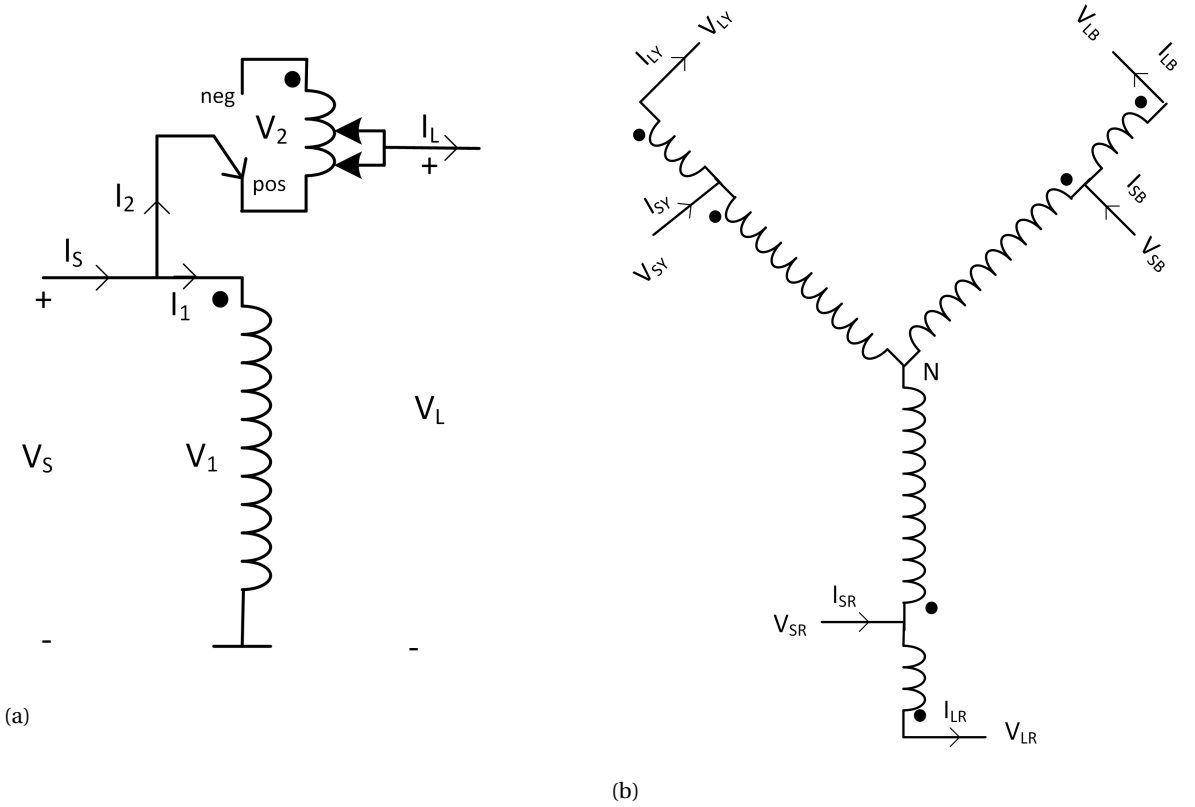

Figure 4.6: (a) Single phase LVR (b) Three phase wye connected LVR

4.4. Mechanical On-Load Tap-Changer

The primary function of a transformer is to transfer energy from one voltage level to another voltage level in an electrical network. Due to power variations in the network, the voltage in the network will not be constant and vary based on the network conditions. Transformers have ideal voltage transformation ratios for ideal network conditions. Due to voltage variations (drop/rise) in the network, transformers should be able adjust the transformer ratio to maintain the voltage within regulation limits. The transformer ratio can be adjusted during de-energized network condition or during energized network condition. The former is called an off-load tap-changer and latter is called an on-load tap-changer. On-load tap-changers are typically used in high-voltage networks and sub-transmission networks. For distribution networks, typically only off-load tap-changers are used due to short lines with less voltage variation and high costs involved. Recently due to high fluctuating loads and generation present in distribution networks, many network operators are using on-load tap changers also for the distribution networks [47].

4.4.1. On-Load Tap-Changer: switching principle and technology

The main function of an on-load tap-changer is to transfer the load from one tap to another tap without any open-circuit, thereby, changing the turns ratio of the transformer to regulate the voltage. Moving from one tap to another tap without a bridging contact, break and make mechanism is shown in fig. 4.7. As the tap transition includes breaking an inductive circuit, a high voltage will be induced to keep the current flowing in the circuit. As the contact keeps moving towards the next tap, there will be a momentary period during which neither of taps are connected to the load creating an open-circuit. This will create disturbances to the consumers during tap changes.

To overcome the shortcomings of an open circuit during a tap change, a bridging contact is introduced so that momentary loss of power is avoided during a tap change. Fig. 4.8 depicts tap transition with the use of a bridging contact. This mechanism has a shortcoming of creating a short-circuit during the contact making process. This high circulating current can be restricted by introducing an impedance within the bridging contact. The impedance used can be either a resistor or an inductance (reactor). Fig. 4.9 shows the bridging

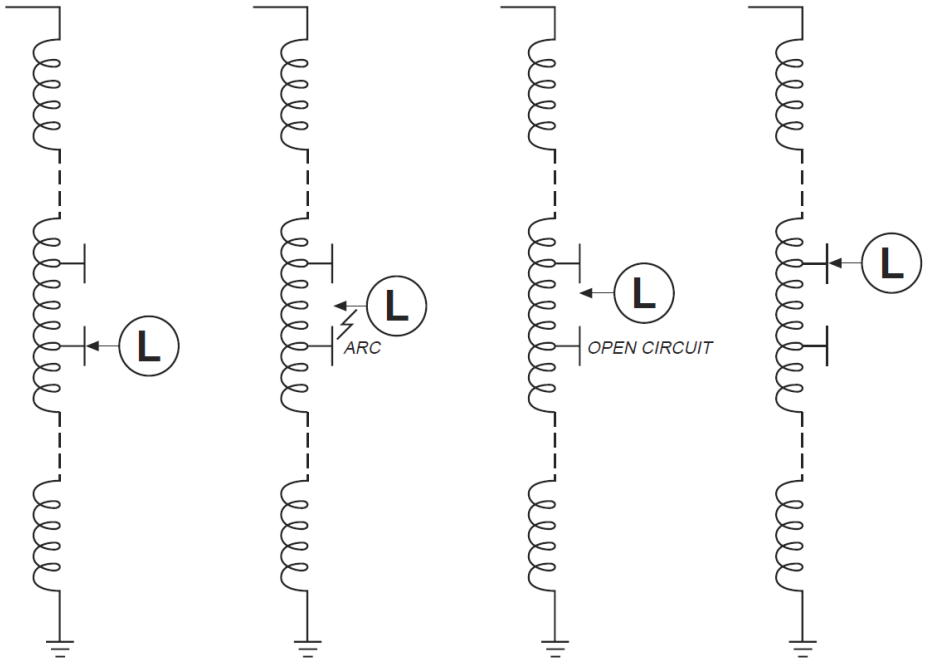

Figure 4.7: Tap transition (left to right) without any bridging contact [32]

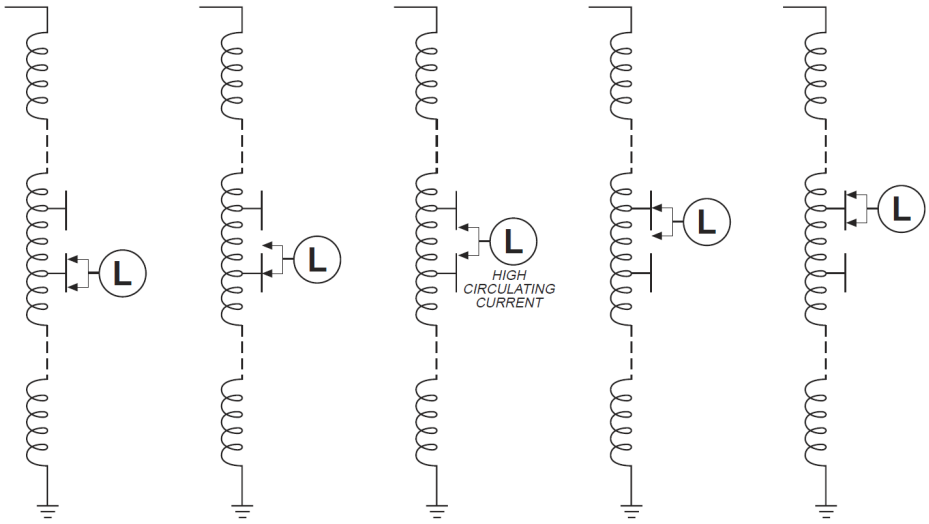

Figure 4.8: Tap transition (left to right) with a bridging contact [32]

contact with an impedance to reduce the circulating current. Fig.4.9 (a) shows a resistor type OLTC with an extra path 'B' to provide a lossless path after a tap change. During the tap change, the transition resistor is present in the circulating current path. Fig.4.9 (b) shows a reactor type OLTC which does not need an extra path after tap change as the mutual flux will be zero leading to negligible voltage drop during steady state operation. During the tap change, circulating current is restricted with the impedance of the reactor.

Oil-type and Vacuum-type OLTCs

Whenever the tap changer breaks a contact, the arc needs to be quenched appropriately to ensure stable operation of the system. Traditionally oil is used in the transformer for cooling and for insulation purposes. It is also used as an arc quenching medium. This type of OLTC can be scaled up for very high power transformers,

Figure 4.9: (a) Bridging contact with a resistor (b) Bridging contact with a reactor [32]

and is used widely in the industry. However, there is an increased fire hazard when the arc is quenched in an oil medium. It also degrades the oil whenever there is a tap change which leads to frequent maintenance. Vacuum-type switching technology was introduced to overcome these problems in mechanical OLTCs. The vacuum interrupter technology is able to provide technical superiority for low and medium voltage transformers [57].

Oil-type OLTC	Vacuum type OLTC
The arc is quenched in the oil and interaction takes place with the medium	The arc is quenched inside a sealed system. There is no interaction of arc with the surrounding medium
Carbon by-products are produced in the oil during arc quenching process	No carbon by-products produced in the oil during arc quenching process
More energy consumption and higher contact wear compared to vacuum-type	Less energy consumption and low contact wear
Higher maintenance costs due to degradation of oil	Low failure rates and reduction in maintenance costs

Table 4.1: Differences between oil-type and vacuum-type OLTCs

4.4.2. Distribution voltage level OLTCs

There are two types of OLTCs available for distribution networks. They are as follows:

- High current carrying OLTCs used for SVRs
- Low current carrying OLTCs used in Voltage Regulated Distribution Transformers (VRDTs)

High current carrying OLTCs

This type of OLTC has been predominantly used by most of the SVR manufacturers. They all have a similar structure and working mechanism with few differences in minor components. VR-32 Quick-Drive Tap-Changer from Cooper Power Systems [68] is taken into consideration here to understand the basic principle and structure of this type of OLTC. But the details discussed here apply to similar OLTCs produced by other manufacturers [24], [64]. The VR-32 OLTCs come as a single-phase OLTCs which have a rated current carrying capacity of up to 668 A. A reversing switch is present to change the polarity of the tapped winding to attain positive and negative regulation in the SVR. Reactor based bridging contact is employed to reduce the circulating current during a tap change operation. Apart from the reactor to restrict circulating current, equalizer windings are used to improve the contact life for high current applications. An Oil medium is used to quench the arc during tap changes due to high currents flowing through the tap-changer. This is one of the main drawback of this kind of tap changer as it contaminates the oil and requires monitoring of the oil, thereby, increasing the maintenance cost of the system. It uses a traditional geneva gear system with synchronous or induction motor to move the taps. Fig. 4.10a shows a VR-32 QD5 single phase tap changer.

(a)

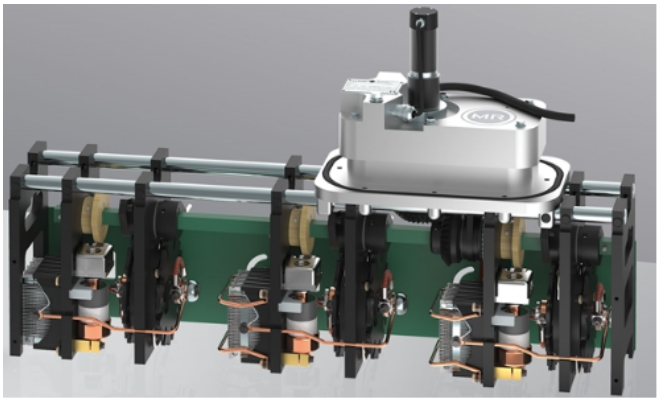

(b)

Figure 4.10: (a) VR-32 Quick-Drive Tap-Changer[68] (b) MR ECPTAP VPD on-load tap-changer [29]

Low current distribution OLTCs

The recent influx of DGs in MV and LV grids has led to the development of OLTCs for distribution transformers to decouple the MV and LV grid similar to HV network. The two main variants of this type of OLTC are GRIDCON iTAP and ECOTAP VPD from Maschinenfabrik Reinhausen (MR). ECOTAP VPD is considered in the study which has a current carrying capability from 30 A to 100 A [29]. The only difference between ECOTAP and GRICON iTAP is current capability of the latter is restricted to only 30A. Oil is not contaminated as vacuum interrupters are used to quench the arc. This OLTC does not come with a reversing switch. The OLTC uses a high-speed resistor type tap changer to restrict the circulating current. The OLTC uses a stationary selector switch and a moving switching module. The selector module has a main and transition tap selector enabling the OLTC to use only one vacuum switch [47]. The current carrying capability is not enough for a typical medium voltage feeder regulation as these are designed for MV/LV distribution transformer to supply LV power distribution network. And a typical MV feeder contains many such LV distribution network points connected to one common MV feeder. For e.g, a 20 kV, 10 MVA MV feeder has a rated current of 288.6 A. Hence, these OLTCs cannot be used in SVR or LVR directly in series with the line due to high currents flowing. This OLTC does not come with a single-phase regulation feature. All the individual phase tap changers act in tandem to perform a three-phase tap change.

This makes the transformer oil maintenance free. The VRDTs can decouple MV and LV grid using the regulation capability but cannot provide feeder specific regulation like a SVR or LVR. There are limited number of manufacturers producing VRDT OLTCs.

4.4.3. OLTC selection

The main advantage of ECOTAP OLTC is the presence of vacuum interrupter to avoid the contamination of oil, which leads to less maintenance and is cheaper compared to high current carrying OLTCs. The cost of high current VR-32 type OLTC is higher because of its higher current rating with medium voltage level insulation requirements, and the use of reactors and equalizing winding to handle high currents. Even though single phase regulation is not possible with ECOTAP OLTC, due to low imbalances in the MV grid, it can be a suitable choice to perform tap changes. The main drawback of the ECOTAP OLTC is the limited current carrying capability and lack of reversing switch for LVR application. The main differences are shown in the table 4.2. The high current carriyng OLTC used in SVRs is referred as VR OLTC, and the low current carrying OLTC used in distribution transformer is referred as DT OLTC.

VR OLTC	DT OLTC
High current carrying capability of up to 688 A.	Low current carrying capacity (up to 100 A).
Comes with an in-built reversing selector switch.	No reversing selector switch is present.
Single phase voltage regulation is possible as they are available as a single phase OLTC.	Single phase voltage regulation not possible as it is available as a three phase OLTC with all phases connected to a common motor drive.
Oil-type OLTC with arcing inside the tank leading oil degradation. Higher maintenance.	Vacuum-type OLTC without any arc interaction with oil inside the tank. Lower maintenance.
More expensive as it is rated for higher line current and requires reactor to restrict the circulating current	Less expensive as it is rated for lower line currents and uses resistor to restrict the circulating current
Manufactured by GE, Siemens and Cooper Power Systems (EATON) – Proprietary equipment of the individual manufacturers	Manufactured by MR and available in the market for other companies

Table 4.2: Comparison of high current carrying (VR) OLTC and low current carrying (DT)OLTC

The ECOTAP OLTC is selected for further analysis as it is economical and also has less maintenance associated with it. The rating of the ECOTAP OLTC taken from the datasheet is given in the table 4.3 [29].

Table 4.3: Technical data of ECOTAP VPD III 100

Paramters	Value
Step Voltage	825 V
Rated current	100 A
Number of switches	9
Reversing switch	No
Rated insulation level	36 kV

The following sections will be focused on different LVR configurations with the ECOTAP OLTC and the additional requirements needed to perform series voltage reversal due to lack of inbuilt reversing switch.

4.5. One active part LVR configuration

This section focuses on LVR configurations that can be constructed using a single active part i.e, only one transformer. This type of configuration has the main benefit of using only one transformer active part which can save space and cost for the LVR. The main transformer which is able to convert the incoming medium voltage to a lower voltage is called a feeder transformer. The primary side of the feeder transformer is connected to the line input voltage. The secondary side of the feeder transformer for single active part configuration is the winding connected in series to the input line to perform voltage regulation. The analysis is carried out for a 20 kV, $\pm 6\%(\pm 1.5\% * 4)$ line voltage regulator. The regulation voltage is divided into steps of 4 with each step contributing to 1.5% of the line voltage. The power handling capability of LVR, voltage requirements, number of taps and contactors for voltage reversal is evaluated individually for each configuration. All the analysis is done for a single phase ideal transformer as per the assumptions from subsec: 4.2.

4.5.1. OLTC on the primary side of the feeder transformer

Fig.4.11 shows the layout of the LVR with an OLTC connected to the primary side of a feeder transformer. The relationship between the induced secondary voltage and primary voltage with the OLTC can be derived as follows:

$$V_2 = V_1 * \frac{N_{sec}}{N_{pri}(OLTC)} \tag{4.15}$$

The number of turns of primary winding depends on the OLTC position which is represented as $N_{pri}(OLTC)$. Assuming the input primary voltage to be constant and number turns in the secondary winding of the feeder transformer is constant, the series voltage V_2 depends on the number of turns of the primary winding of the

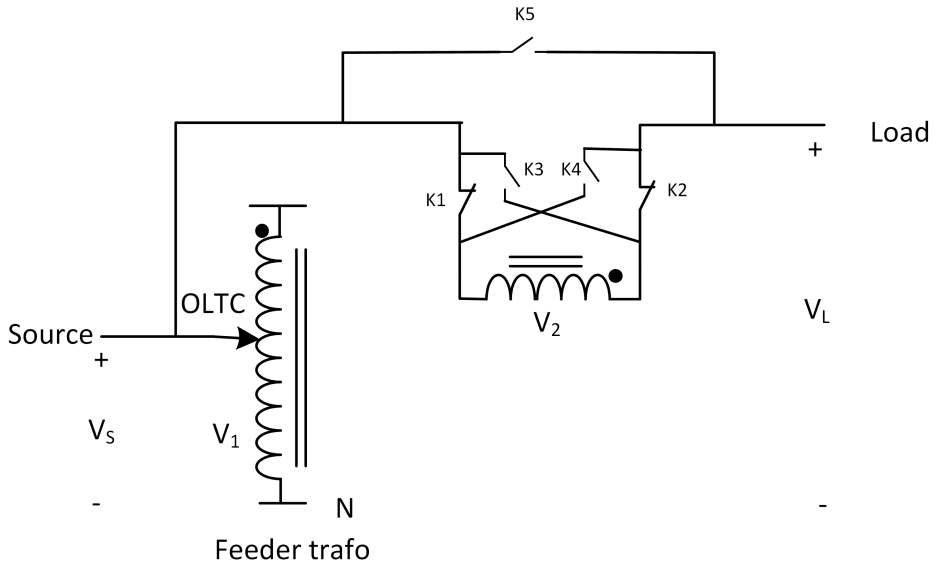

Figure 4.11: Single phase LVR configuration with OLTC on the primary side of the feeder transformer

feeder transformer. The main aspect to be noted in this configuration is the voltage that needs to be controlled is inversely proportional to the number of turns in the winding that can be controlled. Assuming the input voltage to be 1 p.u., The relationship between the primary to secondary turns ratio and series voltage is shown in the graph below.

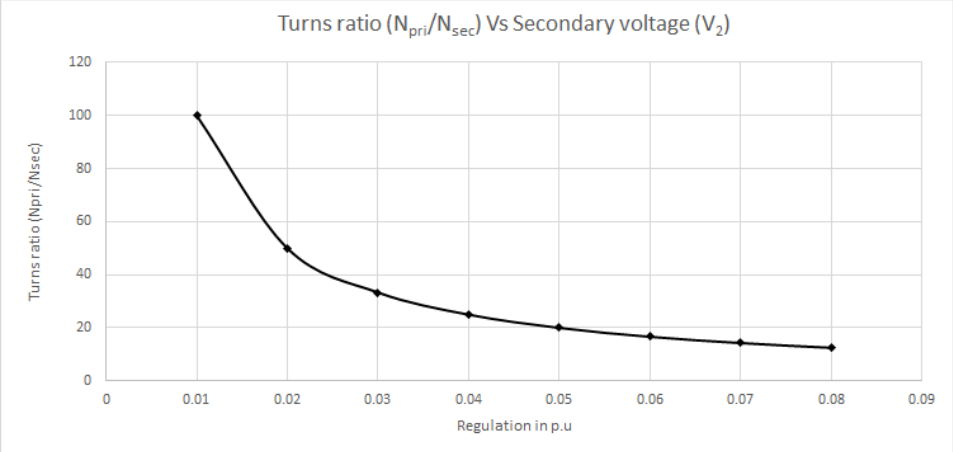

Figure 4.12: Turns ratio Vs Regulation voltage (V_2) for OLTC on the primary side of the feeder transformer

It is very important to note that to change the voltage regulation from 1 % to 2%, the OLTC has to move 50* N_{sec} on the primary side. For further increment in voltage regulation, the number of turns that the OLTC has to move starts to decrease. Due to this effect, the taps on windings should be placed in a non-linear fashion. This also makes the tap to tap (tap - tap) voltage vary for each tap change instead of a constant tap - tap voltage. The tap - tap voltage for a voltage regulation change from 2 % to 1% is very large compared to tap - tap voltage for a voltage regulation change from 8 % to 7%. The calculation for tap - tap voltage for different change in regulation voltage can be derived as follows:

$$N_{pri(8\%)} = 12.5N_{sec} \qquad N_{pri(2\%)} = 50N_{sec}$$
$$N_{pri(7\%)} = 14.285N_{sec} \qquad N_{pri(1\%)} = 100N_{sec}$$
$$\Delta V_{tap(8\%\rightarrow 7\%)} = \frac{V_{pri} * (N_{pri(7\%)} - N_{pri(8\%)})}{N_{pri(8\%)}} \qquad \Delta V_{tap(2\%\rightarrow 1\%)} = \frac{V_{pri} * (N_{pri(1\%)} - N_{pri(2\%)})}{N_{pri(2\%)}}$$
$$\Delta V_{tap(8\%\rightarrow 7\%)} = 0.1428 * V_{pri} \qquad \Delta V_{tap(2\%\rightarrow 1\%)} = 1 * V_{pri}$$

It is clearly seen that the tap-tap voltage for (2% → 1%) and (8% → 7%) is almost 7 times more. This can be particularly difficult for the ECOTAP OLTC to handle as it is designed for a constant (825 V) low tap - tap step voltage.

As the OLTC is on the primary side of the feeder transformer, the volts per turn of the feeder transformer will not be constant for different operating points. It was noted in sec. 4.2, the volts per turn should remain almost constant to avoid saturation of the core of the transformer. We can evaluate volts per turn for different operating points to understand the value for which the core should be designed to avoid saturation of the core material.

$$(\frac{Volts}{Turn}) \propto B_m A_m$$
$$(\frac{Volts}{Turn})_{8\%} = \frac{V_{pri}}{12.5 * N_{sec}} = 0.08 * \frac{V_{pri}}{N_{sec}}$$
$$(\frac{Volts}{Turn})_{1\%} = \frac{V_{pri}}{100 * N_{sec}} = 0.01 * \frac{V_{pri}}{N_{sec}}$$
$$(\frac{Volts}{Turn})_{8\%} = 8 * (\frac{Volts}{Turn})_{1\%}$$

The volts per turn for 8% regulation is much higher than volts per turn for 1% regulation. To compensate for this effect, the area of the core (A_{core}) should be sized for 8% regulation and not for 1 % regulation. This can make the core bigger and make the transformer more expensive and bigger in size.

As it can be seen in the fig.4.11, medium voltage power switches are required to perform regulation voltage reversal. When switch K1 & K2 are connected, positive voltage regulation is performed by adding the regulation voltage to the input voltage. When switch K3 & K4 are connected, negative voltage regulation is performed by subtracting the regulation voltage to the input voltage. The switch K5 is provided to bypass the current and avoid an open line circuit when the regulation voltage reversal takes places.

The key takeaways from this configuration are:

- It requires MV switches to perform series voltage reversal.
- Feeder transformer is an autotransformer which can lead to cost savings. But over-sizing of the core can offset the cost savings as it requires more core material.
- ECOTAP OLTC cannot be used due to large tap -tap voltage required for lower voltage regulation.
- Series voltage regulation cannot be made zero as it requires infinite number of turns (ideally) on the primary side of the feeder transformer.

This configuration is not considered for the final comparison as it is not compatible with the ECOTAP VPD OLTC. Due to the large tap-tap voltage, regular mechanical OLTC is not available for this configuration.

4.5.2. OLTC on the secondary side of the feeder transformer

With the OLTC on the secondary side of the feeder transformer, reversal of voltage can be achieved by either using contactors or by center tapped secondary transformer. Each LVR configuration is dealt with separately to understand the advantages and disadvantages.

LVR configuration 1:

Fig. 4.13 shows the LVR configuration for OLTC on the secondary side of the feeder transformer, i.e., OLTC is on the series winding in-line with the MV network. The relationship between the induced secondary voltage/ series compensation voltage and primary voltage with the OLTC can be derived as follows:

$$V_2 = V_1 * \frac{N_{sec}(OLTC)}{N_{pri}} \tag{4.16}$$

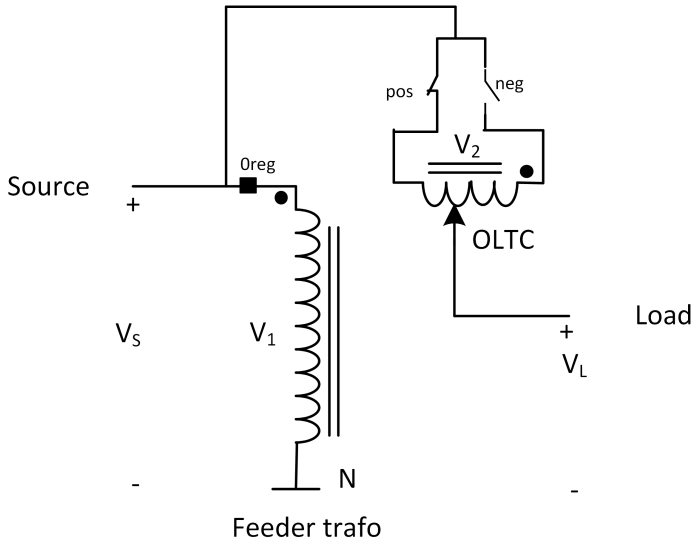

Figure 4.13: Single phase LVR configuration with OLTC on the secondary side of the feeder transformer with contactors for voltage reversal

The number of selected turns in the secondary winding depends on the OLTC position which is represented as $N_{sec}(OLTC)$. As the OLTC is present on the secondary side of the feeder transformer where the voltage needs to be regulated for the LVR, the relationship is directly proportional, making the control and design much simpler compared to the OLTC on the primary side of the transformer. This configuration is widely manufactured by many companies (VR-1 series from GE, JFR series from Siemens) and used in the distribution network.

ECOTAP OLTC can be used in this configuration but its applicability is limited to medium voltage low power networks where the line current is limited to a maximum of 100 A. The maximum line power this configuration can handle is limited by the rated OLTC current. The maximum line power this configuration can handle for a 20 kV line can be derived as follows:

$$S_{max.\,line} = \sqrt{3} * V_S * I_{OLTC\,rated}$$
$$S_{max.\,line} = \sqrt{3} * 20kV * 100A = 3.4\ MVA$$

MV contactors are required apart from the ECOTAP OLTC to perform the series voltage reversal for negative voltage regulation as it lacks an inbuilt reversing switch. As it can be seen in the fig. 4.13, when the contactor 'pos' is in ON condition, the voltage on the load side is higher than the source side due to positive voltage regulation by the LVR. When the contactor 'pos' is in OFF condition, and contactor 'neg' is in ON condition, the voltage on the load side is lower than the source side due to negative voltage regulation by the LVR. As both the contactors are directly connected to the MV network, the contactors should be rated for the corresponding MV level.

The '0reg' point indicates the location at which the OLTC shall move when there is no voltage regulation required or when the sign change of the voltage regulation has to occur. When the regulation changes from positive to negative, to avoid opening the line, OLTC will bypass the series winding by moving to '0reg' shown in the fig. 4.13.

A total of 5 taps is required to achieve $\pm 6\%(\pm 1.5\% * 4)$ voltage regulation. Each tap contributes to 1.5 % of voltage regulation with a 0reg tap for zero voltage regulation in the line. The main advantage of having less number of taps is the ease of manufacturing the transformer. Both the primary and secondary winding is exposed to 20 kV medium voltage. Hence, the primary side winding and the secondary side winding should have a voltage insulation level for 20 kV MV level. Assuming the primary side voltage level to be constant at 20 kV, the secondary side transformer windings should be designed for the voltage derived as follows:

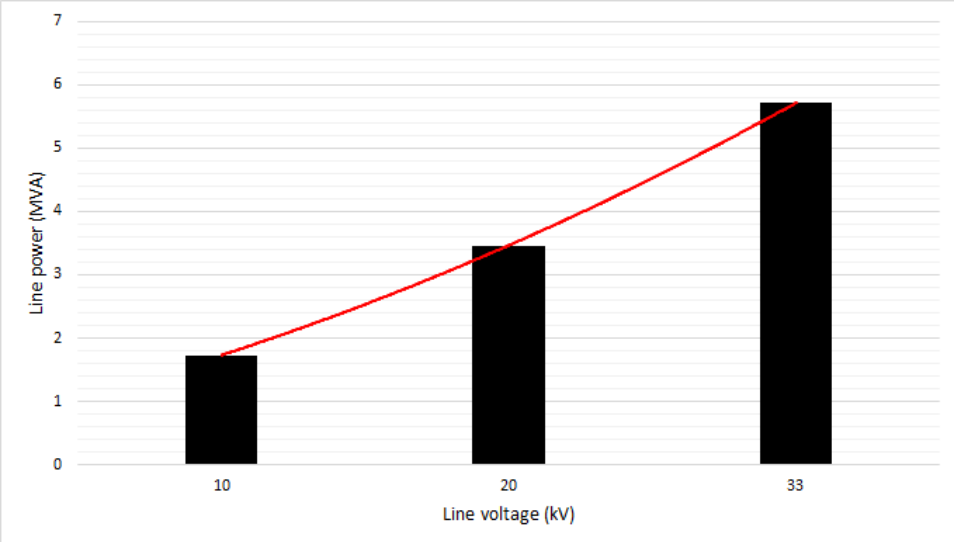

Figure 4.14: Maximum line power that the LVR configuration 1 can handle for the respective line voltage

$$V_{feed.\ sec.(ph-ph)} = Max.Reg(pu) * V_{1(ph-ph)}$$
$$V_{feed.\ sec.(ph-ph)} = 0.06 * 20\ kV = 1200\ V$$
$$\Delta V_{tap} = \frac{V_{feed.\ sec.(ph-ph)}}{N_{taps} - 1}$$
$$\Delta V_{tap} = \frac{1200}{4} = 300V$$

The feeder secondary voltage $V_{feed.\ sec.(ph-ph)}$ should be rated at 1200 V for this configuration with a per-tap voltage (ΔV_{tap}) of 300 V. Table 4.4 shows the main technical parameters related to this configuration. The current rating of the windings will depend on the power rating of the LVR and the line. For a 20 kV network, the maximum power of the line this configuration can handle is around 3.4 MVA.

Table 4.4: Technical parameters for LVR configuration 1

Feeder Trafo		Booster Trafo		No. of MV contactors	Max. line power (MVA)
Primary (kV)	Secondary (kV)	Primary (kV)	Secondary (kV)		
20	1.2	-	-	2	3.4

The key takeaways from this configuration are:

- It requires two MV contactors to perform series voltage reversal.
- Feeder transformer is an autotransformer which can lead to savings in copper and core material.
- ECOTAP OLTC's applicability is limited by the current rating and can be used only for line current less than 100A.

LVR configuration 2:
Fig. 4.15 shows the LVR configuration with secondary side of the feeder autotransformer center tapped to avoid the MV contactors. The center tap of the secondary winding is the point at which there will be no voltage regulation. As the feeder transformer is an autotransformer, when the OLTC is connected to the center tap, there is no magnetic action in the transformer and the whole power is transferred via electrical connections. N_{pri} is the number of turns from the point where the source is connected to the neutral point, number of turns on the secondary side is $N_{sec}(OLTC)$ which is a variable due to the presence of OLTC. Due to autotransformer arrangement, secondary windings used for negative voltage regulation is a part of the primary

windings. This leads to savings in copper material. Windings on the secondary side is from the point '0reg' to the 'pos' for the positive regulation and '0reg' to the 'neg' for the negative regulation as indicated in the schematic diagram. The voltage relationship can be given as follows for the OLTC located between '0reg' and 'pos':

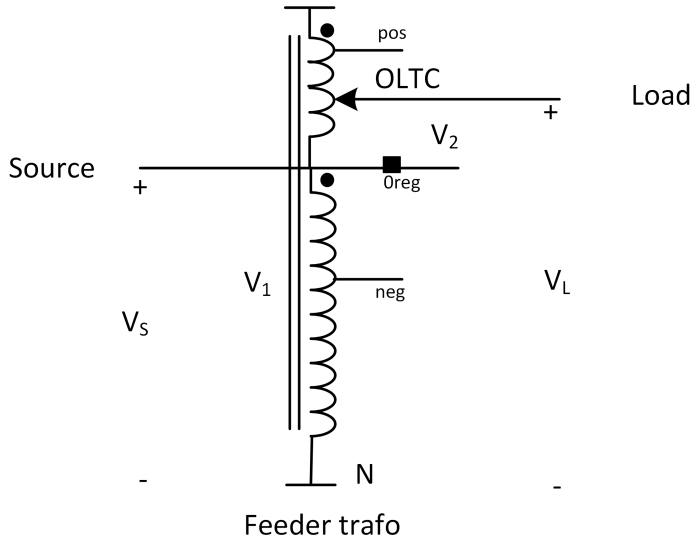

Figure 4.15: Single phase LVR configuration with OLTC on the center-tap secondary side of the feeder transformer

$$V_2 = V_1 * \frac{N_{sec}(OLTC)}{N_{pri}}$$

The voltage relationship can be given as follows for the OLTC located between '0reg' and 'neg':

$$V_2 = -V_1 * \frac{N_{sec}(OLTC)}{N_{pri}}$$

The load voltage V_L is the sum of source voltage and the induced secondary side voltage/ series compensation voltage V_2 of the transformer. It can be given as follows:

$$V_L = V_S + V_2$$

As the OLTC is present on the secondary side of the feeder transformer, the relationship between secondary voltage and the OLTC position on the secondary winding is linear. But the main advantage of this configuration is that there is no requirement of any MV contactors to do voltage reversing operation. This configuration's applicability is limited to network with line current less than 100 A. The maximum line power it can handle is 3.4 MVA, similar to LVR configuration 1.

The point '0reg' acts as the bypass point when no voltage regulation is required by the LVR. A total of 9 taps is required to achieve $\pm 6\%(\pm 1.5\% * 4)$ voltage regulation. As there are no MV contactors used for series voltage reversal, 9 taps are required to achieve both positive and negative voltage regulation. The manufacturing becomes a bit complex with more taps in the transformer. Both the primary and secondary windings are exposed to 20 kV medium voltage. Hence, the primary side winding and the secondary side winding should have a voltage insulation level for 20 kV MV level. Assuming the primary side voltage level to be constant at 20 kV, the maximum secondary side voltage for positive or negative voltage regulation should be designed for the voltage derived as follows:

$$V_{feed.\ sec.(ph-ph)} = Max.Reg(pu) * V_S$$
$$V_{feed.\ sec.(ph-ph)} = 0.06 * 20\ kV = 1200\ V$$
$$\Delta V_{tap} = \frac{V_{feed.\ sec.(ph-ph)}}{((N_{taps} - 1)/2)}$$
$$\Delta V_{tap} = \frac{1200}{4} = 300V$$

The feeder secondary voltage $V_{feed.\ sec.(ph-ph)}$ should be rated at 1200 V. In this configuration, 4 taps are used for positive voltage regulation, 4 taps are used for negative voltage regulation and 1 tap is used for zero voltage regulation. Hence while calculating ΔV_{tap} for this configuration, the no. of taps is subtracted with 1 to exclude the zero voltage regulation tap and divided by 2 to account for positive and negative voltage regulation. For this configuration the per-tap voltage (ΔV_{tap}) is 300 V. Table 4.4 shows the main technical parameters related to this configuration. The current rating of the windings will depend on the power rating of the LVR and the line. For a 20 kV network, the maximum power of the line this configuration can handle is 3.4 MVA. Table 4.5 shows all the technical parameters pertaining to this configuration. The secondary voltage considered in the table is only the voltage between the point '0reg' to 'pos' and not the voltage between point 'neg' and 'pos' marked in the fig. 4.15. This is done as the windings between point '0reg' to 'neg' is a part of the feeder primary windings.

Table 4.5: Technical parameters for LVR configuration 2

Feeder Trafo		Booster Trafo		No. of MV contactors	Max. line power (MVA)
Primary (kV)	Secondary (kV)	Primary (kV)	Secondary (kV)		
20	1.2	-	-	0	3.4

The key takeaways from this configuration are:

- It does not require MV contactors to perform series voltage reversal.
- Feeder transformer is an autotransformer which can lead to savings in copper and core material.
- ECOTAP OLTC's applicability is limited by the current rating and can be used only for line current less than 100A.

4.6. Two active parts LVR configuration

In this section, LVR configuration with two active parts are discussed in detail. Two active parts design consists of two transformers- a feeder transformer and a booster transformer. The feeder transformer is the shunt transformer which converts the incoming medium voltage to a suitable voltage on the secondary side. The secondary side of the feeder transformer is given as the input to the primary side of the booster transformer. Secondary side of the booster transformer is placed in series to the line to perform the voltage regulation operation. If the booster transformer is providing a voltage regulation of X% or (X/100)pu and assuming the load current is 1 pu, the rated power of the series transformer will be (X/100)pu. As the feeder transformer is providing that power to the booster transformer, feeder transformer is also rated at (X/100) pu. As opposed to the single active part design where it requires only one transformer, two active parts design of LVR will require an additional (X/100)pu transformer. This will increase the cost of the LVR as an additional active part of the same rating is required in this case.

The following subsection has been divided based on the reversal techniques used in the configuration. One of the disadvantage of single active part design was the applicability of the OLTC was limited to the line current irrespective of the voltage of the line. To completely utilize the OLTC in a configuration, it should operate at a rated step capacity. Step capacity is defined as the product of step voltage and rated current of the OLTC. The value of the OLTC step capacity and rated current is taken from the table 4.3. It is given as follows for ECOTAP VPD III 100 OLTC:

$$Stepcapacity = V_{step} * I_{rated} = 82500VA$$

For e.g, a 20 kV, 6% voltage regulation for LVR configuration 1 and LVR configuration 2 will have a step capacity as follows:

$$V_{regmax} = \frac{20kV * 0.06}{\sqrt{3}}$$
$$V_{regmaxstep} = \frac{V_{regmax}}{4}$$
$$Stepcapacity = V_{regmaxstep} * I_{rated} = 17321VA$$

Where V_{regmax} is the maximum per phase regulation voltage, $V_{regmaxstep}$ is the maximum per phase step voltage. As it can be seen, only 21 % of the OLTC step capacity has been utilized for the maximum rated power capacity of the single active part configuration. The main advantage with the two active parts design is that by converting the feeder voltage to a suitable voltage and current level, the OLTC can be made to operate at rated step capacity. By operating the OLTC at rated step capacity, the operating power range can be increased for the LVR compared to single active part LVR! The analysis is carried out for a 20 kV, ±6% (± 1.5% * 4) line voltage regulator. The regulation voltage is divided into steps of 4 with each step contributing to 1.5% of the line voltage.

4.6.1. LVR with reversing switches on the secondary side of the feeder transformer

This subsection deals with two active parts LVR configuration with reversing switches to achieve voltage regulation. The voltage reversal can be achieved by using two MV contactors. One important aspect to be considered while evaluating this design with contactors is to have a path for the current flow in the primary side of the booster transformer when the polarity for voltage compensation is reversed. As there is a current flowing through the secondary side of the booster transformer, there should always be a closed path on the primary side of the booster transformer. This subsection focuses on reversing switches on the secondary side of the feeder transformer.

LVR configuration 3:

Fig:4.16 shows the two active parts LVR configuration with a two winding feeder transformer and two winding booster transformer. The OLTC is placed on the secondary side of the feeder transformer. The reversing switches are placed before the connection between secondary feeder and primary booster transformer. The relationship between the feeder voltage and and the series regulation voltage can be given as follows:

$$V_{1T} = V_1 * \frac{N_{sec}(OLTC)}{N_{pri}} \tag{4.17}$$
$$V_{2T} = \pm V_{1T} \tag{4.18}$$
$$V_2 = V_{2T} * \frac{N_{Bsec}}{N_{Bpri}} \tag{4.19}$$

The contactor marked with 'neg' will connect the feeder secondary to booster primary in a such a fashion that the series booster transformer will provide negative voltage regulation and with 'pos' contactor it will provide positive voltage regulation. The voltage reversal transition should be made in a such a way that there is no open circuit created on the primary side of the feeder transformer. If there is an open circuit, then a huge voltage will be developed on the primary side of the booster transformer, which can potentially destroy the insulation of the transformer. When the voltage reversal takes place, both the contactors should be switched ON for a brief amount of time to avoid an open circuit.

A total of 5 taps is required to achieve ±6% regulation in steps of 1.5%. The same taps are used for both positive and negative voltage regulation due to the presence of contactors. The secondary side of the feeder transformer voltage should be designed based on the rated step capacity of the ECOTAP VPD III OLTC to utilize the complete rated capacity of the OLTC. A small change is made in the OLTC connection to the secondary side of the feeder transformer. Alternative switches of the OLTC is connected to the taps on the feeder transformer to increase the power handling capability of the LVR configuration. The secondary side of the feeder transformer voltage and the tap-tap voltage can be derived as follows:

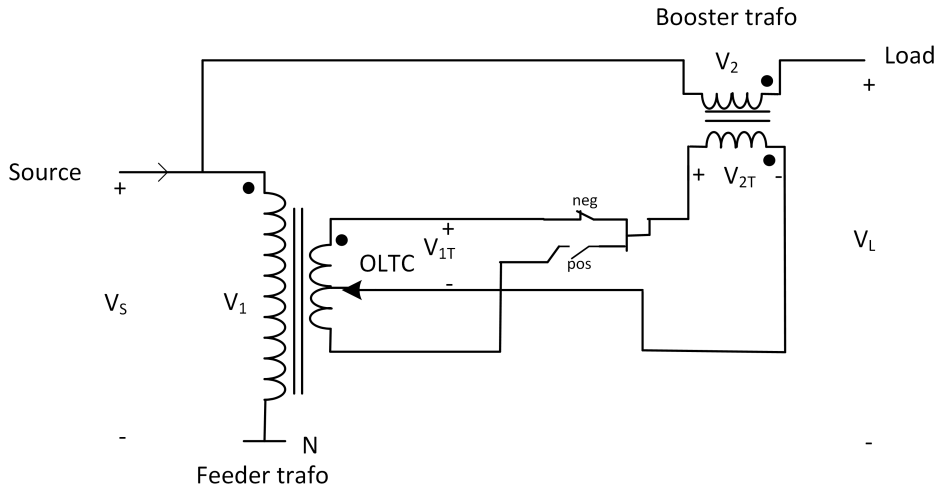

Figure 4.16: Single phase LVR two active parts configuration with OLTC on the secondary side of the feeder transformer and MV contactors for voltage reversal

$$V_{feed.\ sec.(ph-ph)} = \sqrt{3} * V_{step} * (N_{taps} - 1) * 2$$
$$V_{feed.\ sec.(ph-ph)} = 11432.5V$$
$$\Delta V_{tap} = V_{step} * 2$$
$$\Delta V_{tap} = 1650V$$

It can be seen that the per phase tap-tap voltage (ΔV_{tap}) is 1650 V. As the only alternative OLTC switches are connected to the secondary side of the feeder transformer, there are two OLTC switches between 2 taps. This will ensure that the OLTC step voltage of 825 V is not violated during the operation. The contactors voltage rating will be dependent on the secondary feeder voltage. The contactors should be rated for a phase-phase RMS voltage of 11432.5 V or per phase RMS voltage of 6600 V. As the contactors are isolated from the 20 kV MV, it will be less expensive due to lower insulation requirements and lower short circuit current requirements.

Assuming the line voltage to be at 20 kV, the voltage ratings for booster transformer can be derived as follows:

$$V_{booster.\ pri.(ph-ph)} = V_{feed.\ sec.(ph-ph)}$$
$$V_{booster.\ pri.(ph-ph)} = 11432.5V$$
$$V_{booster.\ sec.(ph-ph)} = Max.Reg(pu) * V_S$$
$$V_{booster.\ sec.(ph-ph)} = 1200V$$

The power range for this configuration of LVR will be independent of the current and voltage rating of the network. The maximum power this configuration can handle depends on the rated step capacity of the ECOTAP VPD III OLTC and the regulation range. For a LVR with ±6% voltage regulation, it can be derived as follows:

$$S_{max.\ line} = \frac{V_{step} * I_{rated} * (N_{OLTC\ switches} - 1) * 3}{Max.Reg.(pu)}$$
$$S_{max.\ line} = \frac{825V * 100A * 8 * 3}{0.06} = 33MVA$$

The maximum line power as a function of voltage regulation percentage that the LVR can handle is shown in the fig. 4.17. The function for $S_{max.\ line}$ derived in the equation is used to plot the graph. As it can be

seen in the graph, OLTC's capability is fully exploited to use the LVR for higher line power. Table 4.6 shows all the technical parameters related to this configuration. The current rating of the windings will depend on the power rating of the line.

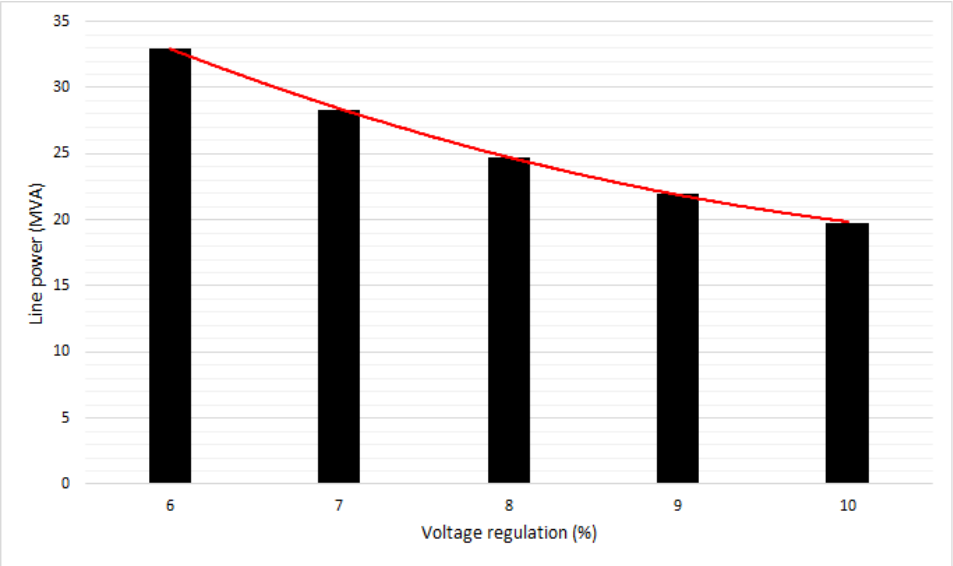

Figure 4.17: Maximum line power that the LVR configuration 3 & 4 can handle for the respective percentage of voltage regulation

Table 4.6: Technical parameters for LVR configuration 3 (‡ - Contactors are rated for 11.4kV level)

Feeder Trafo		Booster Trafo		No. of MV contactors	Max. line power (MVA)
Primary (kV)	Secondary (kV)	Primary (kV)	Secondary (kV)		
20	11.4	11.4	1.2	$2^{‡}$	33

The key takeaways from this configuration are:

- It requires contactors to perform series voltage reversal. It should be rated for the current and voltage of the secondary side of the feeder transformer and not to the MV network level.
- Feeder transformer is a two winding transformer and it needs an extra booster transformer to perform voltage regulation.
- ECOTAP OLTC's applicability is limited only by the rated step capacity of the OLTC, and it can be fully utilized due to the intermediate transformation by the feeder and booster transformer. Ideally the LVR can be used for network power up to 33 MVA with 6% voltage regulation.

LVR configuration 4:
Fig. 4.18 shows the two active parts LVR configuration with a feeder autotransformer and two winding booster transformer. The OLTC is placed on the secondary side of the feeder transformer. The reversing switches are placed before the connection between secondary feeder and primary booster transformer. The relationship between the feeder voltage and and the series regulation voltage can be given as follows:

$$V_{1T} = V_1 * \frac{N_{sec}(OLTC)}{N_{pri}} \tag{4.20}$$

$$V_{2T} = \pm V_{1T} \tag{4.21}$$

$$V_2 = V_{2T} * \frac{N_{Bsec}}{N_{Bpri}} \tag{4.22}$$

The above relationship is similar to one derived for the LVR configuration 3. N_{pri} is the common winding in the autotransformer. The secondary winding is connected to the OLTC, thereby making its effective turns

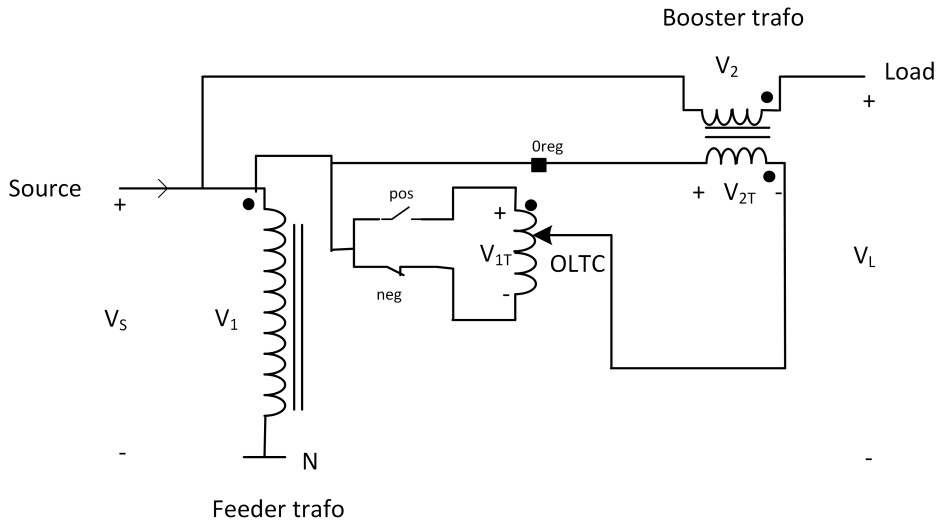

Figure 4.18: Single phase LVR two active parts configuration with OLTC on the secondary side of the feeder autotransformer

controllable.
The reversing contactors are connected via the common winding to the series winding in the autotransformer. As per the dot convention, when 'neg' contactor is connected, the voltage at the load end will be less than the source end. The '0reg' contact will be used by the OLTC when the voltage reversal takes place so that there will be no open circuit on the primary side of the booster transformer. One important aspect to be noted in this configuration is that the contactors are exposed to the medium voltage as the autotransformers do not provide electrical isolation. As the contactors should be rated for MV network, they are more expensive than the LVR configuration 3. In LVR configuration 3, the contactors are exposed only to the secondary feeder voltage as a two winding transformer was used.

The power range for this configuration of LVR will be independent of the current and voltage rating of the network as there is an intermediate stage introduced by two active parts configuration. As the OLTC is placed on the secondary side of the feeder autotransformer, the voltage and current can be chosen in a such a way that the rated step capacity of the OLTC is utilized. Assuming the voltage and current to be 1pu on the load side of the LVR, the maximum line power as a function of voltage regulation percentage that the LVR can handle is similar to the LVR configuration 3 as shown in the fig. 4.17. As it can be seen in the graph, OLTC's step capacity is fully exploited to use the LVR for higher line power.

Table 4.7: Technical parameters for LVR configuration 4

Feeder Trafo		Booster Trafo		No. of MV contactors	Max. line power (MVA)
Primary (kV)	Secondary (kV)	Primary (kV)	Secondary (kV)		
20	11.4	11.4	1.2	2	33

The key takeaways from this configuration are:

- It requires two MV contactors to perform series voltage reversal.
- Feeder transformer is an autotransformer and it needs an extra booster transformer to perform voltage regulation. As feeder transformer is an autotransformer, savings can be realized in copper and core material.
- ECOTAP OLTC's applicability is limited only by the rated step capacity of the OLTC, and it can be fully utilized due to the intermediate transformation by the feeder and booster transformer. Ideally the LVR can be used for network power up to 33 MVA with 6% voltage regulation.

4.6.2. LVR with center tapped transformer

The previous subsection dealt with a two active parts design with contactors for voltage reversal. There is another possibility to avoid contactors and still perform voltage reversal in a LVR. It can be achieved by using

the center tap of the secondary side of the feeder transformer as the common winding to the primary of the booster transformer. The economical advantage of this design will be the possibility to use the OLTC to its rated step capacity and avoid the use of reversing switches.

LVR configuration 5

Fig. 4.19 shows the two active parts LVR configuration with a two winding feeder transformer with center tap on secondary winding and a two winding booster transformer. The center tap from the secondary winding of the feeder transformer is connected to the one end of the booster transformer. OLTC is located on the secondary winding of the feeder transformer. The relationship for this configuration can be given as follows:

$$V_{1T} = V_1 * \frac{N'_{sec}(OLTC)}{N_{pri}} \tag{4.23}$$

$$N'_{sec} = \frac{N_{sec}}{2} \tag{4.24}$$

$$V_{2T} = \pm V_{1T} \tag{4.25}$$

$$V_2 = V_{2T} * \frac{N_{Bsec}}{N_{Bpri}} \tag{4.26}$$

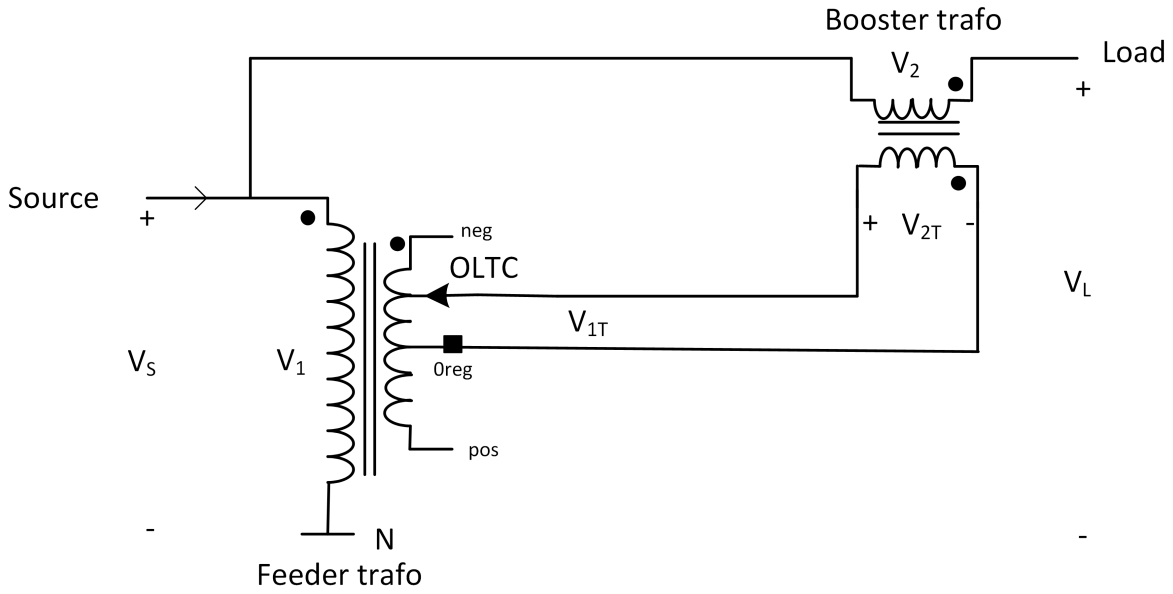

Figure 4.19: Single phase LVR two active parts configuration with OLTC on the secondary side of the center tapped feeder transformer

N'_{sec} is the effective number of turns used for positive/ negative regulation. As indicated by the label 'pos' & 'neg' in the fig. 4.19, eq. 4.25 will be positive for the OLTC position between '0reg' and 'pos', and negative for the OLTC position between '0reg' and 'neg'. When the OLTC position moves to '0reg' there will zero voltage compensation and the current circulates in the primary side of the booster transformer. This position is important so that there is no open circuit is created when the regulation changes the sign (voltage reversal).

As the voltage reversal is achieved by the use of center tap transformer, contactors for reversing the series voltage is not required. This has a huge economical benefit as the medium voltage contactors are expensive due to insulation requirements. A total of 9 taps are required to achieve ±6% voltage regulation in steps of 1.5 %. Out of the 9 contacts available in total from the ECOTAP OLTC, 1 tap is assigned to 0reg (zero regulation), and a total of 4 taps are available for positive and negative regulation respectively. The secondary side of the feeder transformer voltage should be designed based on the rated step capacity of the OLTC to enable the LVR configuration for higher power handling capability. The feeder secondary rated voltage and the tap-tap voltage are given as follows:

$$V_{feed.\ sec.(ph-ph)} = \sqrt{3} * V_{step} * (N_{taps} - 1)$$
$$V_{feed.\ sec.(ph-ph)} = \sqrt{3} * 825 * 8 = 11432.5V$$
$$\Delta V_{tap} = V_{step} = 825V$$

The voltage V_{1T} is divided equally for positive and negative voltage regulation for center tap configuration. For a 20 kV line, voltage ratings for the booster transformer can be derived as follows:

$$V_{booster\ pri.(ph-ph)} = \frac{V_{feed.\ sec.(ph-ph)}}{2}$$
$$V_{booster\ pri.(ph-ph)} = 5716.2V$$
$$V_{2(ph-ph)} = Max.Reg(pu) * V_S$$
$$V_{2(ph-ph)} = 1200V$$

The main advantage of using two active part design is to utilize the OLTC at the rated step capacity. As there is a center tap and only half of the winding is used for positive compensation and the other half is used for negative compensation, the rated power is pumped through half of the winding. Due to this reason, the effective voltage compensation for a given line power is reduced compared to the LVR with two active parts and reversing switch configuration. The maximum line power that can be handled can be derived as follows:

$$S_{max.\ line} = \frac{V_{step} * I_{rated} * ((N_{taps} - 1)/2) * 3}{Max.Reg.(pu)}$$
$$S_{max.\ line} = \frac{825V * 100A * 4 * 3}{0.06} = 16.5MVA$$

The maximum line power as a function of regulation percentage that this LVR confiuration can handle is shown in the fig. 4.20. The maximum line power this configuration can handle for ±6% voltage regulation is 16.5 MVA. Higher voltage regulation percentage will reduce the maximum power handling capability of the LVR. Table 4.8 shows all the technical parameters related to this LVR configuration 5.

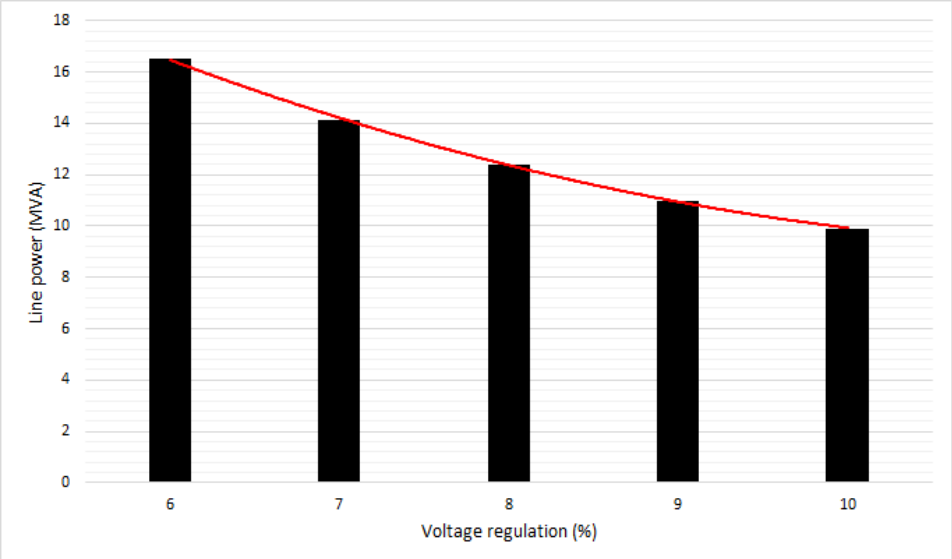

Figure 4.20: Maximum line power that the LVR configuration 5 & 6 can handle for the respective percentage of voltage regulation

The key takeaways from this configuration are:

- It does not require MV contactors to perform series voltage reversal.

Table 4.8: Technical parameters for LVR configuration 5

Feeder Trafo		Booster Trafo		No. of MV	Max. line
Primary (kV)	Secondary (kV)	Primary (kV)	Secondary (kV)	contactors	power (MVA)
20	11.4	5.72	1.2	0	16.5

- Feeder transformer is a two winding transformer and it needs an extra booster transformer to perform voltage regulation.
- ECOTAP OLTC's applicability is limited only by the rated step capacity of the OLTC, and it can be fully utilized due to the intermediate transformation by the feeder and booster transformer. Ideally the LVR can be used for network power up to 16.5 MVA with 6% voltage regulation.

LVR configuration 6

Fig. 4.21 shows the two active parts LVR configuration with a feeder autotransformer with center tap on secondary winding and a two winding booster transformer. The center tap from the secondary winding of the feeder transformer is connected to the one end of the booster transformer. OLTC is located on the secondary winding of the feeder transformer. As a part of primary winding is used as secondary winding in the feeder autotransformer, savings can be realized in copper and core material. The voltage at the point 'neg' marked in the fig. 4.21 is V_1. The total number of turns in the feeder transformer is N_{pri}. The number of turns between 'neg' to '0reg' and the number of turns between 'pos' to '0reg' is equal to $N'sec$. The voltage at the point '0reg' is given as:

$$V_{0reg} = V_1 - (\frac{N'sec}{N_{pri}}) * V_1$$

The voltage at the point 'pos' is given as:

$$V_{pos} = V_1 - (\frac{2 * N'sec}{N_{pri}}) * V_1$$

As the reference voltage for the primary side of the booster transformer is given from the '0reg' point, OLTC is able to create positive and negative voltages across the booster transformer. The relationship between the input and output voltage is given as follows:

$$V_{1T} = V_1 * \frac{N'_{sec}(OLTC)}{N_{pri}} \tag{4.27}$$

$$V_{2T} = \pm V_{1T} \tag{4.28}$$

$$V_2 = V_{2T} * \frac{N_{Bsec}}{N_{Bpri}} \tag{4.29}$$

No contactors are required to perform series voltage reversal. When the OLTC position moves to '0reg' there will be zero voltage compensation and the current circulates in the primary side of the booster transformer. This avoids an open circuit on the primary side of the booster transformer while the voltage reverses. As the insulation level of OLTC is 36 kV, it can handle the network voltage level in this design even though the electrical isolation is lost.

Out of the total 9 contacts from the ECOTAP OLTC, 1 contact is assigned to 0reg (zero regulation), and a total of 4 contacts are available for positive and negative regulation respectively.

Table 4.9: Technical parameters for LVR configuration 6

Feeder Trafo		Booster Trafo		No. of MV	Max. line
Primary (kV)	Secondary (kV)	Primary (kV)	Secondary (kV)	contactors	power (MVA)
20	11.4	5.72	1.2	0	16.5

The key takeaways from this configuration are:

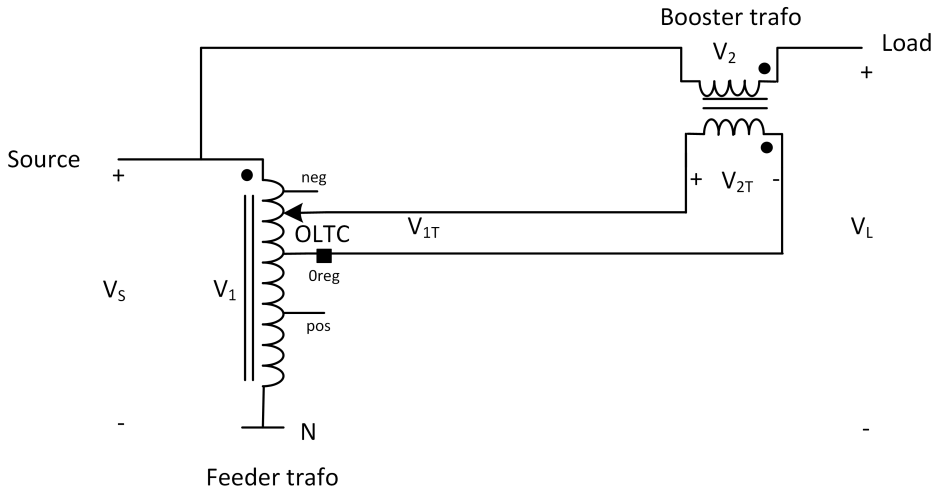

Figure 4.21: Single phase LVR two active parts configuration with OLTC on the secondary side of the center tapped feeder autotransformer

- It does not require MV contactors to perform series voltage reversal.
- Feeder transformer is an autotransformer and it needs an extra booster transformer to perform voltage regulation. As feeder transformer is an autotransformer, savings can be realized in copper and core material.
- ECOTAP OLTC's applicability is limited only by the rated step capacity of the OLTC, and it can be fully utilized due to the intermediate transformation by the feeder and booster transformer. Ideally the LVR can be used for feeder power up to 16.5 MVA with 6% voltage regulation.

4.7. Comparison of LVR configurations

In this section all the LVR configurations are compared based on the range of operation and its cost effectiveness. The one active part LVR configuration with the OLTC on the primary side of the feeder transformer is not considered for comparison as the ECOTAP OLTC cannot be used due to the large tap-tap voltage and other disadvantages elaborated in the subsection 4.5.1. ECOTAP OLTC can be used for all the other LVR configuration discussed. As ECOTAP OLTC has vacuum interrupters, the voltage regulators will have lesser maintenance than the other existing oil-type series voltage regulators which employs oil-type interrupter. Table 4.10 shows the main technical parameters related to different LVR configurations with ±6% voltage regulation for a 20kV feeder line.

Table 4.10: Technical parameters for a 20kV, ±6% LVR configurations (‡ - Contactors are rated for 11.4kV level, † - Feeder is an autotransformer)

Config.	Feeder Trafo		Booster Trafo		No. of MV contactors	Max. line power (MVA)
	Pri. (kV)	Sec. (kV)	Pri. (kV)	Sec. (kV)		
1†	20	1.2	-	-	2	3.7
2†	20	1.2	-	-	0	3.7
3	20	11.4	11.4	1.2	2	33
4†	20	11.4	11.4	1.2	2‡	33
5	20	11.4	5.72	1.2	0	16.5
6†	20	11.4	5.72	1.2	0	16.5

To select the economical configuration, cost of each configuration needs to be individually evaluated. As determining the exact cost depends on various factors, a heuristic approach is used to estimate cost percentages to give a basis for selecting an economical configuration. In general there are four main components in a LVR - feeder transformer, booster transformer, tap changers with contactors, and the enclosure of the system.

The main assumption made to calculate the relative cost percentage is the individual cost contribution of a component to the overall cost of the configuration. For e.g., a transformer will not cost the same as the enclosure in a system. To account for this difference, a weightage factor is assigned to account for the contribution of the component to the overall cost. The cost contribution of each component to the overall cost of the LVR is shown in the table 4.11.

Components	Cost contribution (%)
Feeder transformer	30
Booster transformer	30
OLTC and contactors	30
Enclosure	10
Total	100

Table 4.11: Individual cost contribution of each component to the overall cost of the LVR

LVR configuration 5 (Center-tapped feeder transformer and booster transformer with ECOTAP OLTC) is taken as the reference (100%) based on which the relative cost percentage of the other configurations are determined. Not all the configurations has the same individual components. For e.g., configuration using an feeder autotransformer is cheaper than the configuration using a two winding transformer. This will result in differences in the cost of the overall system. To account for this difference, an individual cost percentages is assigned within the component category. The individual cost percentage of different components is shown in table 4.12. The values are only an approximate indication and are assigned based on discussion with ABB. In each component, one type is taken as the reference cost(100%) and the cost of the other types are determined relative to the reference. Taking the two winding transformer as the reference (100%), if the feeder transformer is constructed with an autotransformer, a relative cost of 80 % is given due to the savings realized in the copper and core. The reflection of this copper and core savings depends on various factor such as the cost of the material, which varies based on the market situation.

Feeder transformer	Individual cost (%)
Two winding transformer (Reference)	100
Autotransformer	80

Booster transformer	Individual cost (%)
Two winding transformer (Reference)	100

Enclosure	Individual cost (%)
Single active part tank	90
Two active part tank (Reference)	100

Tap changers	Individual cost (%)
ECOTAP (Reference)	100
ECOTAP with LV contactors	150
ECOTAP with MV contactors	250

Table 4.12: Individual cost(%) of different components in a LVR

The overall cost percentage of the LVR is calculated by multiplying the component's individual cost with the respective cost contribution and taking the sum for all the components. The eq.4.30 is used to calculate the overall cost of the LVR. 'C' represents the individual cost of the component taken from table 4.12 and 'W' represents the cost contribution of the respective component in a particular category taken from the table 4.11.

$$Overall\ Cost = \frac{\sum_{i=1}^{N} C_i W_i}{\sum_{i=1}^{N} W_i} \tag{4.30}$$

The cost calculation for LVR configuration 5 is shown below:

$$Overall\ Cost_{LVRconfig5} = \frac{100*30+100*30+100*30+100*10}{30+30+30+10} = 100\% \tag{4.31}$$

As the LVR configuration 5 is taken as the reference to determine relative cost of other configuration, the cost of it is 100%. For different configurations of LVR, as the individual cost of the components are varying, the overall cost of the system will vary accordingly.

Table 4.13 shows a comprehensive comparison of operating range and cost for different LVR configurations.

Configuration	Max. line power for 6% voltage regulation (MVA)			Cost (%)
	10 kV	20 kV	33 kV	
1	1.7	3.4	5.7	108
2	1.7	3.4	5.7	63
3	33	33	33	115
4	33	33	33	139
5	16.5	16.5	16.5	100
6	16.5	16.5	16.5	94

Table 4.13: LVR configuration comparison for the maximum line power for different voltage levels and relative cost percentage

The most economical design for a particular line power range can be chosen from the table 4.13 based on the design which has the lowest cost percentage. As it can be seen from the table, even though configuration 2 has the lowest cost, the line power it can handle is only 3.4 MVA for a 20kV distribution line.

LVR configurations 1 & 2 do not require any booster transformer for voltage regulation function. But, the main limiting factor in this design is the OLTC's rated current carrying capability, which limits the LVR application for small line power.

LVR configurations 5 & 6 do not require extra reversing contactors to perform voltage regulation which reduces the overall cost of the system. LVR configuration 6 is more economical as it uses autotransformer as the feeder transformer which leads to savings in copper and core material. For $\pm 6\%(1.5\% * 4)$ voltage regulation, LVR configurations 5 & 6 are capable of handling line network power up to 16.5 MVA. Above this network power, the step capacity of the OLTC will be exceeded.

For line network power above 16.5 MVA and up to 33 MVA, either configuration 3 or 4 can be utilized. Above 33 MVA, the step capaity of the OLTC will be exceeded. In LVR configuration 3, the feeder transformer is a two winding transformer but because of the electrical isolation it provides from the MV network voltage, the contactors will have a lower rating leading to cost savings. In LVR configuration 4, savings can be realized as the feeder transformer is an autotransformer, but the contactors are exposed to MV network voltage which will increase the cost of the system. LVR configuration 3 is more economical than LVR configuration 4 as per the cost calculation performed.

5

Simulation & Experimental Results of LVR

Chapter 4 discussed various LVR configurations with single and two transformer active parts. Technical and cost comparisons were made for different LVR configurations. ECOTAP VPD III 100 from Maschinenfabrik Reinhausen was the chosen mechanical OLTC for the LVR. This chapter will focus on the design and simulation of a 20 kV, 10 MVA LVR with ±6% voltage regulation. The final chosen LVR configuration should satisfy the power handling requirement and should have the lowest cost percentage. A low power experimental setup is used to verify the chosen configuration with the ECOTAP VPD III 100 OLTC.

5.1. Design of the LVR

This section deals with the design of a LVR with ±6% voltage regulation for a 20 kV, 10 MVA feeder line. LVR configurations 3, 4, 5 & 6 are suitable for this voltage and power range. As seen from the table 4.13, LVR configuration 6 is the most economical design for this feeder network level as it does not use reversing contactors, and uses a feeder autotransformer. Since the ABB's oil-transformer factory does not manufacture autotransformers for MV level, so implementing this design would require changes in the factory assembly lines. These changes in a factory assembly line will have major cost implications. LVR configuration 5 with two-winding feeder transformer is considered to avoid such costs. The only difference between LVR configurations 5 & 6 is that the former uses a two-winding transformer and latter uses an autotransformer as the feeder active part. LVR configuration 5 is designed, simulated and validated by a low power experimental setup. Fig. 5.1 shows the LVR configuration 5 that will be used in this chapter.

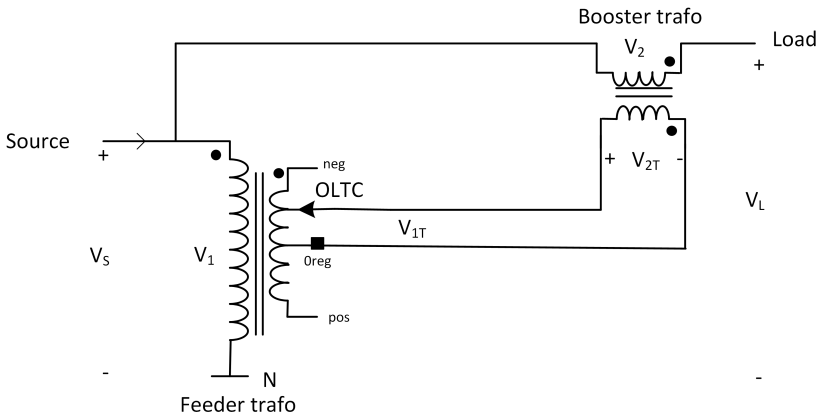

Figure 5.1: Schematic diagram of a single phase LVR configuration 5

5.1.1. Feeder and booster transformer

The ratings for the primary side of feeder transformer and the secondary side of booster transformer is determined by the network ratings and regulation range of the LVR. The power rating of the feeder and the booster transformer is calculated as follows:

$$S_{feeder} = S_{booster} = Reg.\,range(pu) * Line\ power$$
$$S_{feeder} = S_{booster} = 0.06 * 10MVA = 600kVA$$

The ratings for the primary side of the feeder transformer is calculated as follows:

$$V_{1(L-L)} = 20kV$$
$$V_{1(L-N)} = 11.54kV$$
$$I_1 = \frac{600kVA}{\sqrt{3} * 20kV} = 17.32A$$

The ratings for the secondary side of the booster transformer is calculated as follows:

$$V_{2(L-L)} = Reg.\,range(pu) * V_{1(L-L)} = 0.06 * 20kV = 1200V$$
$$V_{2(L-N)} = 692.8V$$
$$I_2 = \frac{600kVA}{\sqrt{3} * 1200} = 288.7A$$

The secondary feeder and primary booster transformer voltage should be designed to fully utilize the operating range of the OLTC. Transformers are always designed with sufficient safety or security factors to handle the over-load and transient conditions as per the network standards. But, over-voltage and over-load safety factors should be taken into consideration also for the OLTC placed on the secondary side of the feeder transformer. The maximum voltage variation above nominal voltage on MV grids as per EN 50160 is 10 %. The typical current overload seen by the line operator is 0.2 pu during 1 h every 8h [44]. If the transformer is designed for OLTCs with maximum step voltage, OLTCs will be stressed with voltages more than the rated step voltage during network over-voltages. So the step voltage or the tap-tap voltage for the secondary side of feeder transformer is designed as follows:

$$V_{Tap-Tap} = \frac{V_{OLTC\ step\ max.}}{1.1} = 750V$$
$$V_{1T(L-N)} = 8 * V_{Tap-Tap} = 6kV$$
$$V_{1T(L-L)} = \sqrt{3} * 6kV = 10.39kV$$
$$a_{feeder} = \frac{V_1}{V_{1T}} = 1.92$$

The secondary side of the feeder transformer is center tapped at 3 kV. The current rating of the secondary side of the feeder transformer is given as follows:

$$I_{1T} = \frac{600kVA}{3 * 3kV} = 66.66A$$
$$I_{Max.\ OLTC} = 100A$$
$$1.2 * I_{1T} = 80A < I_{Max.\ OLTC}$$

The current rating of the feeder transformer I_{1T} including the 20 % overload is within the maximum current the OLTC can handle ($I_{Max.\ OLTC}$).

The primary side ratings of the booster transformer can be calculated as follows:

$$V_{2T(L-N)} = 3kV$$
$$a_{booster} = \frac{V_{2T}}{V_2} = 4.33$$
$$I_1 = \frac{600kVA}{3 * 3kV} = 66.66A$$

Table 5.1: Per-phase ratings of the feeder and booster transformer

Feeder transformer	Booster transformer
HV(primary)/LV(secondary) Voltage: 11.54 kV / 6000 V	HV(primary)/LV(secondary): 3000 V/ 693 V
HV(primary)/LV(secondary) Current: 17.32 A / 66.66 A	HV(primary)/LV(secondary): 66.66 A/ 288.8 A
Vector group: Y III	Vector group: III iii
Tappings (LV): 6000 5250 4500 3750 3000 2250 1500 750 0	

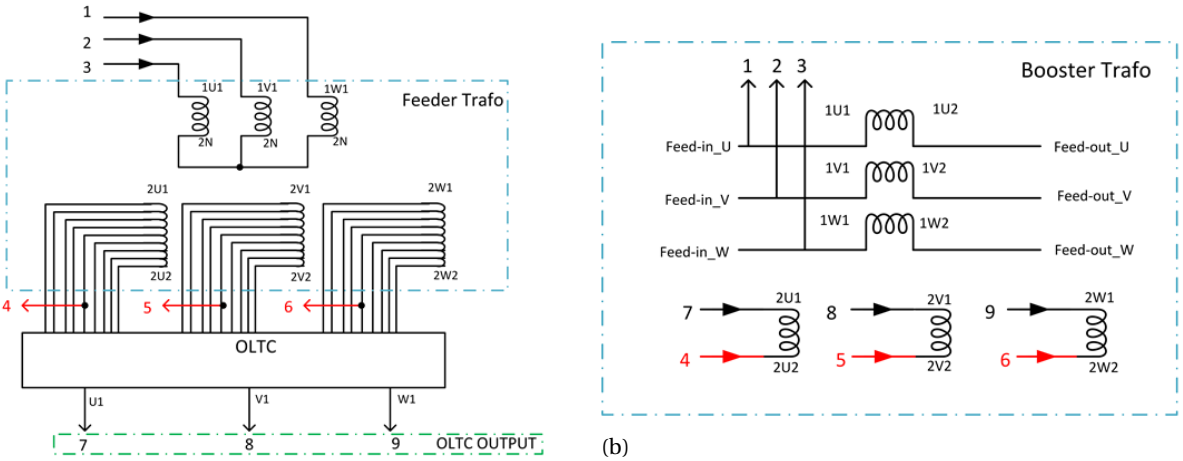

(a) (b)

Figure 5.2: (a) Internal wiring diagram of the feeder transformer (b) Internal wiring diagram of the booster transformer

Table 5.1 shows the per-phase ratings of the feeder and booster transformer. The primary side of the feeder transformer is connected in wye arrangement with a neutral point not connected to ground as indicated in table 5.1 on the feeder transformer vector group. As the secondary side of the feeder transformer is not connected in wye or delta, it is indicated in the vector group as III. Similarly, the primary side of the booster transformer is indictated with III as the vector group, and the secondary side of the booster transformer is connected in series to the MV line to perform voltage regulation. A simple schematic of the wiring diagram of a three phase wye connected LVR with two active parts is shown in fig. 5.2.

The secondary side of the feeder transformer layout is shown in fig. 5.3 with the corresponding tap voltages. Center tap from the secondary side of the feeder transformer is connected to the booster transformer. Center tap becomes the new neutral point and it is assigned a reference value of 0 V. The voltage on the secondary side of the feeder transformer with center tap configuration is shifted accordingly as shown in fig. 5.3. If the OLTC is in the tap position 1, then the primary side of the booster transformer is exposed to 3 kV. If the OLTC is in the tap position 9, then the primary side of the booster transformer is exposed to -3 kV.

5.2. Modeling and Simulation of the system

Simulations are performed in MATLAB/Simulink to verify the design. The simulation model consists of an AC source, distribution line, LVR and a load. The LVR configuration 5 is used in the simulation. The simulation model is shown in the fig. 5.4.

5.2.1. Transformer modeling

The design of the transformer with respect to voltage ratio, current and tapping range was discussed in section 5.1. Impedance is required to completely model the transformer for simulation. The impedance value of the LVR transformer is obtained from ABB. The feeder transformer has an impedance of 6% and the booster transformer has an impedance of 8%. The transformers have a very low no-load and load losses. As discussed in chapter 4 sec.4.2.2, ignoring the power losses and the magnetizing branch will not affect the accuracy of the results [36] [72]. Eq. 4.5 - 4.7 from chapter 4 sec.4.2.2 is used to model the leakage impedance of the transformers. The effective leakage impedance of the transformer is assumed to be divided equally between the

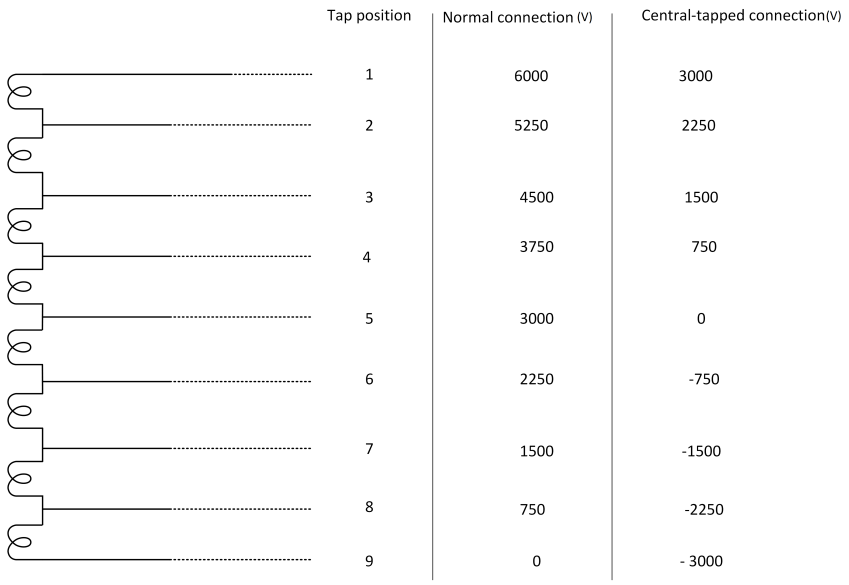

Figure 5.3: Secondary side of the feeder transformer with tappings

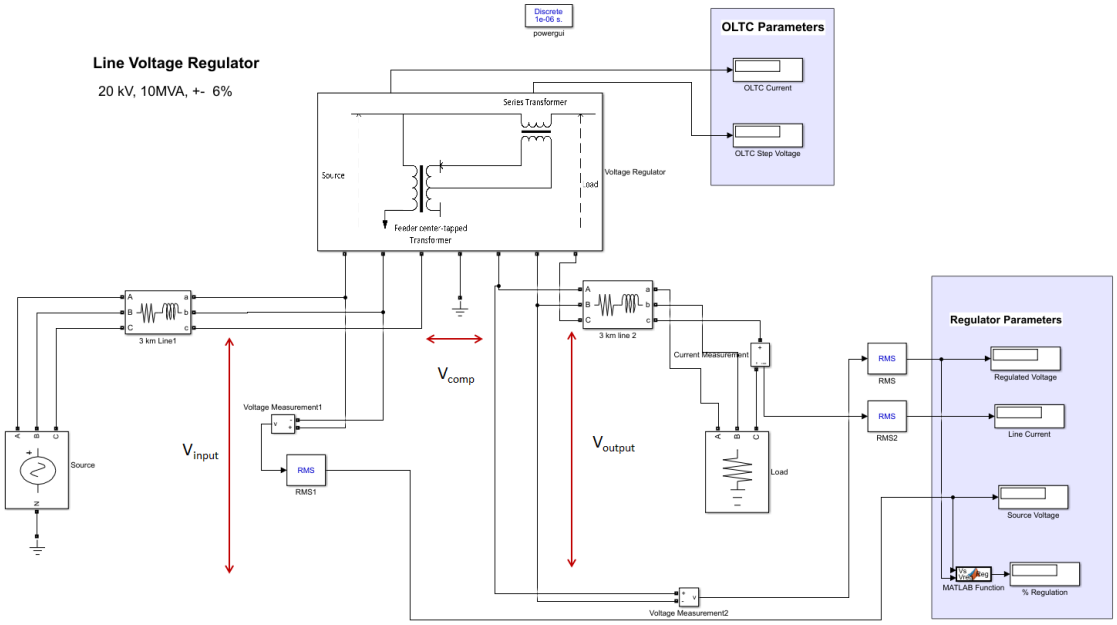

Figure 5.4: MATLAB/ Simulink model of a LVR in a MV distribution line

primary and secondary winding. The leakage impedance for the feeder transformer is calculated as follows:

$$Z_{feeder} = \frac{u_{Zfeeder\%}}{100} * \frac{V^2_{Sfeeder}}{S_{feeder}} = \frac{6}{100} * \frac{(20kV)^2}{600kVA} = 40\Omega$$

$$X_{eq,feedpri} = Z_{feeder}$$

$$L_{eq,feedpri} = \frac{X_{eq,feedpri}}{\omega} = 0.127H$$

$$\frac{L_{eq,feedpri}}{2} = L_{feedpri} = a^2_{feeder} L_{feedsec} = 0.0636H$$

$$L_{feedpri} = 0.0636H$$

$$L_{feedsec} = \frac{0.0636H}{1.92^2} = 0.0172H$$

$$L_{tap} = \frac{L_{feedsec}}{N_{tap} - 1} = \frac{0.0172H}{8} = 2.1465mH$$

The leakage impedance for the booster transformer is calculated as follows:

$$Z_{booster} = \frac{u_{Zbooster\%}}{100} * \frac{V^2_{Sbooster}}{S_{booster}} = \frac{8}{100} * \frac{(\sqrt{3} * 3kV)^2}{600kVA} = 3.6\Omega$$

$$X_{eq,boostpri} = Z_{booster}$$

$$L_{eq,boostpri} = \frac{X_{eq,boostpri}}{\omega} = 0.0114H$$

$$\frac{L_{eq,boostpri}}{2} = L_{boostpri} = a^2_{booster} L_{boostsec} = 5.73mH$$

$$L_{boostpri} = 5.73mH$$

$$L_{boostsec} = \frac{5.73mH}{4.33^2} = 0.3056mH$$

$L_{feedpri}$ is the leakage impedance on the primary side of the feeder transformer. $L_{feedsec}$ & L_{tap} is the leakage impedance on the secondary side of the feeder transformer and per tap leakage impedance on the secondary side of the feeder transformer respectively. $L_{boostpri}$ is the leakage impedance on the primary side of the booster transformer. $L_{boostsec}$ is the leakage impedance on the secondary side of the feeder transformer. Table 5.2 shows the parameters used for modeling the feeder transformer. The secondary feeder transformer voltage shown as $V_{1T(L-L)}$ is the rated voltage, and OLTC will be used to vary the voltage in the simulation. Table 5.3 shows the parameters used for modeling the booster transformer.

Table 5.2: Feeder transformer parameters

Parameter	Value
Primary voltage ($V_{1(L-L)}$)	20 kV
Secondary voltage ($V_{1T(L-L)}$)	10.39 kV
Turns ratio (a_{feeder})	1.92
$L_{feedpri}$	0.0636 H
$L_{feedsec}$	0.0172 H
L_{Tap}	2.1465 mH

It should be noted that even though the impedance of the series transformer is 8 %, the effective impedance of the LVR on the line is very small. It can be calculated as follows:

$$Z_{effLVR}(pu) = \frac{Z_{LVR} * \frac{V_{LVR(L-L)^2}}{MVA_{LVR}}}{\frac{V_{Line(L-L)^2}}{MVA_{Line}}} = 0.06 * 0.08 = 4.8e-3\ pu$$

Table 5.3: Booster transformer parameters

Parameter	Value
Primary voltage ($V_{2T(L-L)}$)	5.19 kV
Secondary voltage ($V_{2(L-L)}$)	1200 V
Turns ratio ($a_{booster}$)	4.33
$L_{boostpri}$	5.73 mH
$L_{boostsec}$	0.3056 mH

$4.8 * 10^{-3}$ pu is the effective impedance offered by the LVR in the 20kV medium voltage line.

The arrangement of the feeder and booster transformer with the OLTC in the simulation model is shown in the fig.5.5. OLTC is formed by parallel switches and the control signal is given to the appropriate switch based on the voltage regulation requirement.

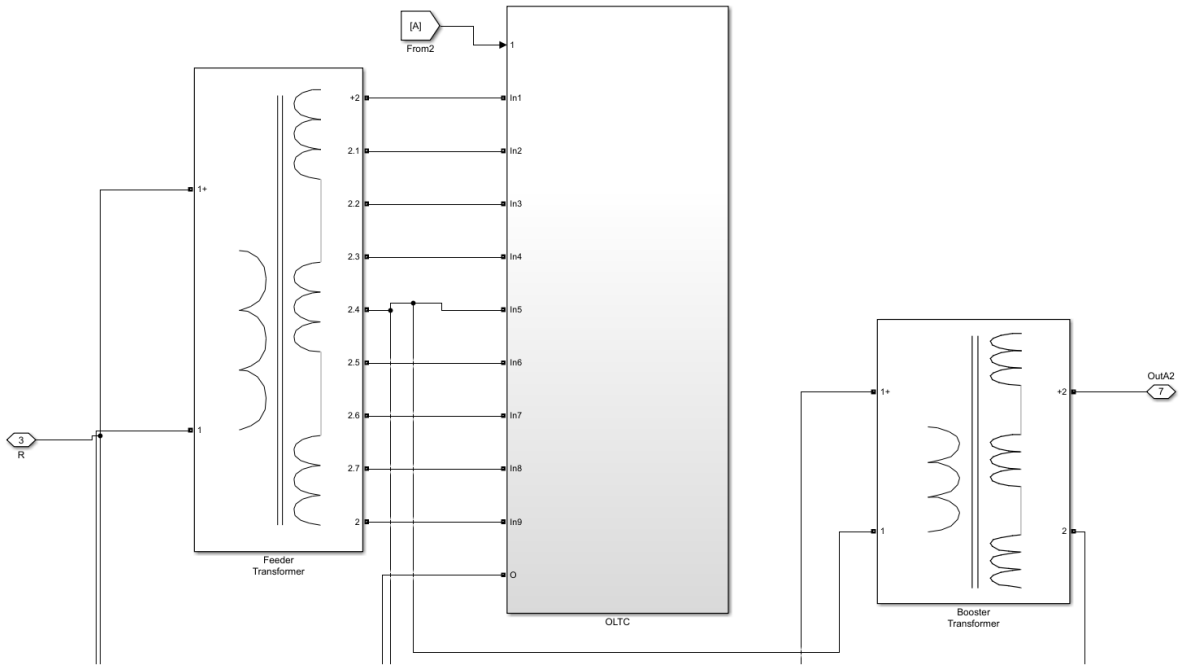

Figure 5.5: The feeder and booster transformer with the OLTC in MATLAB/ Simulink

5.2.2. Line and load modeling

The line is modeled as a lumped resistance and reactance. A 6 KM line is taken and the LVR is placed at 3 KM. The parameters of the line is similar to the model used in chapter 3 and it is shown in table 5.4. The load is modeled as a three phase resistive branch with 1pu (10 MW) capacity.

Table 5.4: Type A1 conductor parameters from IEC 61597

Code number	Stranding	Diameter (mm)	CCC (A)	Resistance(Ω/km)	Inductive reactance (Ω/km)
A1_40	7	8.09	293	0.7165	0.2917

5.2.3. Positive and negative voltage regulation

Positive and negative voltage regulation is individually simulated with the MATLAB/Simulink model. Fig.5.6 shows the LVR (phase - neutral) input voltage (blue), output voltage (orange) and the compensation voltage (green) for 6% positive voltage regulation. The compensation voltage is in-phase with the input voltage of the LVR to increase the output voltage by 6%. There is a voltage drop due to the impedance of distribution line

present before the LVR. The RMS value of input voltage to the LVR is 10.98 kV (phase - neutral) and the RMS value of output voltage of the LVR is 11.63 kV (phase - neutral). The per-phase RMS value of compensation voltage is observed to be 664 V (= 0.06 * 10.98 kV).

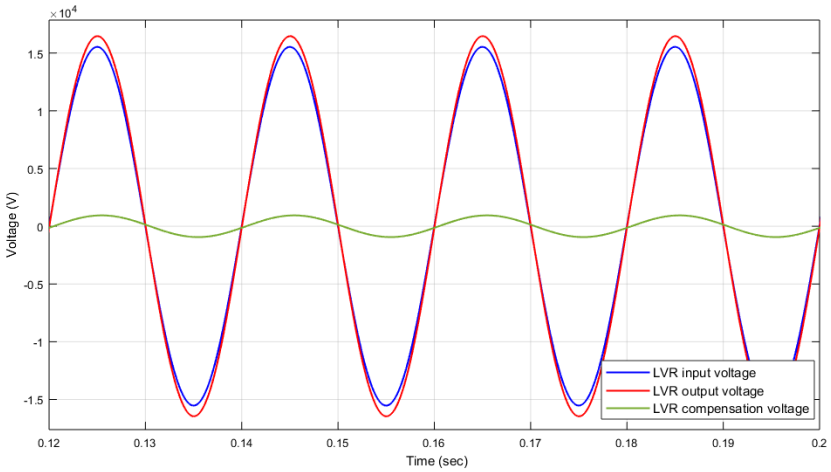

Figure 5.6: Simulation results for 6% positive voltage compensation of phase R

Fig. 5.7 shows the per-phase voltage waveforms for 6% negative voltage compensation. The compensation voltage is out-of-phase with respect to the input voltage. The RMS value of input voltage to the LVR is 11.03 kV (phase - neutral) and the RMS value of output voltage of the LVR is 10.48 kV (phase - neutral). The per-phase RMS value of compensation voltage is observed to be 674 V (= 0.06 * 11.03 kV).

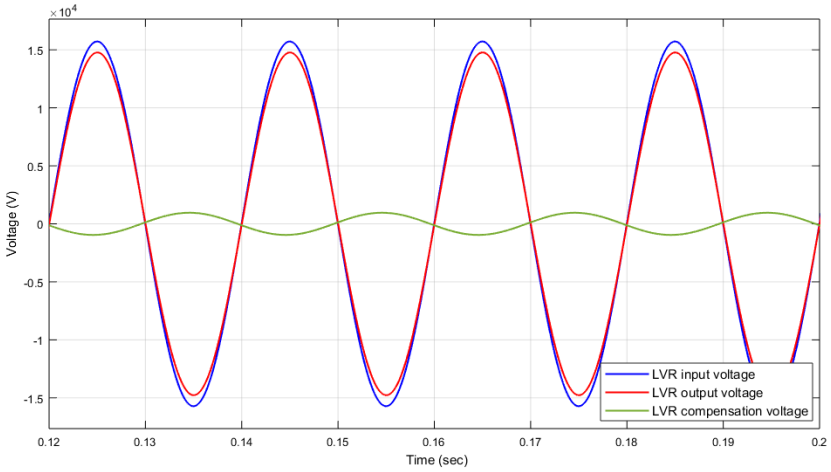

Figure 5.7: Simulation results for 6% negative voltage compensation of phase R

5.3. Experimental results

A low power experimental setup was developed to verify the design of the LVR configuration 5. The concept is tested in a 400 V, 5 kVA LV system. An autotransformer is used to supply a RMS value of 100 V per-phase as the input to the LVR setup. Fig. 5.8 shows the experimental setup from the laboratory. The fig. 5.8a shows the ECOTAP VPD III 100 OLTC with the VPD controller and DSO, and the fig. 5.8b shows the low voltage active parts used in the system. The active part system ratings are given in the table 5.5. Each tapping voltage on the secondary winding of the feeder transformer corresponds to a proportional number of turns(N_5 - N_0). Each step in the feeder transformer varies the output voltage by 1.6 % with a maximum variation of 8%. As the secondary side of the feeder transformer has an even number of taps, it is not possible to have a center tap to attain equal positive and negative regulation. The common winding (0reg) between the feeder and booster transformer is changed for positive and negative regulation to obtain equal compensation of 4.8%.

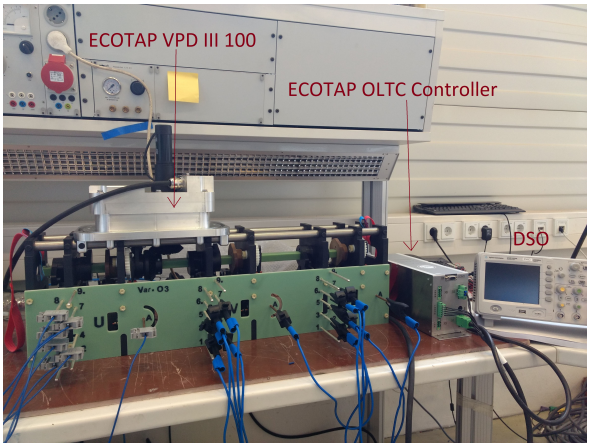

(a)

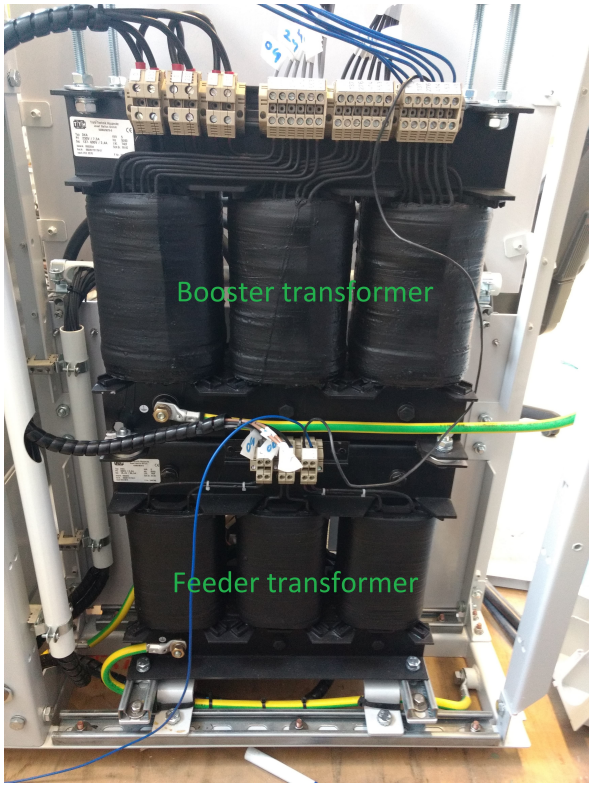

(b)

Figure 5.8: (a) MR ECOTAP OLTC(left), MR controller(center), DSO (right) (b) Feeder transformer (top), Booster transformer (bottom)

The tap changing operation is executed by a Motor Drive and Control (MD & C) unit. A 24 V DC motor is used as the drive for the OLTC. The command to the motor drive is given by the control unit. The control unit is capable of operating in automatic mode (indicated as AVR AUTO in the datasheet), manual mode (indicated as AVR MANUAL in the datasheet) and external input mode (indicated as EXTERNAL CONTROL in the datasheet). The OLTC is controls the output voltage automatically based on the voltage regulation function. A voltage and time bandwidth is set by the user in this mode. The user can manually control the OLTC tap position to change the voltage in AVR MANUAL mode. EXTERNAL CONTROL mode is used by the utility or the customer to control the OLTC tap position from remote end through SCADA. AVR MANUAL mode is used in this work to move the taps locally in the laboratory and extract the results. Agilent DSO1024A is used as the oscilloscope to record the results. The results are stored in a csv file and imported to MATLAB/ Simulink to plot the graphs.

Table 5.5: Per-phase ratings of the feeder and booster transformer used in the experimental test setup

Feeder transformer	Booster transformer
Power: 1.66 kVA	Power: 1.66 kVA
HV(primary)/LV(secondary) Voltage: 230 V/ 690 V	HV(primary)/LV(secondary): 690 V/ 18.4 V
Vector group: Y III	Vector group: III iii
Tappings (LV): 690 V(N_5) 553 V(N_4) 474 V(N_3) 276 V(N_2) 137 V(N_1) 0 V(N_0)	

5.3.1. Positive voltage regulation

The regulation voltage should be in-phase with the input voltage to attain a positive voltage regulation. To obtain +4.8 % regulation, the winding N_2 is used as the common winding (0reg) between the feeder and booster transformer. Table 5.9a explains the redistribution of regulation (%) for positive voltage compensation. As the tap N_2 is used as the common winding, the voltage regulation when the OLTC moves to that winding will be 0 %. Fig.5.9b shows the schematic diagram with the feeder and booster transformers internal connections for the experimental setup. The OLTC is moved to tap N_5 by giving the tap position input to the VPD controller. The waveforms are recorded when the OLTC is on the N_5 winding corresponding to +4.8 % voltage regulation. Fig. 5.10 shows the results for positive voltage compensation. The input voltage (RMS) to the LVR is 100.65 V and the output voltage (RMS) of the LVR is 105.35 V. The compensation voltage (RMS) added by the LVR is 4.7 V which corresponds to 4.67 %. Voltage compensation error (in %) was observed to be 0.13%. Fig. 5.10a shows the per-phase input, output, and LVR compensation voltage waveforms. As it is observed from the plot, the compensation voltage is in-phase with the input voltage to provide positive voltage compensation.

Tapping voltage (V)	Output voltage regulation (%)
N_5	4.8
N_4	3.2
N_3	1.6
N_2 (0reg)	0
N_1	-1.6
N_0	-3.2

(a)

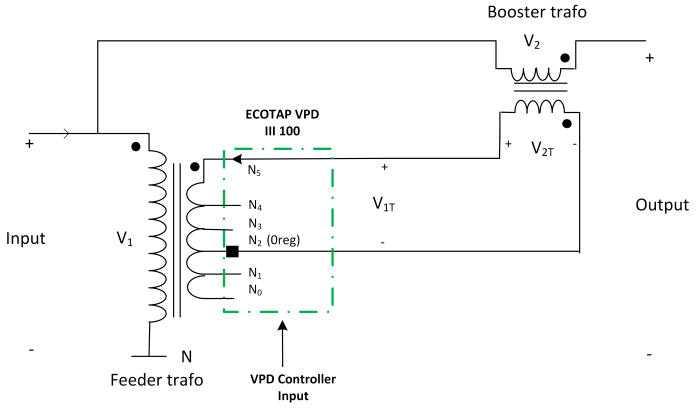

(b)

Figure 5.9: Experimental setup for positive voltage regulation (a) Redistribution of voltage regulation (in %)(b) Schematic diagram of the experimental setup of LVR for positive voltage regulation

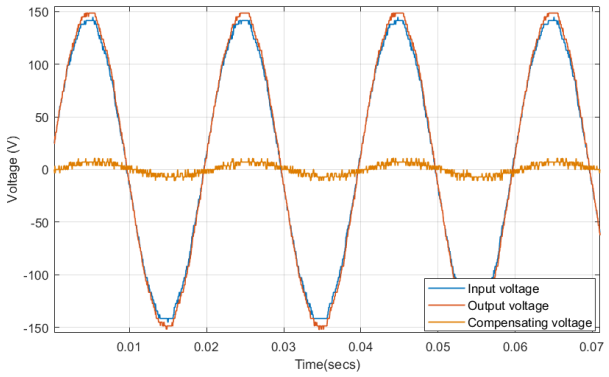

(a)

Input voltage (V)	100.65
Output voltage (V)	105.35
Ideal voltage regulation (%)	4.8
Observed voltage regulation (%)	4.67

(b)

Figure 5.10: Experimental results for positive voltage regulation (a) Per-phase input, output and compensation voltage waveforms (b) Per-phase RMS input, output and compensation voltage values

5.3.2. Negative voltage regulation

The regulation or the compensation voltage should be out-of-phase with the input voltage for negative voltage regulation. To obtain -4.8 % regulation, the common winding (0reg) should be connected to the winding N_3. The table 5.11a explains how the percentage regulation is redistributed for negative voltage regulation. As the tap N_3 is used as the common winding, the voltage regulation when the OLTC moves to that winding will be 0 %. Fig.5.11b shows the schematic diagram with the feeder and booster transformers internal connections for the experimental setup. The OLTC is moved to tap N_0 by giving the tap position input to the VPD controller. The waveforms are recorded when the OLTC is on N_0 winding corresponding to -4.8 % voltage regulation. Fig. 5.12 shows the results for negative voltage compensation. The input voltage (RMS) to the LVR is 100.03 V and the output voltage (RMS) of the LVR is 95.07 V. The compensation voltage (RMS) added by the LVR is - 4.96 V which corresponds to 4.95 %. Voltage compensation error (in %) was observed to be 0.15%. Fig. 5.12a shows the per-phase input, output, and LVR compensation voltage waveforms. As it is observed from the plot, the compensation voltage is out-of-phase with the input voltage to provide negative voltage compensation.

Tapping voltage (V)	Output voltage regulation (%)
N_5	3.2
N_4	1.6
N_3 (0reg)	0
N_2	-1.6
N_1	-3.2
N_0	-4.8

(a)

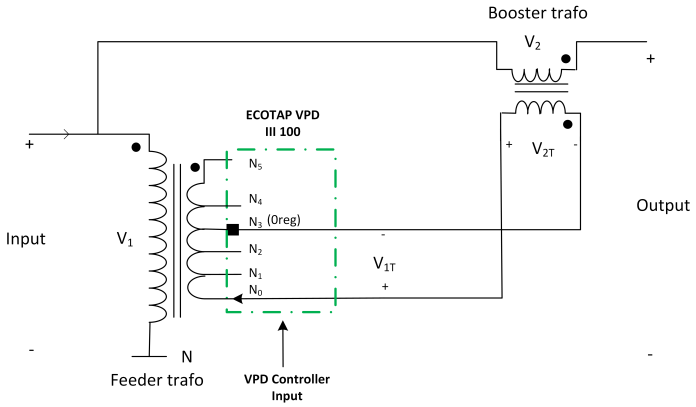

(b)

Figure 5.11: Experimental setup for negative voltage regulation (a) Redistribution of voltage regulation (in %)(b) Schematic diagram of the LVR

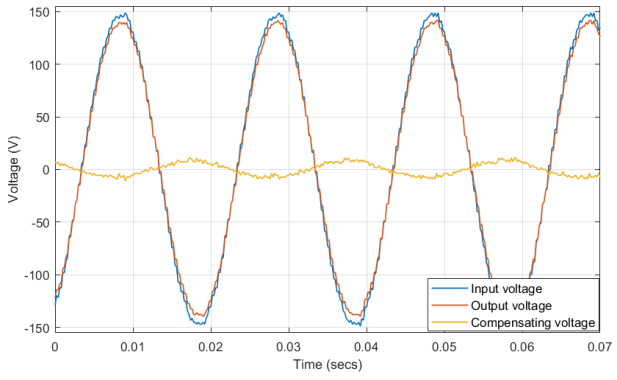

(a)

Input voltage (V)	100.05
Output voltage (V)	95.07
Ideal voltage regulation (%)	- 4.8
Observed voltage regulation (%)	- 4.95

(b)

Figure 5.12: Experimental results for negative voltage regulation (a) Per-phase input, output and compensation voltage waveforms (b) Per-phase RMS input, output and compensation voltage values

6

Feasibility of Power Electronics based OLTCs for LVRs

Mechanical OLTCs have been employed by the transformer manufacturers for a long time due to their robust tap changing capabilities and simple tap changing mechanism using resistors/reactors. However, mechanically moving components are prone to wear and tear which leads to regular maintenance. Frequent maintenance increases the service cost of mechanical OLTCs. The other drawback is the low speed of tap-changers due to mechanically moving components and the time required to store the energy for a tap-changing operation [26]. With the advent of power electronics technology, researchers have been trying to implement tap-changers using solid state switches to avoid any moving parts in the system so as to increase the speed of tap changing operation and reduce maintenance of the OLTC[10][11]. Mechanical tap-changers assisted by power electronic switches have also been proposed to combine the robustness of a mechanical OLTC and arc free commutation of a power electronics based OLTC [48][34]. The advantages of power electronics based OLTCs are as follows[26]:

- Low maintenance cost.
- Fast tap changing operation and no delay between two tap changes.
- No upper limit on the number of tap changing operations.

Even though power electronics based OLTCs have many advantages over mechanical OLTCs, there are some disadvantages associated with them. The initial cost of the solid state switches are high and it has a more complicated control mechanism compared to its mechanical counterpart. It also requires a special protection mechanism to protect the switches during voltage and current disturbances. Increase in unpredictable generators and loads will require higher duty of OLTCs in a distribution line in the near future [60]. Power electronics based OLTCs will be able to perform faster tap changes with lower maintenance for higher duty requirements comapared to mechanical tap-changers. This chapter will focus on the technical and economical feasibility study of power electronics based OLTCs for a 20 kV, 10 MVA LVR with ±6% voltage regulation.

6.1. LVR configuration

One of the drawbacks of power electronics based OLTCs is the cost of the solid-state switches. Power electronic switches are expensive for higher voltage and current ratings. Switches are exposed to surge voltages and short circuit current when directly exposed to a MV line. The power electronic switches should satisfy the short circuit and impulse voltage requirement of the respective medium voltage line if directly exposed to a MV distribution line [18]. Currently there are no electronic switches which can satisfy the requirements for a 20kV MV line; hence, power electronic switches should be used in series and parallel for each tap to meet the requirements. This can drastically increase the cost of the overall system. The switches have to be overrated when series combination of power electronic switches are used to maintain the reliability in operation. LVR with a feeder and booster configuration can be used to avoid series operation of power electronic

switches as it provides isolation from the MV line [44]. This can reduce the number of switches used per tap and also it ensures isolation from system disturbances such as lightning/ switching over-voltage. There are four configurations available for LVR with two active parts as discussed in chapter 4. LVR configuration 5 (subsection: 4.6.2) is used in this thesis work as it does not require a special reversing mechanism due to the use of center-tap configuration on the secondary side of the feeder transformer. Selection of LVR configuration 5 in this feasibility studies also gives a basis of comparison for the operation of the same configuration with mechanical OLTCs. The power electronic switches placement for LVR configuration 5 with feeder and booster transformer is shown in fig. 6.1.

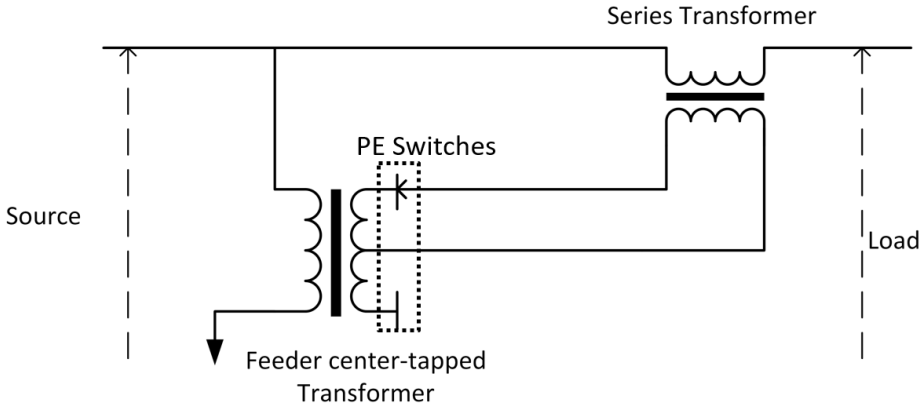

Figure 6.1: Power electronic (PE) switches placement in a LVR with feeder and booster topology

6.2. Solid-state switch selection

As the currents and voltages are AC waveforms, the solid-state switches should be able to handle bi-directional voltages and currents. Thyrsitors can be used in anti-parallel configuration to form a bi-directional switch as shown in fig. 6.2 (b). Both the thyristors have forward and reverse blocking capabilities. When the bi-directional switch is required to conduct, the thyristor pair is switched-on to conduct current in positive and negative directions. At any point in time during switch-on, only one of the thyristors is conducting. The losses will be due to only one thyristor for this bi-directional switch. When the bi-directional switch is switched-off, both the thyristors will be blocking forward and reverse voltage alternatively in each cycle. The main challenge in thyristor based tap-changer is that it requires a resistor or inductor to restrict the short circuit current during tap changes due to the semi-controllable nature of the thyristor switches.

Insulated Gate Bipolar Transistors (IGBTs) can be connected in a common-emitter or common-collector mode to form a bi-directional switch[73]. Fig. 6.2 (a) shows the bi-directional switch using IGBTs with anti-parallel diode in common-emitter configuration. The positive current path is through IGBT T1A and diode D1B, and the negative current path is through IGBT T1B and D1A. The positive voltage is blocked by IGBT T1A and the negative voltage is blocked by IGBT T1B. IGBT based tap-changer can perform commutation without any short circuit by accurately controlling the switching time.

A simple loss and cost calculation is carried out to determine the economical bi-directional switch for LVRs. High power solid-state switches are available for thyristors and IGBTs for voltage ranges between 1 - 6.5 kV. Switches with lower rated voltage are cheaper but will have to carry more current, leading to more losses in the switches. Switches with a rated voltage between 4 - 4.5 kV provide a good trade-off between the cost and the losses. Rated voltage for the switches will be around 4250 V for a secondary feeder voltage ($V_{feedsec}$) of 1500 V. This calculation includes a voltage safety factor of 2 [65]. The feeder secondary current ($I_{feedsec}$) is required to choose the switches and calculate losses. $I_{feedsec}$ for a 20 kV, 10 MVA LVR with ±6% regulation can be calculated as follows:

$$I_{feedsec} = \frac{10\ MVA * 0.06}{3\ *\ 750} = 266.6A$$

Thyristor with part number 5STP 04D4200 and IGBT with part number 5SNA 0650J450300 from ABB satisfies the required voltage and current ratings. The switch parameters are given in the table 6.1.

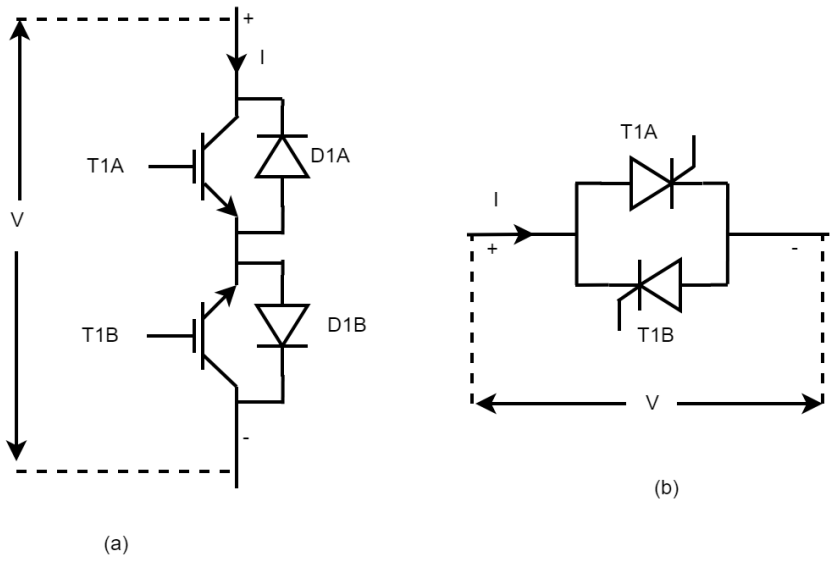

Figure 6.2: (a) Bi-directional IGBT switch in common-emitter configuration (b) Bi-directional thyristor switch connected in anti-parallel configuration

Table 6.1: Thyristor and IGBT parameters used for solid-state switch selection

Thyristor - 5STP 04D4200		IGBT - 5SNA 0650J450300	
Cost - 65 €/switch		Cost - 550 €/ switch	
Parameter	Value	Parameter	Value
V_{DRM}	4500 V	V_{CE}	4500 V
$I_{T(RMS)}$	740 A	I_{Cpeak}	650 A
V_{T0}	1 V	$V_{CE\ sat}$	3.7 V
r_T	1.5 m Ω	V_F	3.4 V

Determination of losses for the switches is given below [59] [63]:

$$P_{L(Thyristor)} = V_{T0} * I_{feedsec(av)} + I^2_{feedsec(RMS)} * r_T \qquad P_{L(IGBT)} = (V_{CE\ sat} + V_F) * Ifeedsec(av)$$

$$P_{L(Thyristor)} = 346.6W \qquad P_{L(IGBT)} = 1704W$$

The thyristors have almost 5 times lower losses and it is 9 times cheaper than the IGBTs for this application. Thyristors are cost- effective with lower losses, thereby, making it an ideal choice for economical on-load tap-changers. As stated before, a resistor or reactor is required to restrict the short circuit current due to the semi-controllable nature of thyristors. However, short circuit current can be limited to a safe value by accurately defining the commutation instant for thyristor based OLTCs [75]. The following sections will deal with the analysis and simulation of thyristor based OLTCs. Fig.6.3 shows the center-tapped secondary side of the feeder transformer with thyristor based OLTCs.

6.3. Commutation principle for a thyristor based tap-changer

A thyristor based tap-changer will experience an uncontrolled short circuit if the commutation instant is not accurately defined. Commutation can be initiated at any instant if a resistor or reactor is present in the tap-changer to avoid large circulating short circuit currents. Therefore, it is very important to define the commutation instant to restrict the short circuit currents for tap-changers without resistor or reactor. The basic principle for commutation can be given as follows[75]:

- Switching up operation can be performed when the tap voltage and current have the same polarity
- Switching down operation can be performed when the tap voltage and current have opposite polarity

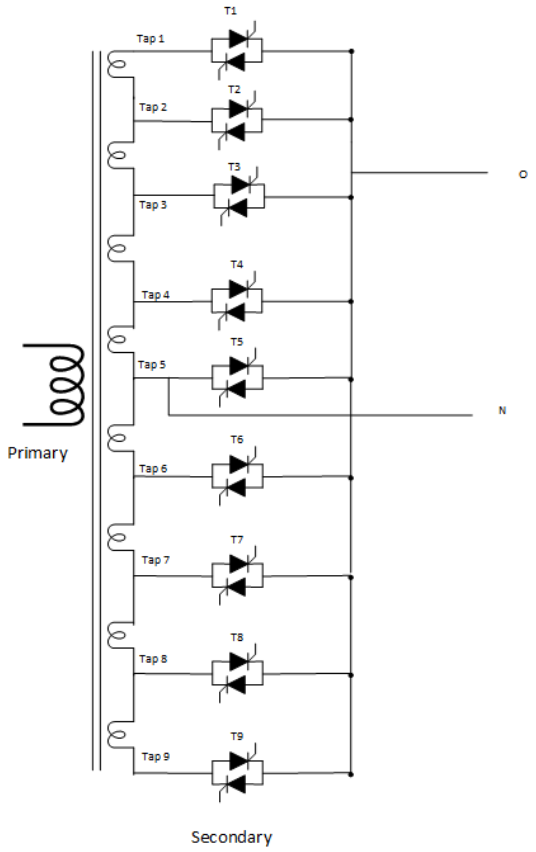

Figure 6.3: Feeder transformer with a thyristor based OLTC on the secondary side of the transformer

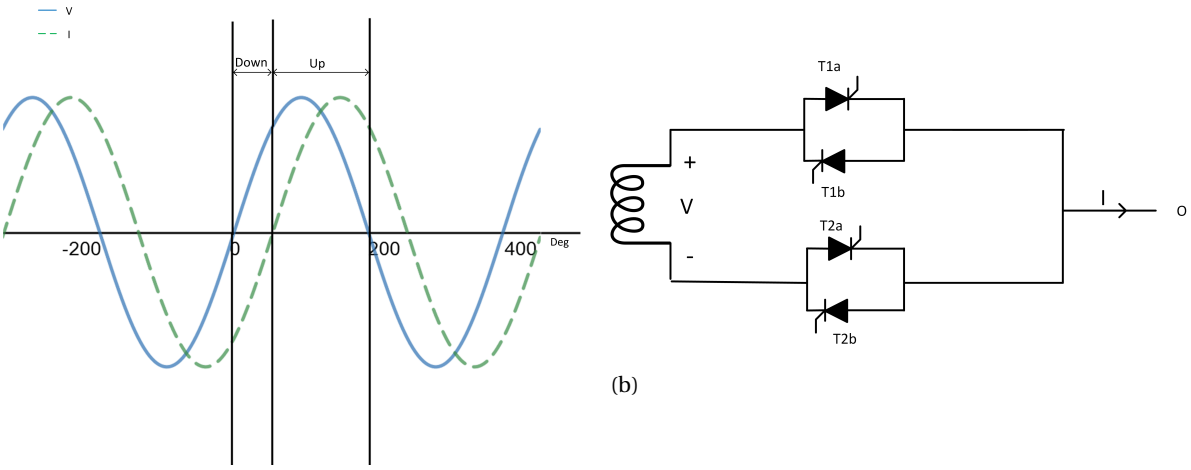

(a)

Figure 6.4: (a) Switching up and down instants for tap-changes without a short circuit for lagging power factor (b) Schematic diagram of one tap with thyristor based tap-changer in feeder secondary transformer

Fig. 6.4a pictorially depicts the region where the switching up and down operation can be performed without creating a short circuit. During switching down operation, the thyristor pair T1 in the fig. 6.4b would be conducting. Assuming the tap voltage is positive and the current direction is negative, the current would be flowing through thyristor T1b. If a commutation is initiated by triggering the thyristor pair T2 during this instant, there will be no short circuit because there is no path for the circulating short circuit current between

the taps. The circulating current path is not available due to the conduction of thyristor T1b, and the thyristor T1a is switched off during this half cycle. Similar logic is applied for switching up when the tap voltage and current have the same polarity.

This commutation logic has limitations for unity and near unity power factors. This logic cannot be applied for switching down at unity power ($\cos(\phi = 1$ or $\phi = 0^\circ)$), as there will be no instant with opposite polarity of voltage and current. It will also not be applicable for switching up for unity power factor with reverse power flow ($\cos(\phi$ = -1 or $\phi = 180^\circ)$) as there will be no instant with the same polarity of voltage and current.

There is also a risk of the thyrsitor prematurely conducting if negative voltage is not applied for an interval more than the thyristor turn-off time (t_q)[46]. The thyristor turn-off time is defined by the manufacturers in the data sheets. Extinction angle is the parameter defined to check for this condition. It is the angle that subtends from the thyristor switch-off instant till a positive voltage is applied to the thyristor.

Each power factor range is separated and analyzed individually to find the optimal firing angles. The analysis is divided into the following categories based on the power factor angle [25]:

1. Inductive mode of operation: $0^\circ < \phi < 180^\circ$
2. Resistive mode of operation: $\phi = 0^\circ$
3. Capacitive mode of operation: $-180^\circ \leq \phi < 0^\circ$

6.3.1. Equivalent circuit of the tap-changer

Equivalent circuit of the secondary side of the feeder transformer is developed for further analysis. Only two taps are considered for simplicity. The impedance is assumed to be divided equally between the primary and the secondary of the feeder transformer. The voltage and the inductance on the secondary side of the feeder transformer is assumed to be divided equally between the taps. This assumption is made to simplify the determination of leakage inductance between the taps. Determination of inductance using this method will give a lower value of the effective inductance. Especially during the controlled short circuit during commutation, the effective inductance is higher due to magnetic circuit coupling between primary and secondary side of the transformer. However, this assumption simplifies the analysis and gives the value of short circuit currents higher than the actual value as the calculated reactance value is lower. Resistance is not included in the calculation due to low power losses in the transformers. V_{tap} is the per-tap voltage of the transformer. The equivalent circuit of the tap-changer with a leakage inductance (L_{tap})of the transformer is shown in the fig. 6.5a.

Leakage inductance does not allow the current to become zero in the previously conducting tap instantaneously. This also helps in reducing the rate of change of current in the circuit. During commutation both the thyristor pairs are conducting, and the current in the previously conducting tap will gradually come to zero based on the value of the leakage inductance[75]. A commutation between the taps is complete only when the previously conducting tap has no current and the current is completely transferred to the next tap. This time or angle elapsed during commutation is defined as overlap angle (γ) as shown in fig. 6.5b. α is the firing angle from the zero crossing of the voltage. The firing angle is always applied from the rising edge of the tap voltage in this work. δ is the extinction angle of the thyristor. δ should always be higher than t_q/ω (δ_q) to avoid false firing of the thyristor. The following subsections will deal with determining the firing angle for the thyristor to have no/controlled short circuit during tap changes. The optimum firing angle as a function of power factor angle is determined for switching down operation. The same relation can be extended for switching up operation by inverting the tap voltage and applying the same firing angle. The firing angle as a function of power factor angle determined for switching down operation is shifted by 180° for switching up operation [75].

6.3.2. Switching down in an inductive power factor region

Current lags the voltage for inductive power factors. The firing angle can be anywhere between the voltage zero crossing and the current zero crossing. During this period the current and the voltage have opposite polarity, which is ideal for switching down operation. The most optimum firing angle would be just after the zero crossing of voltage[25]. T1b thyrsitor will experience a reverse bias after the commutation till the next zero voltage crossing (10 ms), ensuring sufficient extinction angle (γ) greater than the thyristor turn-off angle (δ_q).

However, the extinction angle is not enough for the thyristor to recover for power factor angles close to 180°. Fig. 6.6 highlights the scenario near the voltage zero crossing. Thyristor T1a was conducting before the

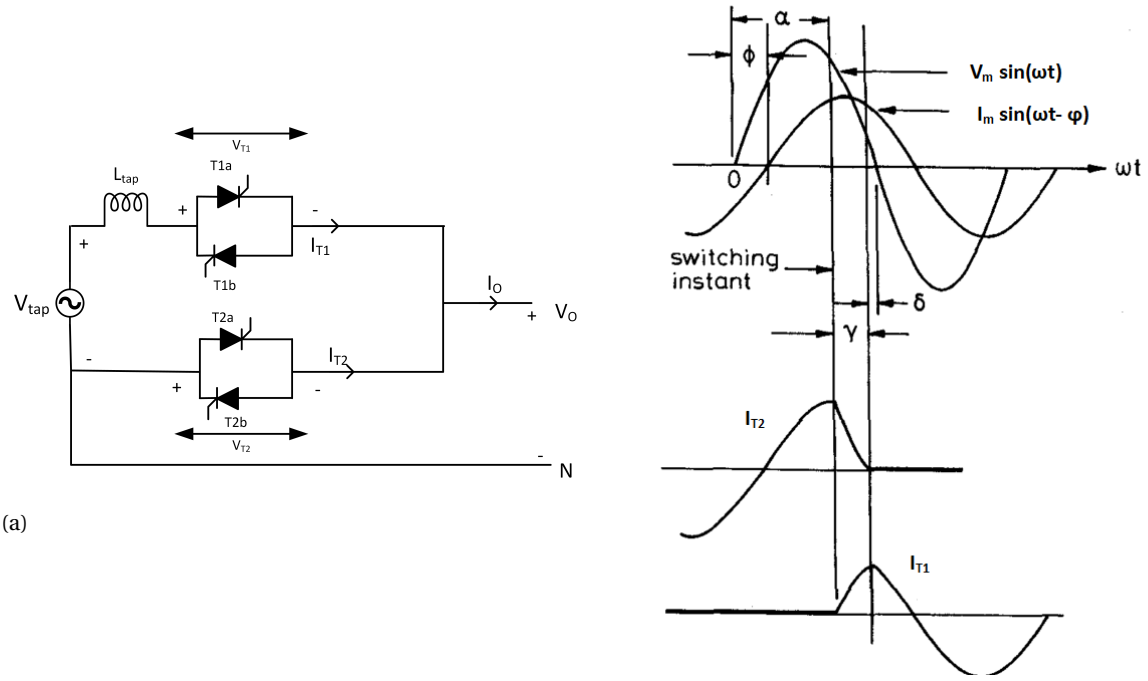

Figure 6.5: (a) Equivalent circuit of two taps with thyristor based tap-changers (b) Voltage and current waveforms during switching up operation [75]

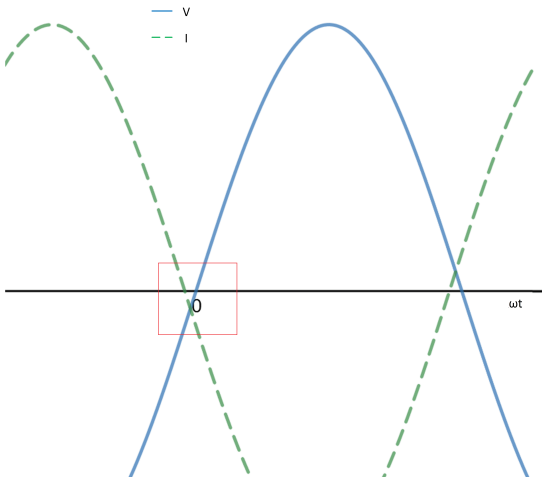

Figure 6.6: Voltage and current waveforms for inductive power factors close to 180°

current crosses zero and becomes negative. If the thyristor T2 pair is triggered close to voltage zero crossing, thyristor T1a will experience a positive forward bias after the commutation before the thyristor turn-off time leading to a false triggering. To avoid this false firing of thyristor T1a, the firing angle should be slightly shifted away from the zero for this power factor range. The relationship between firing angle and power factor angle can be summarized as follows:

Table 6.2 shows the firing angle corresponding to the power factor angle in the inductive region. For power factor angles ranging between 180° - δ_q and 180°, the firing angle is shifted by the thyristor turn-off angle (δ_q). This is done to allow the thyristor T1a to fully recover after switch-off.

Table 6.2: Power factor angle and firing angle relationship for switching down operation in an inductive power factor region

Power factor angle (deg)	Firing angle (deg)
$0^\circ < \phi < 180^\circ - \delta_q$	0°
$180^\circ - \delta_q \leq \phi < 180^\circ$	$\phi - (180^\circ - \delta_q)$

6.3.3. Switching down in unity power factor

Switching down at unity power factor is not possible without a short circuit as there is no region in which the voltage and the current have opposite polarities. The thyristor pair T2 can be triggered slightly before the voltage zero crossing. This will induce a controlled short circuit. As the firing angle is chosen close to zero, the peak value of the circulating short circuit current will be low.

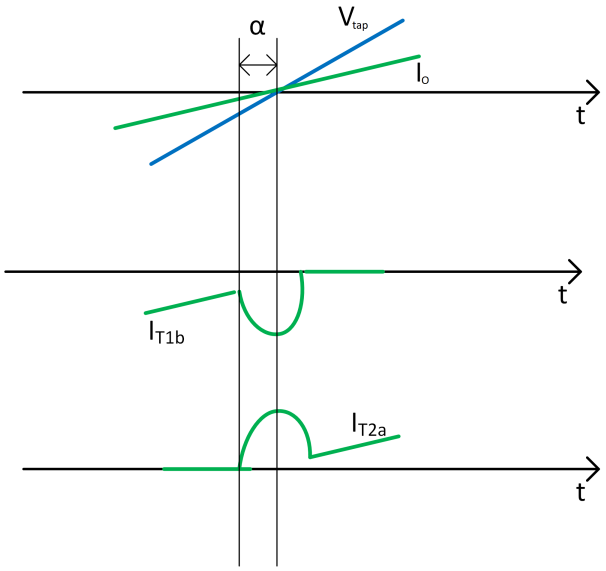

Figure 6.7: Voltage and current switching waveforms at unity power factor

Fig. 6.7 shows the waveforms for switching at unity power factor. The firing angle is negative in this case as the thyristors are triggered before the voltage zero crossing. The circulating short circuit current flows through the thyristor T1b and T2a. After the short circuit is over, the thyristor pair T2 starts conducting as a result of a successful tap change with a controlled short circuit. Equation for the short circuit current through I_{T1b} can be determined as follows[25]:

$$V_{tap} = L_{tap}\frac{di_{T1b}}{dt} \tag{6.1}$$

$$i_{T1b}(\omega t) = \left(\frac{1}{L_{tap}} * \int_{\alpha}^{\omega t} V_m sin(\omega t)\right) + i_o(\alpha) \tag{6.2}$$

$$I_{T1b} = \frac{V_m}{\omega L_{tap}}(cos(\alpha) - cos(\omega t)) + I_m sin(\alpha) \tag{6.3}$$

Eq. 6.2 has an extra term $i_o(\alpha)$ to account for the base current above which the short circuit current will be added to the total current i_{T1b}. During short circuit, the tap voltage is connected across the leakage inductance of the transformer leading to current lag the voltage by 90°. When the voltage reaches zero, the current reaches its maximum value. Maximum short circuit current through the thyristor T1b is determined by substituting ωt as zero in the Eq. 6.3. The peak value of the circulating short circuit is given in Eq. 6.4.

$$I_{T1b} = \frac{V_m}{\omega L_{tap}}(cos(\alpha) - 1) + I_m sin(\alpha) \tag{6.4}$$

6.3.4. Switching down in a capacitive power factor region

Current leads voltage for capacitive power factors, hence the switching down operation can be performed after the current zero crossing till the voltage zero crossing as both the polarities are opposite in that region. However, thyristor turn-off time would play a crucial role in near unity capacitive power factors as the thyristor that switches-off will experience a positive bias when the voltage zero crossing occurs. It is also dangerous to have the firing angle close to current zero crossing because the thyristor that was previously conducting would experience a positive bias before the thyristor turn-off time (t_q).

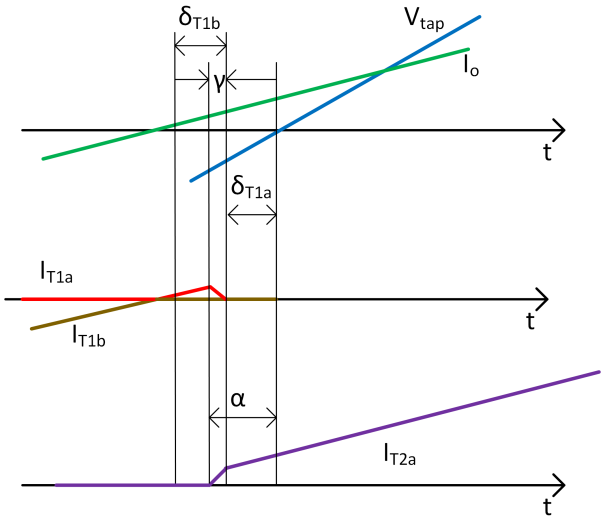

Figure 6.8: Voltage and current commutation waveforms for capacitive power factors without a short circuit

Fig. 6.8 shows the commutation waveforms for capacitive power factors. The extinction δ_{T1b} & δ_{T1a} as depicted in the fig.6.8 should be greater than the thyristor turn-off angle δ_q. For extinction angles lower than δ_q, unwanted triggering of thyristors will occur leading to a short circuit which can damage the equipment. There will be a critical angle at which the extinction angle for both the thyristor T_{1a} & T_{1b} will just be equal to the thyristor turn-off angle (δ_q). For angles greater than the critical angle, commutation can only be performed with a short circuit. To incorporate a controlled short circuit, commutation is performed similar to unity power factor by triggering the T2 thyristor pair before the current zero crossing. The analysis for capacitive power factor is separated into two parts: capacitive power factor commutation region without a short circuit and capacitive power factor commutation region with a short circuit.

Capacitive power factor commutation region without a short circuit

The minimum firing angle should be displaced by the thyristor turn-off angle from the current zero crossing to have a sufficient extinction angle for the thyristor T_{1b}. The minimum firing angle for this region is given as follows:

$$\alpha_{min} = \phi + \delta_q \tag{6.5}$$

The above equation gives the lower bound of the firing angle in this region. The upper bound of the firing angle in this region can be given as follows:

$$\alpha_{max} = -\gamma - \delta_q \tag{6.6}$$

The firing angle is negative, and the overlap angle and the thyristor turn-off angle are positive, hence the negative sign for γ & δ_q. The overlap angle depends on the magnitude of current and the tap inductance. The magnitude of the current depends on the power factor at a given firing angle.

The overlap angle can be found by solving the equation for current i_{T1a} within the commutation period. Similar to eq. 6.2, current i_{T1a} can be written as follows:

$$i_{T1a}(\omega t) = \Big(\frac{1}{L_{tap}} * \int_{\alpha}^{\omega t} V_m sin(\omega t)\Big) + i_o(\alpha - \phi) \tag{6.7}$$

$$I_{T1a}(\omega t) = \frac{V_m}{\omega L_{tap}}(cos(\alpha) - cos(\omega t)) + I_m sin(\alpha - \phi) \tag{6.8}$$

As observed from the fig. 6.8, at $\omega t = \alpha + \gamma$, the current I_{T1a} reaches zero. This condition is used to solve for the overlap angle (γ). The relationship for γ can be derived as follows:

$$I_{T1a}(\alpha + \gamma) = \frac{V_m}{\omega L_{tap}}(cos(\alpha) - cos(\alpha + \gamma)) + I_m sin(\alpha - \phi) \tag{6.9}$$

$$0 = \frac{V_m}{\omega L_{tap}}(cos(\alpha) - cos(\alpha + \gamma)) + I_m sin(\alpha - \phi) \tag{6.10}$$

$$cos(\alpha + \gamma) = cos(\alpha) + \frac{\omega L_{tap} I_m}{V_m} sin(\alpha - \phi) \tag{6.11}$$

$$\alpha + \gamma = cos^{-1}\Big(cos(\alpha) + \frac{\omega L_{tap} I_m}{V_m} sin(\alpha - \phi)\Big) \tag{6.12}$$

As cosine is positive in both fourth and first quadrant, a negative sign should be added to the right hand side of the eq. 6.12 [25]. The final equation for γ is given as follows:

$$\gamma = -cos^{-1}\Big(cos(\alpha) + \frac{\omega L_{tap} I_m}{V_m} sin(\alpha - \phi)\Big) - \alpha \tag{6.13}$$

As stated before, the critical power factor angle is the limiting angle at which thyristor T1a & T1b will have an extinction angle equal to the thyristor turn-off time. The critical power factor angle can be calculated by equating the maximum firing angle and minimum firing angle [25]. The critical power factor angle (ϕ_c) is derived as follows:

$$\alpha_{max} = \alpha_{min} \tag{6.14}$$

$$\phi_c + \delta_q = -\gamma - \delta_q \tag{6.15}$$

$$\phi_c + 2\delta_q + \gamma = 0 \tag{6.16}$$

$$\phi_c + 2\delta_q - cos^{-1}\Big(cos(\alpha_{min}) + \frac{\omega L_{tap} I_m}{V_m} sin(\alpha_{min} - \phi_c)\Big) - \alpha_{min} = 0 \tag{6.17}$$

$$\phi_c = -cos^{-1}\Big(cos(\delta_q) - \frac{\omega L_{tap} I_m}{V_m} sin(\delta_q)\Big) - \delta_q \tag{6.18}$$

Eq.6.18 gives the expression for the critical power factor angle above which thyristor T1 pair will have an extinction angle less than thyristor turn-off angle. For power factor angle above the critical angle, commutation technique similar to unity power factor mode is implemented.

Capacitive power factor commutation region with a short circuit

For power factor angles greater than the critical angle (ϕ_c), the thyrsitor pair T2 is triggered before the current zero crossing. This will a create a short circuit between the taps. Fig. 6.9 shows the commutation waveforms above critical power factor angle. The thyristor pair T2 is triggered before the current zero crossing.

The peak short circuit current can be determined by eq. 6.8 and it occurs when voltage zero crossing occurs ($\omega t = 0°$). The peak short circuit can be given as follows:

$$I_{T1a} = \frac{V_m}{\omega L_{tap}}(cos(\alpha) - 1) + I_m sin(\alpha - \phi) \tag{6.19}$$

The firing angle is slightly less than the power factor angle to initiate a controlled short circuit for commutation. During the commutation, the tap T2 will provide the short circuit current with the load current I_o. The peak current in thyristor pair T2b occur at voltage zero crossing and can be given as follows:

$$I_{T1b} = -\frac{V_m}{\omega L_{tap}}(cos(\alpha) - 1) - I_m sin(-\phi) \tag{6.20}$$

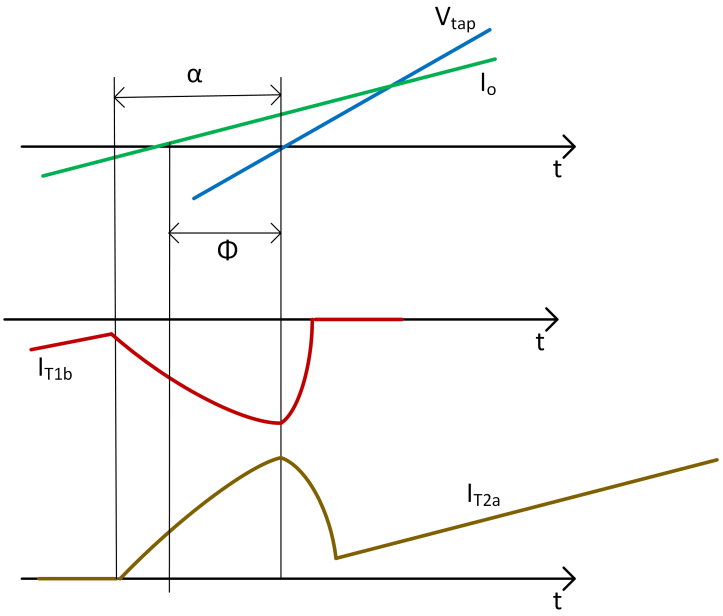

Figure 6.9: Voltage and current commutation waveforms for capacitive power factors with a short circuit

6.4. Determination of firing angle for switching down operation

A generalized approach was followed in the previous section to determine the relationship between the firing angle and power factor angle. In this section, the optimal firing angle is determined for a 20 kV, 10 MVA LVR with ±6% voltage regulation. Table 6.3 shows the parameters for the transformer and the thyristor used for the calculation.

Table 6.3: Transformer, tap, & thyristor parameters used to determine the firing angle

	Parameters	Values
Feeder transformer	Primary side voltage	20 kV
	Secondary side voltage	2598 ($\sqrt{3}$ * 1500) V
	Impedance	6 %
	Taps	9
Tap	Peak tap voltage (V_m)	265.16 V
	Peak tap current (I_m)	376.12 A
	Tap inductance	0.136 mH
Thyristor	Rated peak voltage (V_{DRM})	4200 V
	Rated current ($I_{T(RMS)}$)	740 A
	Turn-off angle (δ_q)	10.9 °

The firing angle for inductive power factors should be 0° until ϕ is 169.1°. For ϕ from 169.1° to 180°, the firing angle is given by ϕ - (180° - δ_q), which is ϕ - 169.1°. The firing angle at unity power factor is chosen to be -5.45° (-δ_q/2). This value ensures that a controlled short circuit is initiated for commutation. The peak value of short circuit current will not be high as the firing angle is small.

The minimum firing angle (α_{min}) for the capacitive region without a short circuit is directly given by a linear relationship $\alpha_{min} = \phi + 10.9°$. The maximum firing angle (α_{max}) is given by a cosine and sine function that needs to be solved numerically in MATLAB (code in Appendix B). The α_{max} relationship is given as follows:

$$\alpha_{max} = -\gamma - \delta_q \tag{6.21}$$

$$\alpha_{max} = -\Big(- cos^{-1}\Big(cos(\alpha_{max}) + \frac{\omega L_{tap} I_m}{V_m} sin(\alpha_{max} - \phi)\Big) - \alpha_{max}\Big) - \delta_q \tag{6.22}$$

$$cos(\alpha_{max}) + \frac{\omega L_{tap} I_m}{V_m} sin(\alpha_{max} - \phi) - cos(\delta_q) = 0 \tag{6.23}$$

Eq. 6.23 is solved numerically for ϕ ranging from -180° to ϕ_c. The value of ϕ_c is determined by substituting the values in eq. 6.18. The value of ϕ_c for the given configuration is -24.8°. The firing angle is selected such that the $|\alpha|$ is within 30 °. This ensures the voltage stress on the thyristor to be restricted to half of the peak tap voltage (V_m) during the switching process [75].

The firing angle for the capacitive commutation region with a short circuit needs to have a firing angle slightly higher than the power factor angle to initiate a controlled short circuit. For power factor angles from ϕ_c to 0°, a line equation for the firing angle is formulated so that the firing angle is slightly lower than the power factor angle. The firing angle equation for power factor angles from ϕ_c to 0° is given as follows :

$$\alpha(\phi_1) = -26^\circ \quad \phi_1 = \phi_c = -24.8^\circ$$
$$\alpha(\phi_2) = -5.45^\circ \quad \phi_2 = 0^\circ$$
$$(\alpha - \alpha(\phi_2)) = \frac{\alpha(\phi_2) - \alpha(\phi_1)}{\phi_2 - \phi_1} (\phi - \phi_2)$$
$$\alpha = 0.828\,\phi - 5.45 \qquad \phi_c \le \phi < 0^\circ$$

Fig. 6.10 shows the plot depicting the relationship between the firing angle and the power factor angle for the complete power factor range for the switching down operation. As calculated with eq. 6.18, the numerically solved α_{max} & α_{min} values converge at a critical power factor angle (ϕ_c) of -24.8°, which can also be calculated with eq. 6.18. This proves the validity of the MATLAB code. The same relationship is phase shifted by 180° to obtain the plot for the switching up operation.

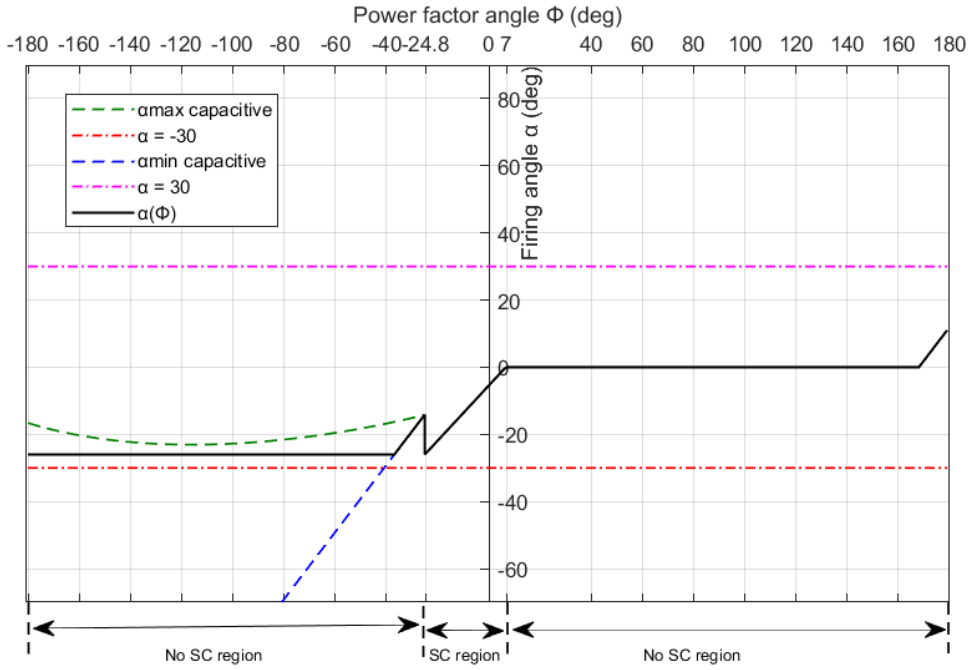

Figure 6.10: Firing angle (α) vs Power factor angle (ϕ) for switching down operation

6.5. Simulation results of thyristor based tap-changer

An equivalent circuit of the thyristor based tap-changer with two taps is simulated in a MATLAB/ Simulink environment. As suggested by the author in [75], a thyristor based tap-changer does not require a snubber circuit. Though the thyristor is rated with a safety factor of 2 for the feeder secondary side voltage, the maximum voltage during turn-off is less than 50 % ($|\alpha| \leq 30°$) of the tap voltage (265.16 V). The rate of change of current ($\frac{di}{dt}$) is limited by the leakage inductance of the transformer.

The parameters from table 6.3 are used in the model. Fig. 6.11 shows the model used in the simulation. The firing circuit in the figure triggers the thyristor based on the voltage zero crossing. The model is analyzed in different power factor regions for switching down and up operation. The thyristors are triggered around 0.4 s based on the firing angle in all the individual cases.

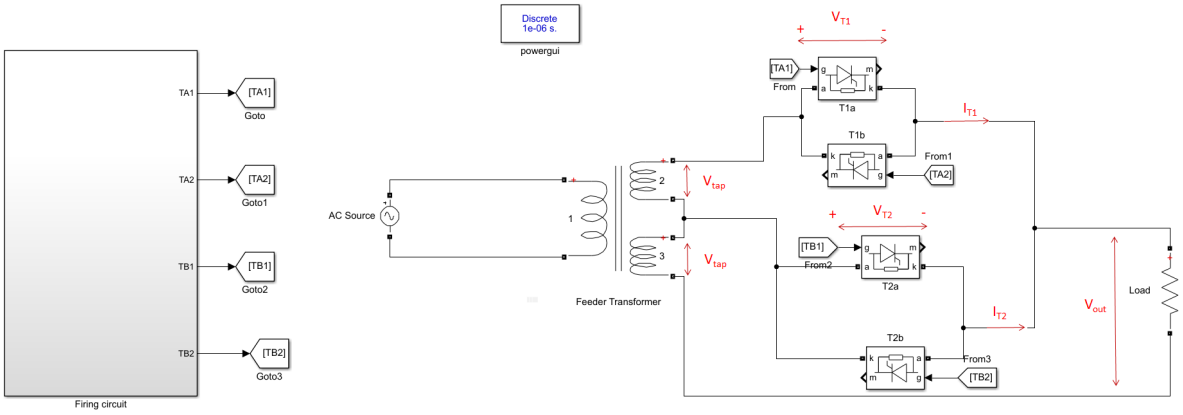

Figure 6.11: MATLAB/ Simulink model of two taps with a thyristor based tap-changer

6.5.1. Inductive power factor

The system has an inductive power factor angle of 30°. The firing angle for switching down operation is 0 °. The T2 thyristor pair is triggered at 0.4 s, and the firing signal for T1 pair is made zero at the same instant. The T1 pair stops conducting when the current naturally reaches zero. Fig. 6.12 shows the waveforms for switching down operation. Short circuit does not occur as predicted in the analysis. The thyristor pair T1 experiences a voltage of 68.5 V at the switch - off instant. This voltage is 0.016 times the rated voltage of the thyristor. Fig. 6.12b shows the output voltage (V_o) variation for switching down operation. The voltage reduces from $2V_{tap}$ to V_{tap}. The firing angle for switching up operation is -26°. The thyristor is triggered 26° before the voltage zero crossing. This is determined by phase shifting the switching down characteristics by 180°. The firing angle for switching up at an inductive power factor angle of 30° is equal to the firing angle for switching down at capacitive power factor angle of 150°. Fig. 6.15 shows the waveforms for switching up operation. The thyristor pair T2 experiences a voltage of 48.1 V at the switch - off instant. Fig. 6.12b shows the output voltage (V_o) variation for switching up operation. The voltage increases from V_{tap} to $2V_{tap}$.

6.5.2. Unity power factor

The system is operated at unity power factor. The firing angle for switching down operation is -5.45° as per the fig. 6.10. The T2 thyristor pair is triggered 5.45° before 0.4 s, and the firing signal for T1 pair is made zero at the same instant. A short circuit is initiated for the commutation and the peak short circuit current I_{T1} is 38.7 A. The peak short circuit current when calculated by the eq.6.3 is 63.7 A. The difference comes due to the approximation used for the calculation of the tap inductance. A simulation with only the equivalent tap inductance of 0.136 mH is performed instead of the transformer to verify the above statement(simulation model in appendix B). The peak short current in that simulation is observed to be 59.3 A, which is close to the value obtained through equation, thus validating the equation used for the analysis(plot in appendix B). The thyristor ratings are sufficient in this mode as the value obtained from the simulation with the transformer model is lower than the estimated value through the equation. The controlled short circuit current is very low compared to the thyristor rated current. Fig. 6.14 shows the waveforms for switching down operation. The thyristor pair T1 experiences a voltage of 31.4 V at the switch - off instant. Fig. 6.12b shows the output voltage

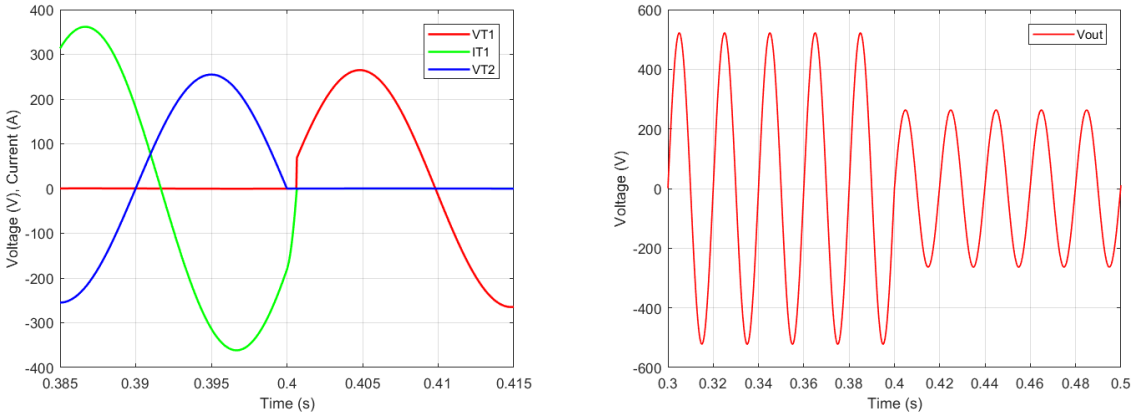

(a) (b)

Figure 6.12: Simulation results at an inductive power factor angle of 30 ° for switching down operation (a) Thyristor voltages V_{T1}, V_{T2} and thyristor current I_{T1} (b) Tap output voltage (V_o)

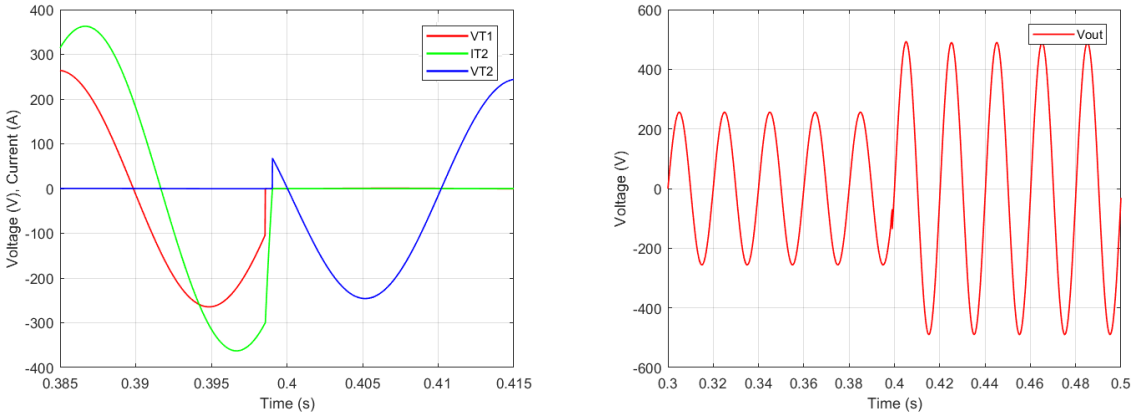

(a) (b)

Figure 6.13: Simulation results at an inductive power factor angle of 30 ° for switching up operation (a) Thyristor voltages V_{T1}, V_{T2} and thyristor current I_{T2} (b) Tap output voltage (V_o)

(V_o) variation for switching down operation. The voltage reduces from $2V_{tap}$ to V_{tap}.

The firing angle for switching up operation is -26°. The thyristor is triggered 26° before the voltage zero crossing. This is determined by phase shifting the switching down characteristics by 180°. The firing angle for switching up at an unity power factor is equal to firing angle for switching down at capacitive power factor of 180°. Fig. 6.15 shows the waveforms for switching up operation. The thyristor pair T2 experiences a voltage of 67.2 V at the switch - off instant. Fig. 6.12b shows the tap output voltage variation for switching up operation. The voltage increases from V_{tap} to $2V_{tap}$.

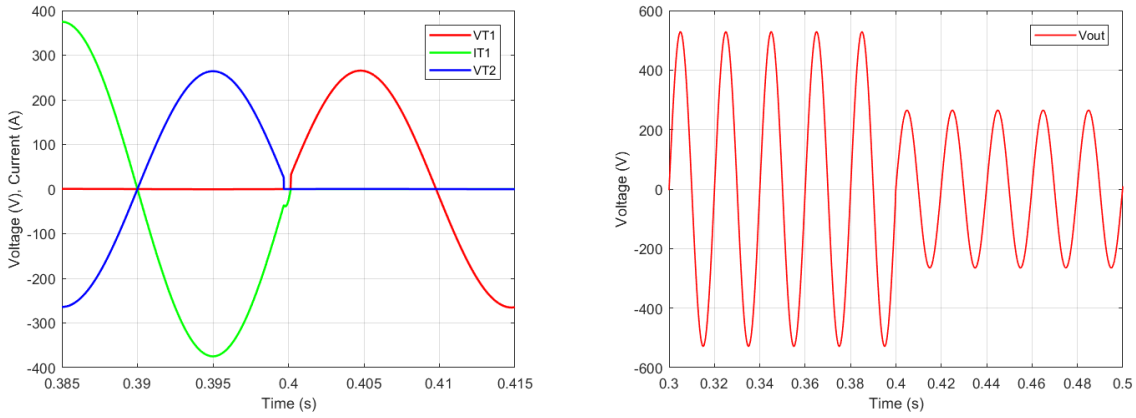

(a) (b)

Figure 6.14: Simulation results at unity power factor for switching down operation (a) Thyristor voltages V_{T1}, V_{T2} and thyristor current I_{T1} (b) Tap output voltage (V_o)

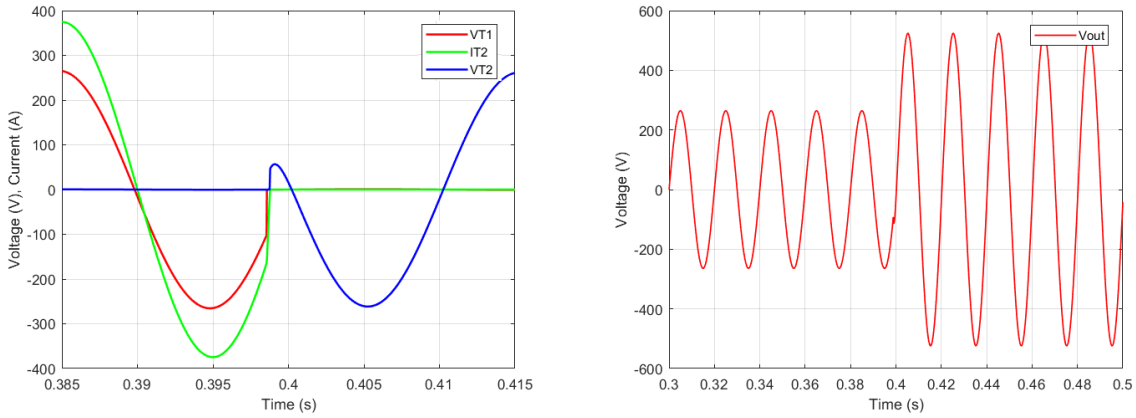

(a) (b)

Figure 6.15: Simulation results at unity power factor for switching up operation (a) Thyristor voltages V_{T1}, V_{T2} and thyristor current I_{T2} (b) Tap output voltage (V_o)

6.5.3. Capacitive power factor

The switching down operation in the capacitive region is analyzed for commutation with a short circuit and commutation without a short circuit. The capacitive region with a short circuit commutation is studied first. The system has a capacitive power factor angle of -24.8° (critical power factor angle ϕ_c). The firing angle for switching down operation in this mode is -26° as per the fig. 6.10. The T2 thyristor pair is triggered 26° before 0.4 s, and the firing signal for T1 pair is made zero at the same instant. A short circuit is initiated for the commutation and the peak short circuit current I_{T1} is 415.2A as shown in fig. 6.16a. The peak current through I_{T2} is 558.2 A (figure in appendix B). The current in T2 is higher compared to the current in T1 as it carries also the output load current. The value of I_{T1} & I_{T2} using the eq. 6.19 & eq.6.20 are 635.6 A & 792.5 A respectively. The difference between the calculated and the observed value comes due to the approximation used for the calculation of tap inductance. The value obtained from simulation is lower than the estimated value, hence,

the thyristor current ratings are sufficient in this region during commutation. This controlled short circuit current is lower than the thyristor rated current. The thyristor is capable of handling a peak non-repetitive surge current of 7.1 kA. Fig. 6.16b shows the output voltage (V_o) variation for switching down operation. The voltage reduces from $2V_{tap}$ to V_{tap}.

The system for switching down operation in capacitive region without a short circuit has a capacitive power factor angle of 30°. The firing angle for switching down operation is -19.1° as per the fig. 6.10. The T2 thyristor pair is triggered 19.1° before 0.4 s, and the firing signal for T1 pair is made zero at the same instant. Short circuit does not occur as predicted in the analysis. Thyristor T1b has an extinction angle greater than the thyristor turn-off angle ($|\phi - \alpha| = 11°$). The extinction angle for T1a is 12.45°, which is greater than thyristor turn-off angle (figure in appendix). Fig. 6.17 shows the waveforms for switching down operation without a short circuit for commutation. The thyristor pair T1 experiences a voltage of 57 V at the switch - off instant. Fig. 6.17b shows the output voltage (V_o) variation for switching down operation. The voltage reduces from $2V_{tap}$ to V_{tap}.

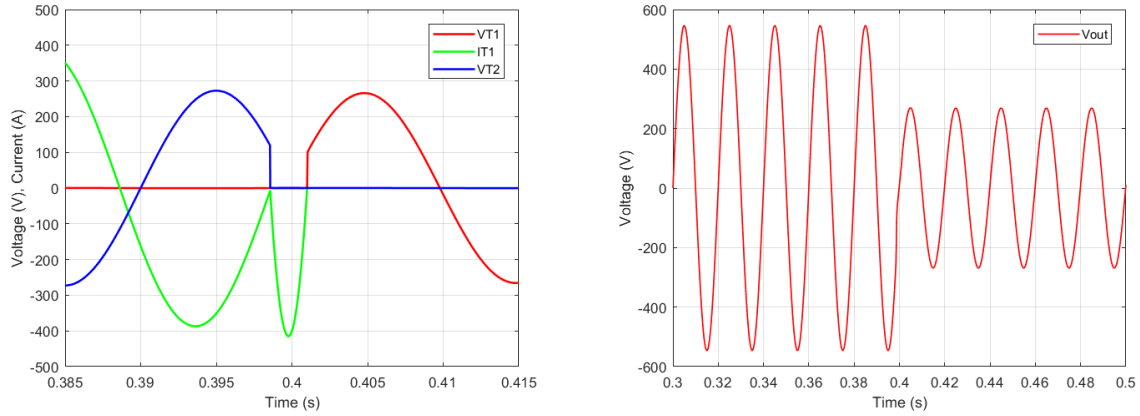

(a) (b)

Figure 6.16: Simulation results at capacitive power factor angle of 24.8° (ϕ_c) for switching down operation (a) Thyristor voltages V_{T1}, V_{T2} and thyristor current I_{T1} (b) Tap output voltage (V_o)

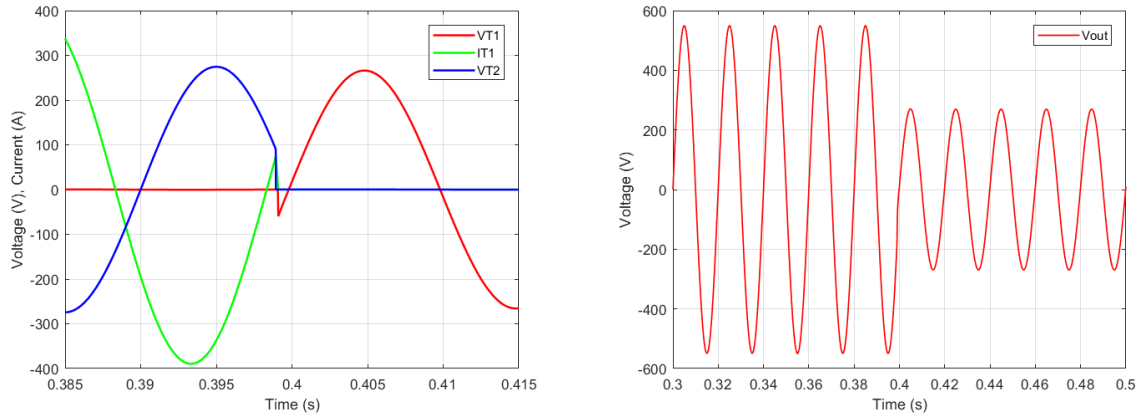

(a) (b)

Figure 6.17: Simulation results at capacitive power factor angle of 30° for switching down operation (a) Thyristor voltages V_{T1}, V_{T2} and thyristor current I_{T1} (b) Tap output voltage (V_o)

The firing angle for switching up operation is 0°. The thyristor is triggered at the instant of voltage zero crossing. This is determined by phase shifting the switching down characteristics by 180°. The firing angle for switching up at a capacitive power factor of 30° is equal to firing angle for switching down at an inductive power factor of 150°. Fig. 6.18 shows the waveforms for switching up operation. The thyristor pair T2 experiences a voltage of 19.8 V at the switch - off instant as observed in fig. 6.18a. Fig. 6.18b shows the tap output voltage variation for switching up operation. The voltage increases from V_{tap} to $2V_{tap}$.

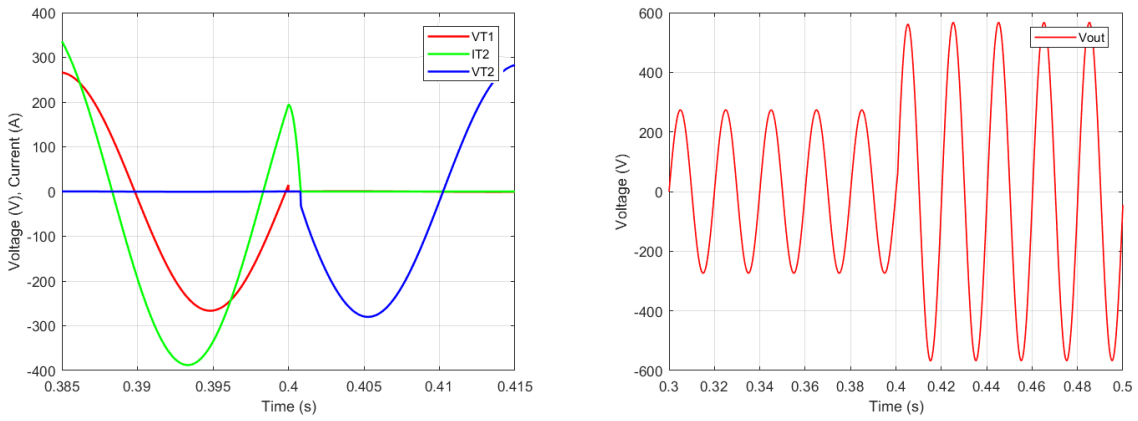

(a) (b)

Figure 6.18: Simulation results at capacitive power factor angle of 30° for switching up operation (a) Thyristor voltages V_{T1}, V_{T2} and thyristor current I_{T2} (b) Tap output voltage (V_o)

6.6. Simulation results of LVR with PE based OLTC

The thyristor based tap-changer is simulated for the complete LVR system in this section. The same LVR setup used in the previous chapter (sec. 5.2) for the simulation is used in this section, except for the transformer parameters and the OLTC. Fig.6.19 shows the simulink model used for the simulation with transformer parameters from table 6.3 and the thyristor based OLTC (figure in appendix B). The firing circuit is used to trigger the thyristor pair based on the firing angle corresponding to the power factor angle. The thyristor based OLTC is also implemented to the other phases of the transformer. The firing angle for phase Y is 120° displaced and for phase B is -120° displaced from phase R's firing angle.

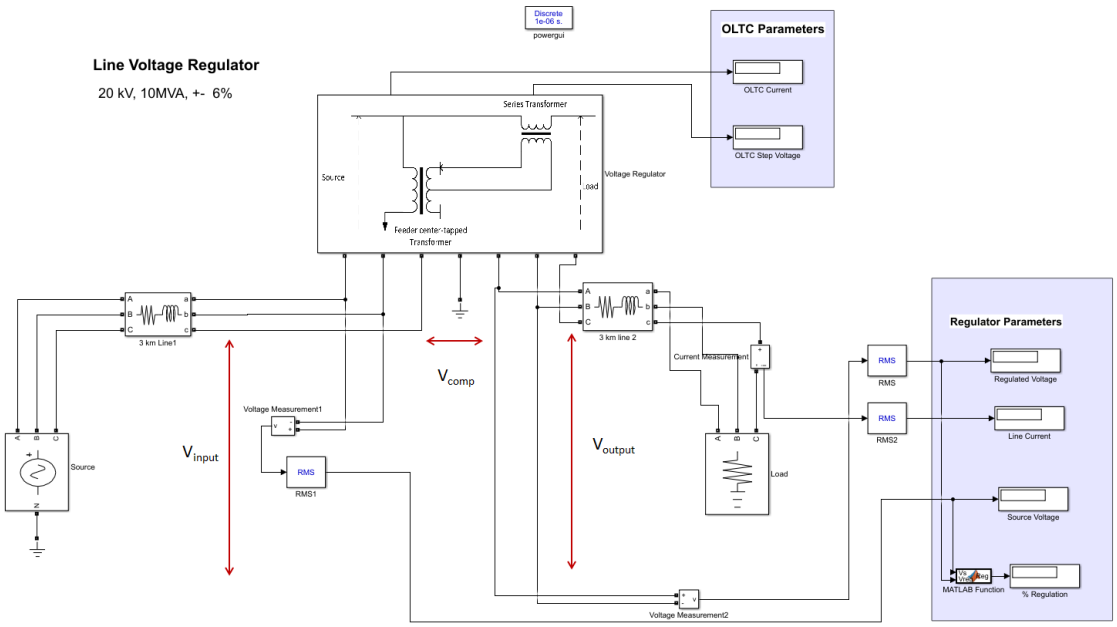

Figure 6.19: MATLAB/ Simulink model of a LVR with thyristor based OLTC in a MV distribution line

6.7. Switching down operation

The switching down operation is performed from a 6% voltage regulation to a 4.5% voltage regulation. The load is purely resistive, but the distribution lines have inductances which introduces a small inductive power

factor angle between line voltage and current. The system has an inductive power factor angle of 1.8°. The firing angle for switching down operation for an inductive power factor angle of 1.8° is - 4°. This firing angle will induce a controlled short circuit during the commutation process. The per-phase input RMS voltage to LVR is 10.91 kV (phase-phase voltage is 18.9 kV). The voltage drop from the 20 kV (phase-phase) source is due to the impedance in the line. The tap voltage (V_{tap}) is 250.4 V and the tap current is 358 A. The peak value of the short circuit current in thyristor T1b is 21.6 A, which is very low compared to the rated current of the components. Fig. 6.20a shows the compensation voltage of the LVR reducing from 934 V (6%) to 703.9 V (4.5%) after switching down operation around 0.4 s. Fig. 6.20a also shows the voltages and current of thyristor T1 & T2. Fig. 6.20b shows the LVR input and output voltage during the switching down operation with the voltage regulation (in %) highlighted in the figure. The LVR per-phase RMS output voltage reduces from 11554 V to 11412 V.

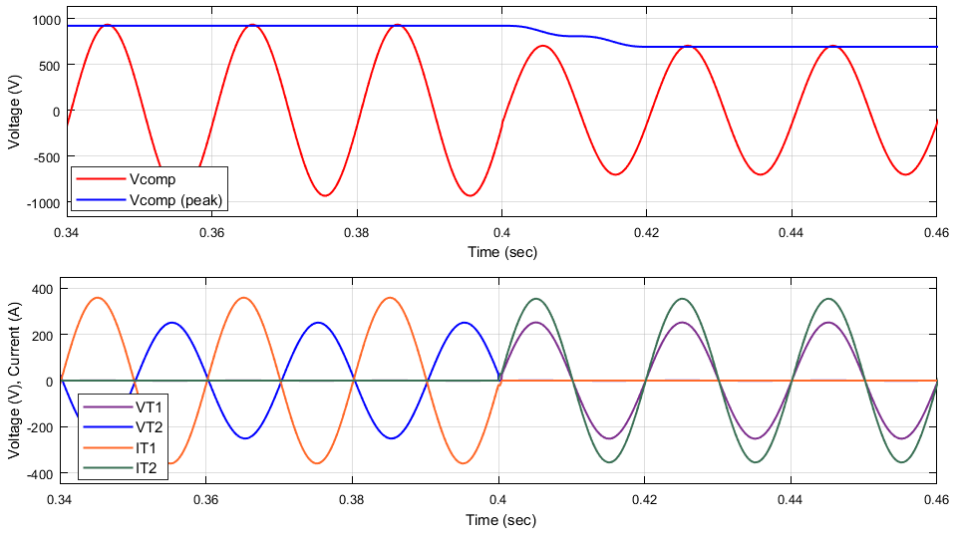

(a)

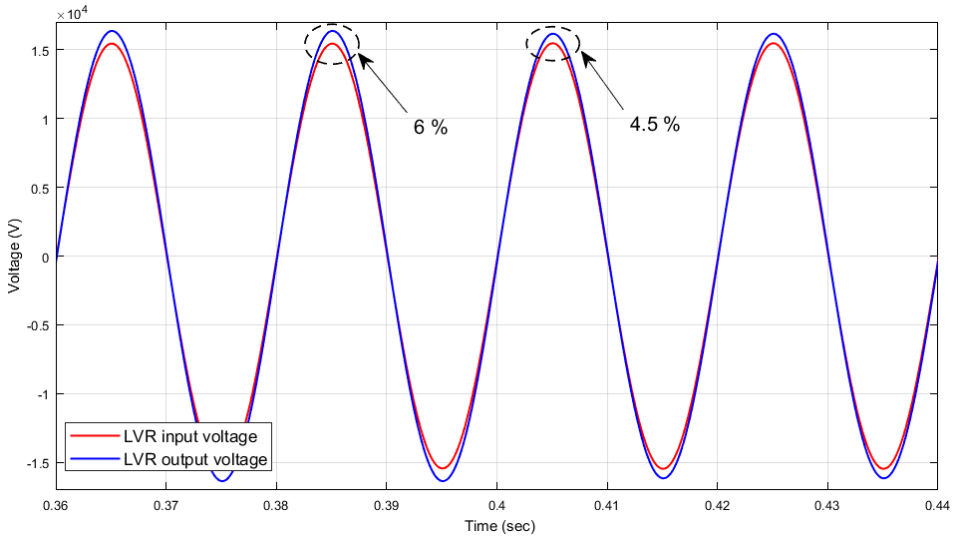

(b)

Figure 6.20: Simulation results of phase R for switching down operation in a LVR (a) Top: Compensation voltage, Bottom: Thyristor voltages (V_{T1}, V_{T2}) and Thyristor current (I_{T1}, I_{T2}) (b) LVR input and output voltages

6.8. Switching up operation

The switching up operation is performed from a 4.5% voltage regulation to a 6% voltage regulation. The system has an inductive power factor angle of 1.8°. The firing angle for switching up operation for an inductive power factor angle of 1.8° is - 26°. The commutation takes without the short circuit between the taps. The per-phase input RMS voltage to LVR is 10.91 kV (phase-phase voltage is 18.9 kV). The tap voltage (V_{tap}) is 251 V and tap current is 358 A. The thyristor pair T2 experiences a voltage of 97V at the switch - off instant. Fig. 6.21a shows the per-phase peak compensation voltage of the LVR increasing from 703.4 V (4.5%) to 934 V (6%) after switching up operation of around 0.4 s. Fig. 6.20a also shows the voltages and current of thyristor T1 & T2. Fig. 6.20b shows the LVR input and output voltage during the switching up operation with the voltage regulation (in %) highlighted in the figure. The LVR per-phase RMS output voltage increases from 11412 V to 11561 V.

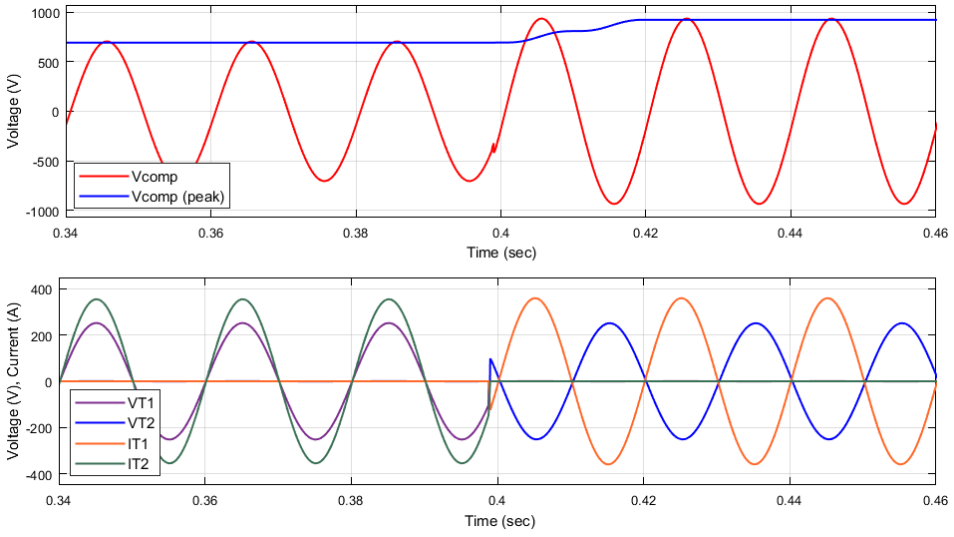

(a)

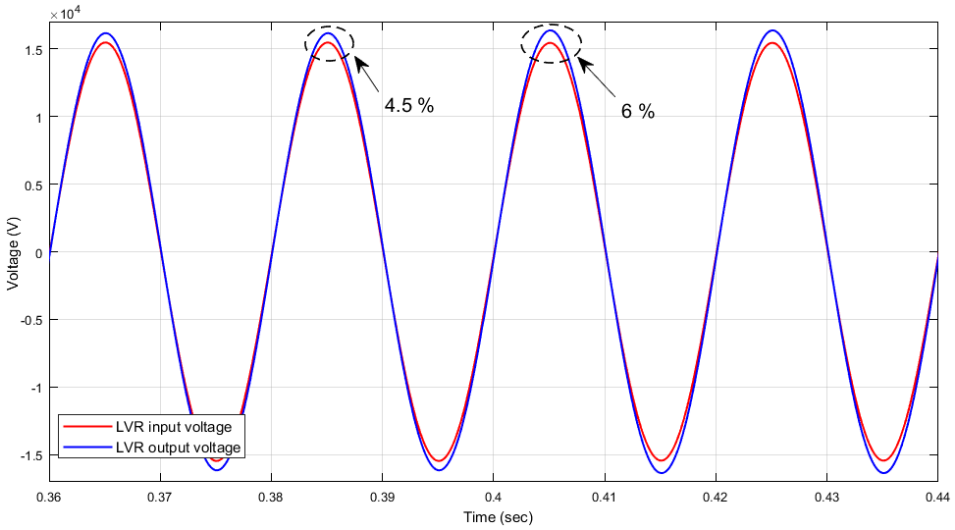

(b)

Figure 6.21: Simulation results of phase R for switching up operation in a LVR (a) Top: Compensation voltage, Bottom: Thyristor voltages (V_{T1}, V_{T2}) and Thyristor current (I_{T1}, I_{T2}) (b) LVR input and output voltages

6.9. Comparison of PE based OLTC and mechanical OLTCs

Chapter 5 analyzed LVR configuration 5 with a mechanical OLTC, and this chapter focused on analyzing LVR with thyristor based OLTC. A brief technical and economic comparison of both OLTCs is presented in this

section to understand the advantages and disadvantages.

Mechanical OLTCs have a simple commutation principle using of oil or vacuum switches to quench the arc. The commutation can be executed at any instant due to the use of a bridging resistor or reactor to restrict the circulating short circuit currents. The mechanical OLTC used in this thesis, ECOTAP VPD III 100, takes approximately 300 ms per tap change operation and requires a minimum of 3 s between each tap change operation[29]. Mechanical OLTCs have maximum number of tap changing operations due to the use of mechanical components for quenching the arc. It has a maximum number of 500,000 tap changing operations before being decommissioned for maintenance. It can withstand a short circuit peak current up to 5000 A for 2 s. This is one of the advantages of having mechanical contacts which can withstand large currents without any special mechanism to protect the contacts. ECOTAP VPD III 100 with the VPD Motor Drive & Control (MD & C) cost approximately 12,000 €.

A thyristor based OLTC takes less than one cycle for a three-phase tap change operation and it requires only one cycle (20 ms) delay between each tap change operation. One cycle delay between each tap change operation is required for the new rising edge of voltage zero crossing, around which thyristors are triggered. Ideally, thyristor based OLTCs do not have limitations on the number of tap changing operations. It requires a fault deviation switch on the primary side of the series transformer [44] for the protection of solid state switches. A fault deviation switch has an important function of bypassing the currents in the secondary of the feeder transformer during line short circuit. A total of 18 solid state switches are required per-phase. The cost of thyristors (ABB 5STP 04D44200) for a three-phase 20kV, 10 MVA LVR with ±6% voltage regulation is approximately 3510 €. The cost of fast acting fault deviation switches, controllers and gating circuits for thyristors are not included in the cost calculation. Only by including the previously mentioned costs, can a more accurate cost estimation of a thyristor based OLTC be calculated.

Table 6.4: Technical and cost comparison of ECOTAP VPD III 100 and thyristor based OLTC(* Includes only the cost of thyristor switches)

	ECOTAP VPD III 100	Thyristor based OLTC
Runtime per tap-change operation	~300 ms	<20ms
Minimum time delay between tap-change operations	3 s	20 ms
Maximum number of tap-change operations	500,000	NA
Short circuit capability	5000 A for 2 s	Requires a fault deviation switch
Cost	12000 €	3510* €

7

Conclusion and Future Work

7.1. Thesis overview

The impact of a shunt voltage compensation, series voltage compensation and conductor upgradation on grid capacity of a MV radial feeder distribution line was studied. LVR was effective in significantly improving the grid capacity without violating the power and voltage limits of the distribution line. Various configurations of LVR with single and two active parts were studied. ECOTAP VPD III 100 from Maschinenfabrik Reinhausen (MR) was chosen as the OLTC for the LVR as it was economical and it required low maintenance for the oil in the transformer due to vacuum interrupters. LVR with center tapped autotransformer as the feeder transformer and a two winding transformer as the booster transformer was economical for the 20 kV, 10 MVA line. As ABB's oil-transformer factory does not manufacture autotransformers for MV levels, implementing this design would require changes in the factory assembly lines, which will lead to major cost implications. Hence, the design and simulation was carried out for the LVR configuration 5 with center tapped two winding transformer as the feeder transformer, and a two winding transformer as the booster transformer. A small scale experimental setup was built to test the LVR configuration 5 with the ECOTAP VPD III 100 OLTC. The simulation and experimental results with LVR configuration 5 were found to be satisfactory. As mechanical OLTCs require regular maintenance, a feasibility study of a power electronics based OLTC was conducted. LVR configuration 5 was chosen for this feasibility study as it provides isolation to the solid-state switches and enables the system to use thyristors without a series/parallel connection for the taps. The thyristor switches were found to have almost 5 times lower losses and were 9 times cheaper than the IGBT switches for this application. The commutation instants were defined based on the power factor of the system to have controlled short circuit currents for certain power factor angles with thyristor based OLTCs. A transformer model with two taps was simulated for the complete power factor range. The thyristor based OLTC was also implemented to a 20 kV, 10 MVA LVR with ±6% voltage regulation. The switching up and switching down operation was performed and the simulation results were found to be satisfactory. A brief technical and cost comparison between mechanical OLTCs and thyristor based OLTCs was also presented.

7.2. Results and conclusion

Impact of LVRs on the grid capacity

The main results and conclusions from studying the impact of different voltage regulation strategies on grid capacity for a 20 kV, 10 MVA radial feeder are as follows:

- Voltage variation limits pose a serious bottleneck to utilize the full grid capacity in a MV distribution network. It was shown that the voltage limits are violated before the thermal or power limits of long MV distribution lines.

- Shunt compensation using reactive elements or FACTS devices helps to increase the grid capacity only by a small percentage. Shunt compensation is not very effective in regulating the voltage in distribution networks due to the high R/X ratio.

- Series compensation with a LVR is able to effectively increase the grid capacity up to 73.59 % in load scenario and 63.78 % for the generation scenario as shown in the fig. 7.1. For a MV distribution feeder line with loads and generators, LVR enables the DSO to utilize the existing line for longer lengths without voltage violation and avoids the expensive grid reinforcements such as conductor upgradation.

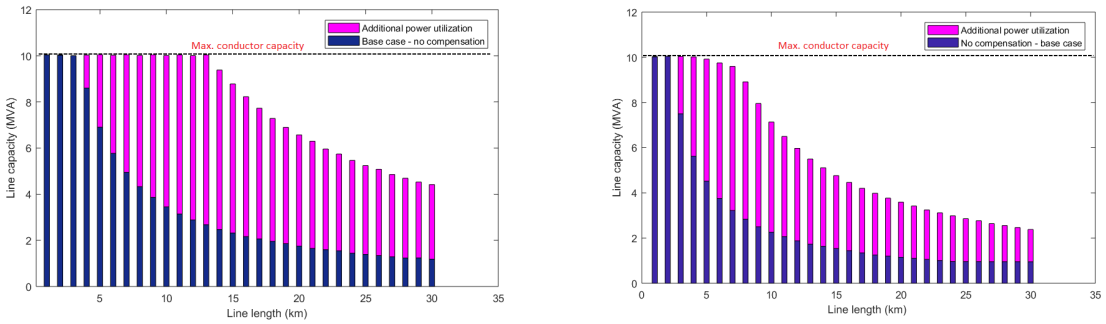

(a) (b)

Figure 7.1: (a) Line capacity (MVA) vs line length (km) for the load scenario with a ±10% LVR (b) Line capacity (MVA) vs line length (km) for the generation scenario with a ±10% LVR

Economical LVR configuration with mechanical OLTCs

The main results and conclusions from analyzing different configurations with oil-type transformers and mechanical OLTC for a 20 kV, 10 MVA LVR system with ±6% voltage regulation are as follows:

- ECOTAP VPD III 100 from MR was selected as the preferred OLTC because of its low cost and no oil maintenance required in the transformer due to vacuum interrupters to quench the arc during tap changes.
- Various configurations of LVRs with single and two active parts with OLTC were analyzed. All the configurations were compared for the cost and range of operation.
- Single active part configuration has a limited power range due to the rated current limitation of 100 A by the OLTC. For a 20 kV system, single active part configuration could handle a maximum line power of 3.4 MVA.
- For a 20 kV, 10 MVA feeder line, LVR configuration 6 was found to be the most economical configuration with operating power range up to 16.5 MVA. LVR configuration 6 uses a feeder center tapped autotransformer and a booster two winding transformer with OLTC without any reversing contactors for voltage reversal.
- LVR configuration 5 with a two winding feeder transformer is selected for further analysis due to the cost involved in setting up new assembly lines at ABB for LVR configuration 6, which requires MV autotransformers. The only difference between LVR configuration 5 and 6 is that the former uses a two winding transformer and the latter uses an autotransformer as the feeder transformer.
- A 20 kV, 10 MVA LVR with ±6% voltage regulation was simulated in MATLAB/ Simulink and was experimentally verified with a LV setup. The selected LVR configuration with ECOTAP VPD III has a satisfactory performance for positive and negative voltage regulations.

Feasibility of power electronics based OLTCs

A feasibility study of power electronics based OLTCs was conducted for a 20kV, 10 MVA LVR with ±6% voltage regulation. The main results and conclusions were as follows:

- LVR configuration 5 was chosen for implementing the power electronics based OLTC as it provides voltage isolation to the switches from the MV distribution line disturbances.

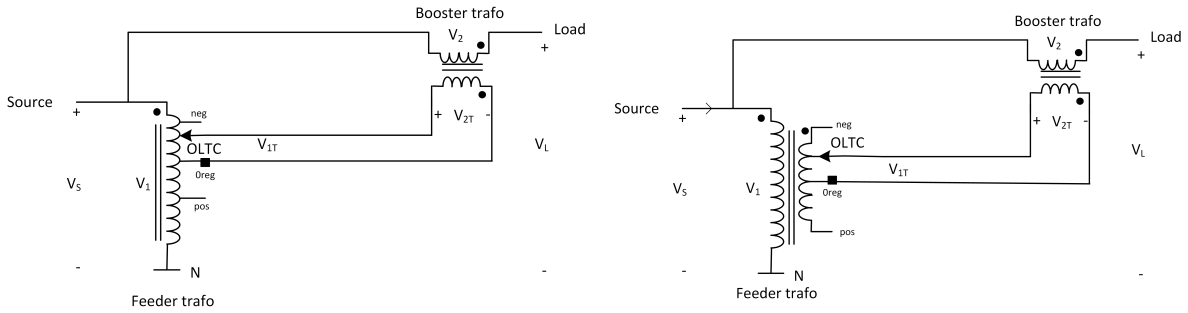

Figure 7.2: (a)LVR configuration 6 (b) LVR configuration 5

- Thyristors in anti-parallel configuration were chosen as the solid state bi-directional switch for the OLTC as it was 9 times cheaper and has 5 times lower losses compared to IGBT in common-emitter mode for this application. The thyristor with part number 5STP 04D4200 from ABB satisfies the required voltage and current ratings.
- Commutation instants were defined for the complete power factor range for the thyristor based OLTC to have no/controlled short circuit during tap changes.
- The feeder transformer model with two taps was simulated for switching up and switching down operation with a thyristor based OLTC for capacitive, inductive and resistive power factors. The peak short circuit current for switching down operation at unity power factor was found to be 38.7 A. The peak short circuit current for switching down operation at critical power factor angle (ϕ_c = -24.8°) was found to be 558.2 A. The controlled short circuit peak currents are less than the rated non-repetitive surge current rating of the thyristor and less than 2 pu of the rated current on the secondary side of the feeder transformer.
- The LVR was placed in a distribution line and tap changing operations was performed using the thyristor based OLTC. The system was able to switch up and switch down satisfactorily, confirming the robust operation of a thyristor based OLTC for LVR applications.
- Thyristor based OLTC proves to be superior compared to the ECOTAP VPD III 100 OLTC in terms of maximum number of tap-changes before maintenance, time taken per tap-change and minimum delay time between two consecutive tap-changes. The cost of thyristors (ABB 5STP 04D44200) for a three-phase 20kV, 10 MVA LVR with ±6% voltage regulation is approximately 3510 €. The cost of fast acting fault deviation switches, controller and gating circuits for thyristors should be included to have an accurate cost comparison against ECOTAP VPD III 100 mechanical OLTC.

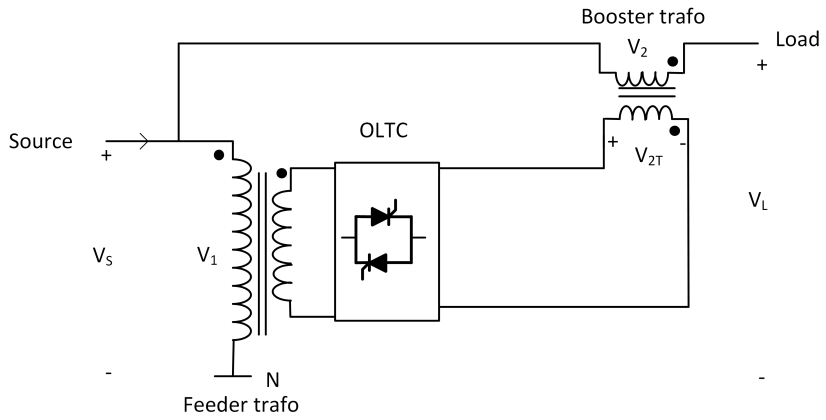

Figure 7.3: Schematic of LVR configuration 5 with thyristor based OLTC

7.3. Future Work

Although this thesis work focused on various aspects of LVR in a MV distribution grid, there is a scope for further improvement which can be incorporated in the future. In this section some suggestions for future work are presented.

- The impact study of different voltage regulation strategies only considered radial grids for simulations in this project work. The same study could be extended to a meshed distribution grid configuration.
- Distribution OLTCs on MV/LV transformers are being installed by the DSOs to regulate the voltages in the grid. Either all the load centers with MV/LV transformers could be installed with a OLTC to regulate the LV voltage or the MV line could be installed with a LVR to regulate the MV voltage, which will in turn regulate the LV voltage. These two methodologies could be studied in detail to find the most technically beneficial and economical solution for the voltage regulation in distribution grids.
- Due to time constraints, the selected LVR configuration could be tested only on a low voltage setup. The complete prototype with a MV oil-type transformer, OLTC, protection and bypass switches and controller could be tested to make the concept ready to be introduced into the market.
- This work could be extended by including the primary side inductance for the determination of tap inductance to accurately predict the short circuit current during tap-changes. In this study, the analysis for commutation with thyristor based OLTCs considered an approximate model of tap inductance, which led to differences in predicted short circuit currents using analytically derived equations and observed short circuit current in the simulations.
- A low voltage setup of LVR could be used to experimentally verify the control algorithm applied in this thesis work for the thyristor based OLTC.
- A fault deviation switch could be designed and tested as it plays a crucial role in the protection of solid state switches during fault conditions.

Appendix A

The MATLAB code to run the simulink model for studying the impact of different voltage regulations strategies on grid capacity of a distribution line

```
%% Loading parameters for tech-eco analysis
clear all;
clc;
%%

N_l = 5;
Z = zeros(30,1);
s= 1;
%% P_s load apparent power
for L = 0.2: 0.2 : 6
    for P_s = 1.1e6: 0.05e6 : 10e6
    P_a = ( P_s * 1); %%active power
    P_r = sqrt(P_s^2 - P_a^2); %% reactive power
    %PC = 0.666 * P_r ;
    R_line = 0.455* L;
    X_line = 0.2772* L;
    L_line = (X_line)/(2*pi*50);
    LF = power_loadflow('-v2','techecoanalysis5','solve');
    bu = LF.bus;
    x = struct2table(bu);
    V_load = abs(table2array(x (6,13)));
    P_line = abs(table2array(x(1,15)));
        if P_line >= 0.1 || V_load <= 0.96
            break
        end
    end
Z(s) = P_line;
s=s+1;
end
%L = 1.4 ; line length in Km
Len = 0.2:0.2: 6;
Z= Z*100e6;
plot (Len*5,Z)
```

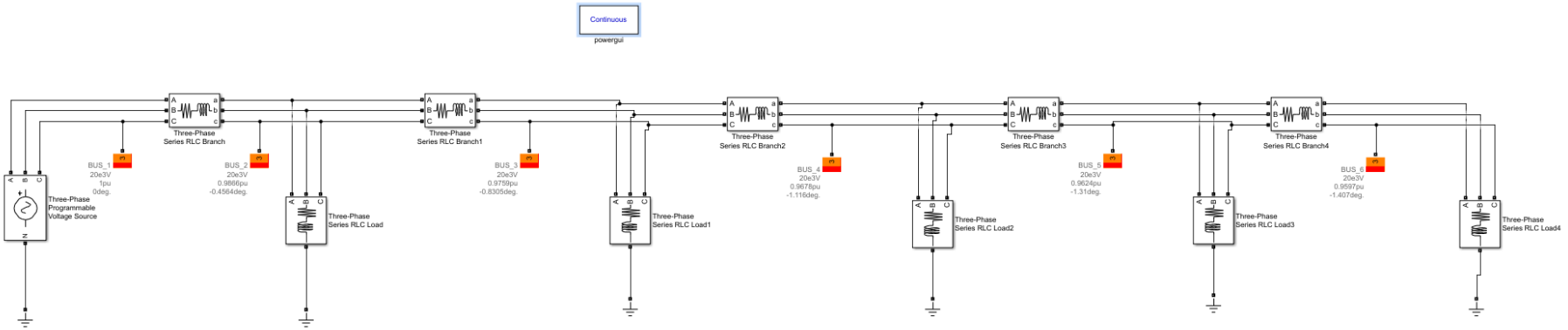

Figure 4: MATLAB/Simulink model used for technical benefit analysis

Appendix B

```
%% Code for calculating alpha maximum for switching down operation in capacitive power factor region
clear all;
clc;
%%

syms x
%phi = [30 29 28 27 26 25 24 23 22 21];
%firing_angle = zeros(1,10);
alpha30 = 30*ones(1,156);
phi_slicap = -1* [24.99 23 22 21 20 19 18 17 16 15 14 13 12 11
10 9 8 7 6 5 4 3 2 1 0 -1 -2 -3 -4 -5 -6];
alpha_slicap = (0.822*phi_slicap) - 5.45;
for i = 1 : 156
syms x
phi(i) = 181 - i;
E = cos (x)+(0.06*sin(x+((181 - i)*.017)))+0.98 == 0;
[x] = solve (E,x);
vpa (x)
alpha = double (x);
alpha = real(alpha);
alpha = rad2deg(alpha);
firing_angle(i) = 180 - alpha(1);
end

plot (-phi, -firing_angle)
hold on
plot (-phi, (-phi+10.9))
hold on
plot (-phi, -alpha30)
```

```
%% Loading parameters for the thyristor based OLTC
clear all;
clc;
%%
%% firing angle
ON_TA1 = 1; %TA1 1, TA2 zero -> switching down
ON_TA2 = 0; % TA2 0 , TA2 1 -> switching up
fir_ang = -4.45;
fir_inst = 0.400; %0.40029
t_TA1 = fir_inst + (fir_ang*55.556e-6);
t_TA2 = fir_inst + (fir_ang*55.556e-6);
t_TB1 = fir_inst + (fir_ang*55.556e-6);
t_TB2 = fir_inst + (fir_ang*55.556e-6);
%%

%% Thyristor parameters
Ron_TA1 = 1e-3 ; %1e-3
Lon_TA1 = 0 ;
Vf_TA1 = 0.01 ; %.01
Rs_TA1 = 5000 ; %5000
Cs_TA1 = 250e-9 ;

Ron_TA2 = 1e-3 ;
Lon_TA2 = 0 ;
Vf_TA2 = 0.01 ;
Rs_TA2 = 5000 ;
Cs_TA2 = 250e-9 ;

Ron_TB1 = 1e-3 ;
Lon_TB1 = 0 ;
Vf_TB1 = 0.01 ;
Rs_TB1 = 5000 ;
Cs_TB1 = 250e-9 ;

Ron_TB2 = 1e-3 ;
Lon_TB2 = 0 ;
Vf_TB2 = 0.01 ;
Rs_TB2 = 5000 ;
Cs_TB2 = 250e-9 ;
%%

%% Load parameters
S_load = 99702.05;
ang_phi = 0;
PF = cosd(ang_phi);
P_load = S_load * PF;
Ql_load = 0;
Qc_load = P_load* tand(ang_phi);
%%
```

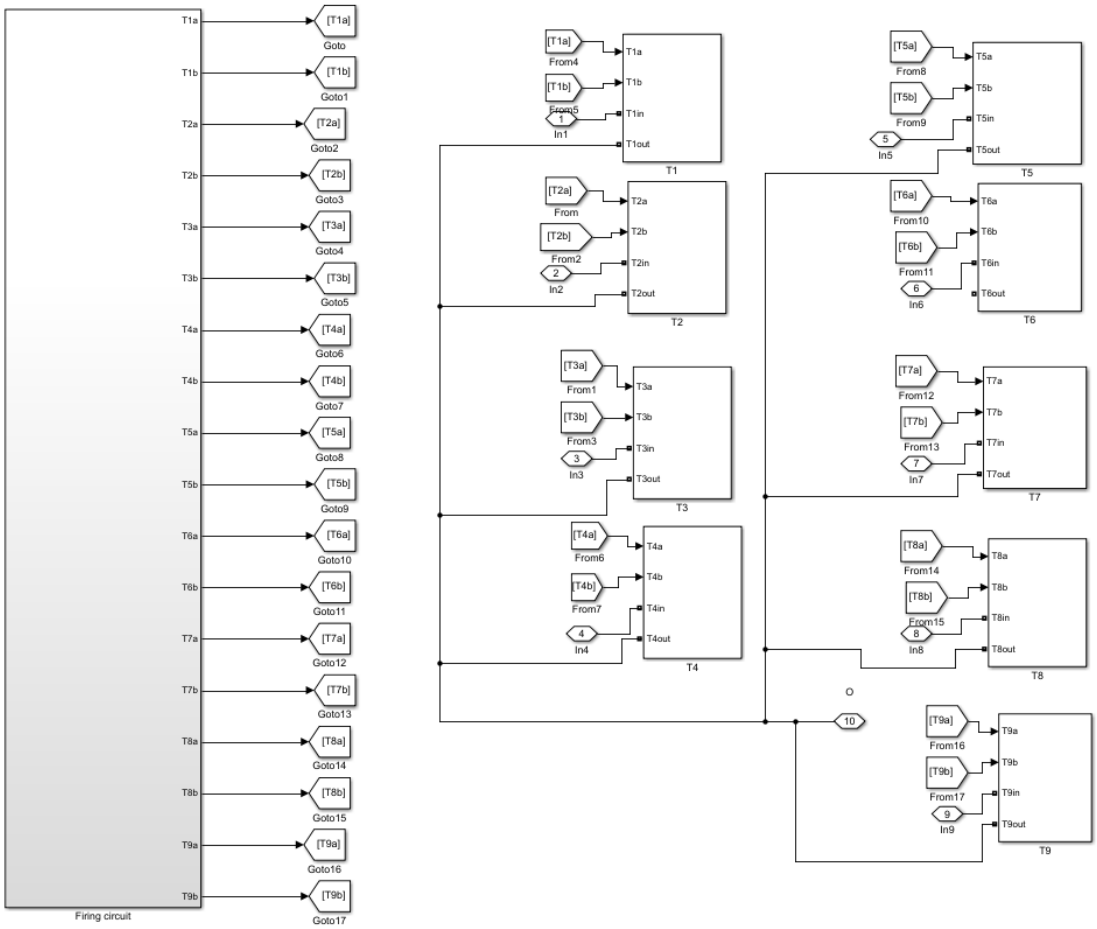

Figure 5: MATLAB/ Simulink model of a single phase thyristor based OLTC

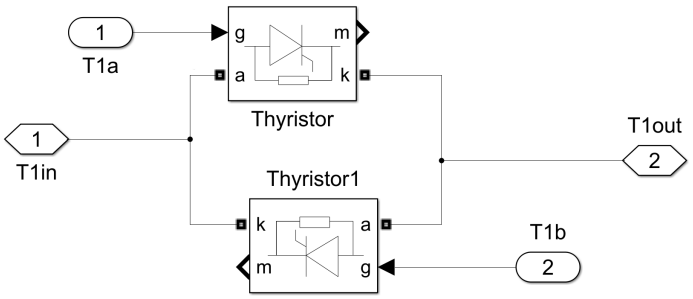

Figure 6: MATLAB/ Simulink model of thyristor cell subsystem used in fig.5

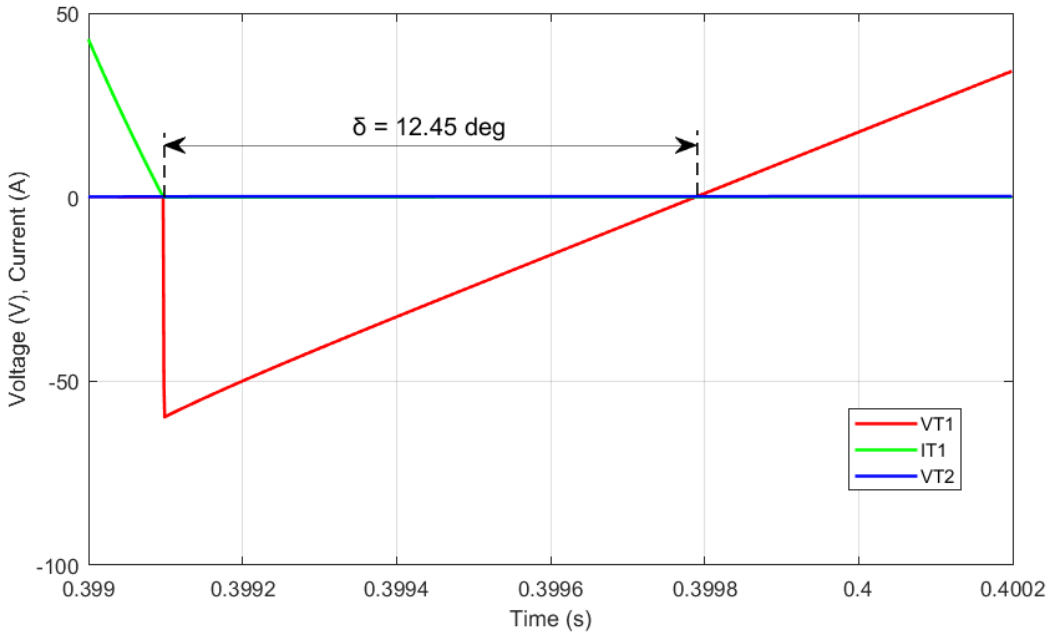

Figure 7: Extinction angle of T1a for switching down at capacitive power factor angle of 30°

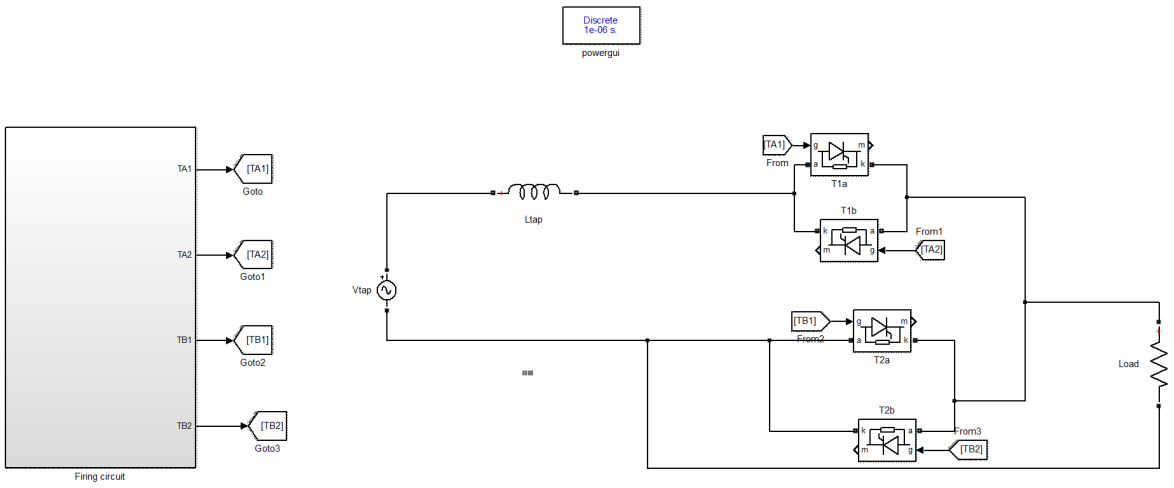

Figure 8: MATLAB/ Simulink model of two taps with equivalent tap inductance and thyristor based tap-changer

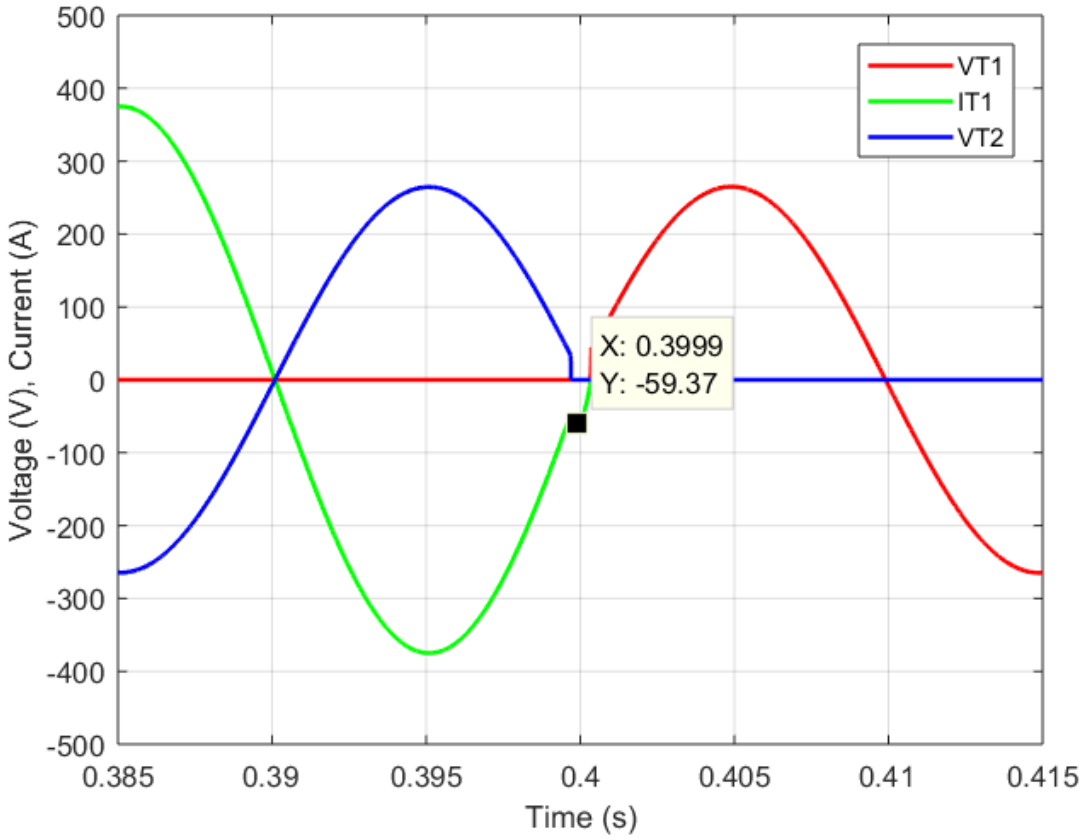

Figure 9: Simulation results of V_{T1}, V_{T2} & I_{T1} at unity power factor with tap inductance instead of feeder transformer model

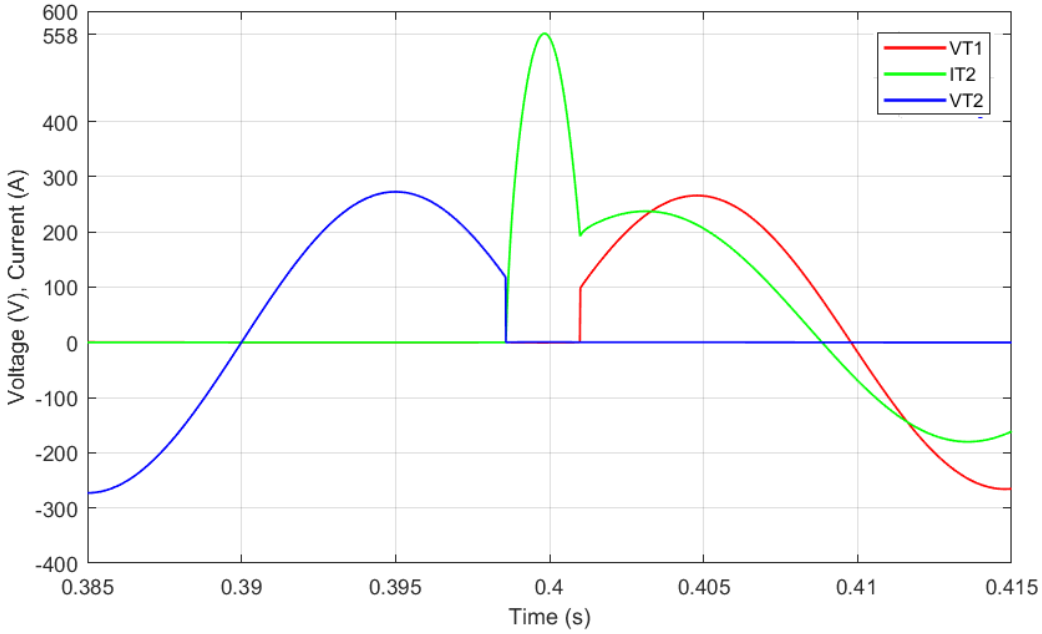

Figure 10: Simulation results of V_{T1}, V_{T2} & I_{T2} at capacitive power factor angle of 24.8°

Bibliography

[1] ANSI C84.1-2011, Voltage ratings for electric power systems and equipment (60 hz).

[2] GB/T 12325-2003, Power quality– Admissible deviation of supply voltage.

[3] Linking Renewable Energy to Rural Development, Executive Summary Brief for Policy Makers.

[4] NRS-048-2, Quality of supply part 2: Voltage characteristics, compatibility levels, limits and assessment methods.

[5] EN50160, Voltage characteristics of electricity supplied by public distribution networks.

[6] Transmission line constraints. URL `http://nptel.ac.in/courses/108101040/6`.

[7] Global trends in renewable energy, Jan 2018. URL `https://www.rsm.global/insights/economic-insights/global-trends-renewable-energy`.

[8] Line voltage regulator for medium voltage grids with RESIBLOC ® technology Reliable answer to voltage variations. Tec. Report 2014.

[9] Tao AAXu and PC Taylor. Voltage control techniques for electrical distribution networks including distributed generation. *IFAC Proceedings Volumes*, 41(2):11967–11971, 2008.

[10] J. Arrillaga and R. M. Duke. A static alternative to the transformer on-load tap-changer. *IEEE Transactions on Power Apparatus and Systems*, PAS-99(1):86–91, 1980. ISSN 00189510. doi: 10.1109/TPAS.1980.319612.

[11] P. Bauer and S. W. H. de Haan. Electronic tap changer for 500 kva/10 kv distribution transformers: design, experimental results and impact in distribution networks. In *Conference Record of 1998 IEEE Industry Applications Conference. Thirty-Third IAS Annual Meeting (Cat. No.98CH36242)*, volume 2, pages 1530–1537 vol.2, Oct 1998. doi: 10.1109/IAS.1998.730344.

[12] Danilo Bertini, D Falabretti, M Merlo, D Moneta, J SILVA DE ASSIS CARNEIRO, and Andrea Silvestri. Hosting capacity of italian lv distribution networks. In *CIRED 2011*, pages 1–4, 2011.

[13] M. T. Bishop, J. D. Foster, and D. A. Down. The application of single-phase voltage regulators on three-phase distribution systems. In *Proceedings of 1994 IEEE Rural Electric Power Conference*, pages C2/1–C2/7, Apr 1994. doi: 10.1109/REPCON.1994.326251.

[14] David Block, John Harrison, Paul Brooker, FS Center, and Ms Denise Dunn. Electric vehicle sales for 2014 and future projections. *Florida Solar Energy Center*, pages 1949–3053, 2015.

[15] Ben O Brewin, Samuel CE Jupe, Marc G Bartlett, Katherine T Jackson, and Clare Hanmer. New technologies for low voltage distribution networks. In *Innovative Smart Grid Technologies (ISGT Europe), 2011 2nd IEEE PES International Conference and Exhibition on*, pages 1–8. IEEE, 2011.

[16] Martin Carlen and et al. Voltage control system, Sep 2017.

[17] Martin Carlen, Frank Cornelius, Jens Tepper, Rainer Jakobs, Michael Schneider, Harald Wiesler, Adam Slupinski, and Irma Buschmann. LINE VOLTAGE REGULATOR FOR VOLTAGE ADJUSTMENT IN MV-GRIDS. *CIRED*, (June):15–18, 2015.

[18] Nan Chen and Lars E. Jonsson. A new Hybrid power electronics on-load tap changer for power transformer. In *Conference Proceedings - IEEE Applied Power Electronics Conference and Exposition - APEC*, 2015. ISBN 9781479967353. doi: 10.1109/APEC.2015.7104475.

[19] Carter-brown Clinton. Increasing Network Capacity By Optimising Voltage Regulation on Medium. (May):12–15, 2003. ISSN 1021447X.

[20] California Energy Commission. *MODELING AND TESTING OF UNBALANCED LOADING AND VOLTAGE REGULATION*. Number March. 2009. ISBN 5002008054.

[21] Stefania Conti and Andrea Maria Greco. Innovative voltage regulation method for distribution networks with distributed generation. In *19th International Conference on Electricity Distribution*, 2007.

[22] Juan Dixon, L. Moran, J. Rodriguez, and Ricardo Domke. Reactive power compensation technologies: State-of-the-art review. *Proceedings of the IEEE*, 93(12):2144–2164, 2005. ISSN 0018-9219. doi: 10.1109/JPROC.2005.859937. URL `http://ieeexplore.ieee.org/lpdocs/epic03/wrapper.htm?arnumber=15457685Cnhttp://ieeexplore.ieee.org/xpls/abs_all.jsp?arnumber=1545768`.

[23] Edition. Capacity of Distribution Feeders for Hosting DER. 2014.

[24] General Electric Digital Energy. Voltage regulators - robust, maintenance free solutions, 2014.

[25] S. P. Engel and R. W. De Doncker. Control of thyristor-based commutation cells. In *2012 IEEE Energy Conversion Congress and Exposition (ECCE)*, pages 2030–2037, Sept 2012. doi: 10.1109/ECCE.2012.6342562.

[26] Jawad Faiz and Behzad Siahkolah. *Electronic tap-changer for distribution transformers*, volume 2. Springer Science & Business Media, 2011.

[27] L. A. Gallego and A. Padilha-Feltrin. Voltage regulator modeling for the three-phase power flow in distribution networks. In *2008 IEEE/PES Transmission and Distribution Conference and Exposition: Latin America*, pages 1–6, Aug 2008. doi: 10.1109/TDC-LA.2008.4641843.

[28] Frederik Geth, Koen Willekens, Kristien Clement, Johan Driesen, and Sven De Breucker. Impact-analysis of the charging of plug-in hybrid vehicles on the production park in belgium. In *MELECON 2010-2010 15th IEEE Mediterranean Electrotechnical Conference*, pages 425–430. IEEE, 2010.

[29] ECOTAP VPD Maschinenfabrik Reinhausen GmbH. URL `https://www.reinhausen.com`.

[30] John J. Grainger. *Power system analysis*. McGraw-Hill, 1994.

[31] Björn Gwisdorf, Thorsten Borchard, Torsten Hammerschmidt, and Christian Rehtanz. Technical and economic evaluation of voltage regulation strategies for distribution grids with a high amount of fluctuating dispersed generation units. In *Innovative Technologies for An Efficient and Reliable Electricity Supply (CITRES), 2010 IEEE Conference on*, pages 8–14. IEEE, 2010.

[32] James H Harlow. Transformer tap changing under load: a review of concepts and standards. In *Proc. 1993 64th Annual Engineering Conf.*, pages 305–310, 1993.

[33] Ali Ipakchi and Farrokh Albuyeh. Grid of the future. *IEEE power and energy magazine*, 7(2):52–62, 2009.

[34] Hao Jiang, Roger Shuttleworth, Bashar A.T. Al Zahawi, Xiaolin Tian, and Andrew Power. Fast response GTO assisted novel tap changer. *IEEE Transactions on Power Delivery*, 16(1):111–115, 2001. ISSN 08858977. doi: 10.1109/61.905608.

[35] Takehiko Kojima, Hitoshi Isotani, and Makato Yamada. Distribution Static Var Compensators and Static Synchronous Compensators for Suppressing Voltage Fluctuation. Technical report, Fuji Electric.

[36] SV Kulkarni and SA Khaparde. Transformer engineering design and practice. *Indian Institute of Technology, Bombay (Mumbai)*, 2004.

[37] G Leci and F Cornelius. Increasing grid capacity to connect renewable energies. *CIRED*, pages 1–9, 2016.

[38] Yang Liu, Shuitao Yang, Shao Zhang, and Fang Zheng Peng. Comparison of synchronous condenser and STATCOM for inertial response support. *2014 IEEE Energy Conversion Congress and Exposition, ECCE 2014*, pages 2684–2690, 2014. doi: 10.1109/ECCE.2014.6953761.

[39] JA Peças Lopes, Filipe Joel Soares, and PM Rocha Almeida. Identifying management procedures to deal with connection of electric vehicles in the grid. In *Powertech, 2009 IEEE bucharest*, pages 1–8. IEEE, 2009.

[40] M.A. Mahmud, M.J. Hossain, and H.R. Pota. Analysis of Voltage Rise Effect on Distribution Network with Distributed Generation. *IFAC Proceedings Volumes*, 44(1):14796–14801, 2011. ISSN 14746670. doi: 10.3182/20110828-6-IT-1002.01305. URL http://linkinghub.elsevier.com/retrieve/pii/S1474667016460064.

[41] Nasif Mahmud and A. Zahedi. Review of control strategies for voltage regulation of the smart distribution network with high penetration of renewable distributed generation. *Renewable and Sustainable Energy Reviews*, 64:582–595, 2016. ISSN 18790690. doi: 10.1016/j.rser.2016.06.030. URL http://dx.doi.org/10.1016/j.rser.2016.06.030.

[42] Philippe Maibach and System Engineering. STATCOM Technology for Wind Parks to Meet Grid Code Requirements. pages 1–10.

[43] Paul E. Marken, Arthur C. Depoian, John Skliutas, and Michael Verrier. Modern synchronous condenser performance considerations. *IEEE Power and Energy Society General Meeting*, pages 1–5, 2011. ISSN 19449925. doi: 10.1109/PES.2011.6039011.

[44] Salvador Martínez García, Juan Carlos Campo Rodríguez, José Antonio Jardini, Joaquin Vaquero López, Alfonso Ibarzábal Segura, and Pedro María Martínez Cid. Feasibility of electronic tap-changing stabilizers for medium voltage lines - Precedents and new configurations. *IEEE Transactions on Power Delivery*, 24(3):1490–1503, 2009. ISSN 08858977. doi: 10.1109/TPWRD.2009.2021032.

[45] Barry Mather and Araya Gebeyehu. Field demonstration of using advanced PV inverter functionality to mitigate the impacts of high-penetration PV grid integration on the distribution system. *2015 IEEE 42nd Photovoltaic Specialist Conference, PVSC 2015*, pages 1–6, 2015. doi: 10.1109/PVSC.2015.7356169.

[46] Undeland Tore M. Robbins Mohan, Ned and William P. *Power Electronics - Converters, Applications, and Design (3rd Edition)*. John Wiley & Sons, 2003.

[47] S. Mokkapaty, J. Weiss, F. Schalow, and J. Declercq. New generation voltage regulation distribution transformer with an on load tap changer for power quality improvement in the electrical distribution systems. *CIRED - Open Access Proceedings Journal*, 2017(1):784–787, 2017. doi: 10.1049/oap-cired.2017.0881.

[48] G. R. Chandra Mouli, P. Bauer, T. Wijekoon, A. Panosyan, and E. Bärthlein. Design of a power-electronic-assisted oltc for grid voltage regulation. *IEEE Transactions on Power Delivery*, 30(3):1086–1095, June 2015. ISSN 0885-8977. doi: 10.1109/TPWRD.2014.2371539.

[49] M. I. Muhamad, N. Mariun, and M. A. M. Radzi. The effects of power quality to the industries. In *2007 5th Student Conference on Research and Development*, pages 1–4, Dec 2007. doi: 10.1109/SCORED.2007.4451410.

[50] A Notholt. Germany's new code for generation plants connected to medium-voltage networks and its repercussion on inverter control.

[51] KR Padiyar. Facts controllers in power transmission and distribution. 2007.

[52] N. Papazacharopoulos, M. Gibescu, and P. Vaessen. Smart voltage control in distribution networks with a large share of distributed renewable generation. In *2015 IEEE Eindhoven PowerTech*, pages 1–6, June 2015. doi: 10.1109/PTC.2015.7232497.

[53] Nikolaos Papazacharopoulos, Madeleine Gibescu, and Peter Vaessen. Smart voltage control in distribution networks with a large share of distributed renewable generation. *PowerTech*, 2015.

[54] White Paper and Juan Tobias. Specifying HV / MV Transformers at Large Sites for an Optimized MV Electrical Network.

[55] Robert Passey, Ted Spooner, Iain MacGill, Muriel Watt, and Katerina Syngellakis. The potential impacts of grid-connected distributed generation and how to address them: A review of technical and non-technical factors. *Energy Policy*, 39(10):6280–6290, 2011.

[56] Prof. P. Sasidhara Rao Prof. Krishna Vasudevan, Prof. G. Sridhara Rao. NPTEL lectures on Voltage Regulation. pages 57–64.

[57] MR publication. Vacutap® technology new standard for users of regulating transformers.

[58] Christian Puret. Mv public distribution networks throughout the world. *E/CT*, 155, 1992.

[59] N Rao and D Chamund. Calculating power losses in an igbt module. *Application Note, Dynex Semiconductor Ltd.*, 2014.

[60] Daniel J. Rogers and Tim C. Green. An active-shunt diverter for onload tap changers. *IEEE Transactions on Power Delivery*, 28(2):649–657, 2013. ISSN 08858977. doi: 10.1109/TPWRD.2013.2243171.

[61] M. Schael and C. Sourkounis. Impact of voltage variations on a grid-connected shredder system. In *IECON 2014 - 40th Annual Conference of the IEEE Industrial Electronics Society*, pages 641–647, Oct 2014. doi: 10.1109/IECON.2014.7048568.

[62] Helge Seljeseth, Thomas Rump, and Krister Haugen. Overvoltage immunity of electrical appliances laboratory test results from 60 appliances. In *Proc. Int. Conf. Electricity Distribution (CIRED)*, 2011.

[63] ST semiconductors. How to select the right thyristor (scr) for your application. *AN4608 Application note*, 2014.

[64] SIEMENS. Jfr distribution step voltage regulator instructions, 2008.

[65] MD Singh. *Power electronics*. Tata McGraw-Hill Education, 2008.

[66] S. Sithole, N. Mbuli, and J. H C Pretorius. Voltage regulation in the douglas area using shunt capacitor banks and controllable shunt reactors. *2013 13th International Conference on Environment and Electrical Engineering, EEEIC 2013 - Conference Proceedings*, pages 85–90, 2013. doi: 10.1109/EEEIC-2.2013.6737888.

[67] Management Summary, I E A Task, Recommendations Based, and Field Experience Report Iea-pvps. Do It Locally : Local Voltage Support by Distributed Generation – A Management Summary Do It Locally : Local Voltage Support by Distributed Generation – A Management Summary. (January 2017), 2017.

[68] Cooper Power Systems. Vr-32 voltage regulator with quik-drive™ tap-changer installation, operation, and maintenance instructions, 2017.

[69] Seyed Abbas Taher, Hosein Tahami Fard, and Ehsan Boloor Kashani. New switching approach for DVR using one cycle control method. *Ain Shams Engineering Journal*, 2017. doi: 10.1016/j.asej.2017.03.003.

[70] John Olav Tande, Giuseppe Di Marzio, and Kjetil Uhlen. System Requirements for Wind Power Plants. 2007.

[71] John Olav Giœver Tande. Exploitation of wind-energy resources in proximity to weak electric grids. In *Applied Energy*, 2000. doi: 10.1016/S0306-2619(99)00098-7.

[72] LP Teshmont Consultants and Shaarbafi Karim. Transformer modelling guide. *aeso, Alberta Electric System Operator, Revision*, 2, 2014.

[73] M. Tewolde and S. P. Das. A novel control of bi-directional switches in matrix converter. In *2006 International Conference on Power Electronic, Drives and Energy Systems*, pages 1–6, Dec 2006. doi: 10.1109/PEDES.2006.344404.

[74] I N Power Transmission. *Facts Controllers in Power Transmission*. 2007. ISBN 9788122425413.

[75] F. Q. Yousef-Zai and D. O'Kelly. Solid-state on-load transformer tap changer. *IEE Proceedings - Electric Power Applications*, 143(6):481–491, Nov 1996. ISSN 1350-2352. doi: 10.1049/ip-epa:19960578.

[76] A. Zahedi. A review of drivers, benefits, and challenges in integrating renewable energy sources into electricity grid. *Renewable and Sustainable Energy Reviews*, 15(9):4775–4779, 2011. ISSN 13640321. doi: 10.1016/j.rser.2011.07.074. URL `http://dx.doi.org/10.1016/j.rser.2011.07.074`.

[77] Baosen Zhang, Albert Y. S. Lam, Alejandro Dominguez-Garcia, and David Tse. An Optimal and Distributed Method for Voltage Regulation in Power Distribution Systems. pages 1–13, 2012. ISSN 0885-8950. doi: 10.1109/TPWRS.2014.2347281. URL `http://arxiv.org/abs/1204.5226`.